Aalto University
School of Engineering
Department of Energy Technology

Cichong Liu

Optimization of a new system combining district heating with underground thermal energy storage

Master's Thesis submitted in fulfilment of the requirements for the degree of Master of Science in Technology

Espoo 14.08.2014

Supervisor Markku Lampinen, Professor
Instructor Kari Saari, Lic. Sc. (Tech)

Author: Cichong Liu

Title of thesis: Optimization of a new system combining district heating with underground thermal energy storage

Department: Department of Energy Technology

Major: Innovative Sustainable Energy Engineering **Code of professorship:** Ene-39

Thesis supervisor: Markku Lampinen, Professor

Thesis advisor: Kari Saari, Lic. Sc. (Tech)

Date: 14.08.2014 **Number of pages:** 98 **Language:** English

Abstract

This thesis is focusing on optimizing a new system combining underground thermal energy storage with district heating. The system is operated by storing heat during summer time to lower the heat demand during winter.

By analyzing the heat transfer model of the new system, the effects from mass flow rate of the circulating fluid on the heat transfer rate, the exiting fluid temperature and the ground temperature are significant. After economic analysis, it is possible to draw a conclusion that with a lower mass flow rate during summer time and a higher mass flow rate during winter time, the heat utilization can be maximized thus the economic profits can be maximized as long as the ground mean temperature after a whole year is higher than the initial ground temperature.

For Turku case, the minimum payback years is 3.54 years with one borehole operated for the whole year, while in summer, the mass flow rate is 0.05 kg/s and in winter, the fluid is circulated with a mass flow rate of 0.5 kg/s and the corresponding COP of the connected heat pump ranges from 2.8 to 3.

Keywords: Underground thermal energy storage, District Heating, Turku, Heat Pump, Heat Transfer, Economic Analysis, Mass Flow

Cichong Liu
400079
cichong@aalto.fi

Contents

Abstract I

1 Introduction 1

1.1 Introduction to the underground thermal energy storage system 1

1.1.1 What is the underground thermal energy storage system 1

1.1.2 Types of the underground thermal energy storage systems 2

1.1.3 Advantages and Disadvantages of the underground thermal energy storage systems 4

1.1.4 Parallel & Series connections of borehole heat exchangers 5

1.1.5 Typical case realized 6

1.1.6 Aim of the new system combining district heating with underground thermal energy storage 8

1.1.7 Cost of the underground thermal energy storage 9

1.2 Introduction to the project 11

1.3 Purpose of the project 14

2 Heat transfer model of the UTES 15

2.1 Short introduction of the heat transfer models for calculating heat exchange of the UTES 15

2.1.1 Heat transfer outside borehole 16

2.1.2 Heat transfer inside boreholes 17

2.2 Matlab programming 21

2.2.1 Baseline Scenario (Scenario 0) 23

2.2.2 Other scenarios analysis 33

2.2.3 Scenarios comparison 35

3 The analysis of heat pump connected with underground thermal energy storage 39

4 Economic Analysis of the new system 41

4.1 Baseline Scenario (Scenario 0) 41

4.1.1 Matlab programming 41

4.1.2 Results 43

4.1.3 How the cost of heat in summer affects the results 45

4.2 Other scenarios analysis 46

5 Case in Turku 47

5.1 New system 47

5.1.1 Winter mass flow rate = 0.5 kg/s 49

Cichong Liu
400079
cichong@aalto.fi

5.1.2 Winter mass flow rate = 0.25 kg/s 53
5.2 Geothermal heat pump analysis 56
5.2.1 Winter heat transfer prediction 56
5.2.2 Economic analysis 57
6 Discussion 59
7 Conclusions 61
8 Acknowledgement 62
9 References: 63
10 Appendix 67
10.1 Matlab Code 67
10.1.1 Summer iterating 67
10.1.2 Winter iterating 72
10.1.3 Economic analysis 78
10.1.4 Turku case analysis 80
10.2 Scenario Results 82
10.2.1 Scenario 1 (mass flow rate in summer = 0.1kg/s, mass flow rate in winter =0.5 kg/s) 82
10.2.2 Scenario 2 (mass flow rate in summer = 1 kg/s, mass flow rate in winter = 0.5 kg/s) 86
10.2.3 Scenario 3 (mass flow rate in summer = 0.5 kg/s, winter mass flow rate in winter = 0.1 kg/s) 89
10.2.4 Scenario 4 (mass flow rate in summer = 0.5 kg/s, mass flow rate in winter =1 kg/s) 91

Cichong Liu
400079
cichong@aalto.fi

α	Thermal diffusivity of soil (m^2/s)
τ	Time (s)
c	Specific capacity of the circulating fluid (J/kg·K)
COP	Coefficient of performance
$C_{electricity}$	Electricity cost (€/MWh)
C_{summer}	Cost of heat in summer time (€/MWh)
C_{winter}	Cost of heat in winter time (€/MWh)
D	Half distance between two legs of the U-tube (m)
h	Thermal convection efficient between circulating fluid and inner U-tube wall (W/m^2K)
H	The length of the borehole heat exchanger (m)
k_b	Thermal conductivities of the grouting material (W/mK)
k_{ground}	Thermal conductivity of soil (W/mK)
k_U	Thermal conductivities of the U-tube material (W/mK)
$\dot{m}$	mass flow rate (kg/s)
n	Number of borehole heat exchangers built
n_{used}	Number of borehole heat exchanger used hourly in summer time
P	Power consumed in running compressor (W)
q_l	Heating/cooling rate per length (W/m)
$q_{lsummer}$	Heating rate per length in summer (W/m)
$q_{lwinter}$	Cooling rate per length in winter (W/m)
q_{summer}	Hourly heat capacity charged to the borehole in summer (W)
q_{winter}	Hourly heat capacity discharged from the borehole in winter (W)
Q_h	Useful thermal energy (W)
Q_{heat}	Hourly heat demand for the whole year (W)
$Q_{heatsummer}$	Hourly heat demand for summer time (W)
$Qheat_{winter}$	Hourly heat demand for winter time(W)
r	Horizontal distance to the borehole center (m)
r_b	Borehole radius (m)
r_{ext}	Outer radius of the U-tube (m)
r_{int}	Inner radius of the U-tube (m)
R_{11}/R_{22}	Thermal resistance between one U-tube leg and borehole wall (mK/W)
R_{12}	Thermal resistance between two legs of the U-tube (mW/W)
Sh	Summer hours in the range from 1 to 3672 (hour)
SD	Summer Day (Day)
T	Ground temperature (°C)
T_b	Borehole wall temperature (°C)
T_{exit}	Exiting fluid temperature from the U-tube (°C)
T_{f1}	Fluid temperature in the inlet leg of U-tube (°C)
T_{f2}	Fluid temperature in the outlet leg of U-tube (°C)
T_h	High temperature level of the heat pump (K)
T_{in}	Entering fluid temperature into the U-tube (°C)
Tin_{summer}	Entering fluid temperature into the U-tube in summer (°C)
Tin_{winter}	Entering fluid temperature into the U-tube in winter (°C)
T_l	Low Temperature level of the heat pump (K)
T_o	Initial ground temperature (°C)
T_{return}	Return temperature from district heating networks (°C)
T_{supply}	Supply temperature from district heating networks (°C)
Wh	Winter hours in the range from 3672 to 8761 (hour)
WD	Winter Day (Day)
z	Vertical distance to the ground surface (m)

1 Introduction

1.1 Introduction to the underground thermal energy storage system

1.1.1 What is the underground thermal energy storage system

Underground thermal energy storage system is one typical type of seasonal thermal energy storage. Seasonal thermal energy storage is a term used for describing various technologies of storing heat/energy for months especially for some renewable energy which is very productive during the low demand period. Seasonal thermal energy storage can be classified into three typical groups: Sensible heat storage, latent heat storage and chemical storage (Xu et al., 2013). Among which, sensible heat storage is the most commonly used technology for underground thermal energy storage thanks to its simplicity, low costs and relative mature technology. According to Schmidt et al. (2003) research's results, water, rock-sort materials and soil are the possible candidates of storage media of sensible heat storage systems.

Underground thermal energy storage is developed based on the theory that beneath the ground 10 meters, the temperature is roughly equal to the mean annual air temperature at the latitude at the surface (GTK, 2010).As shown in Figure 1 which is a test run in east Finland, underground around 10 meters, the temperature starts to remain constant irrelative with the months.

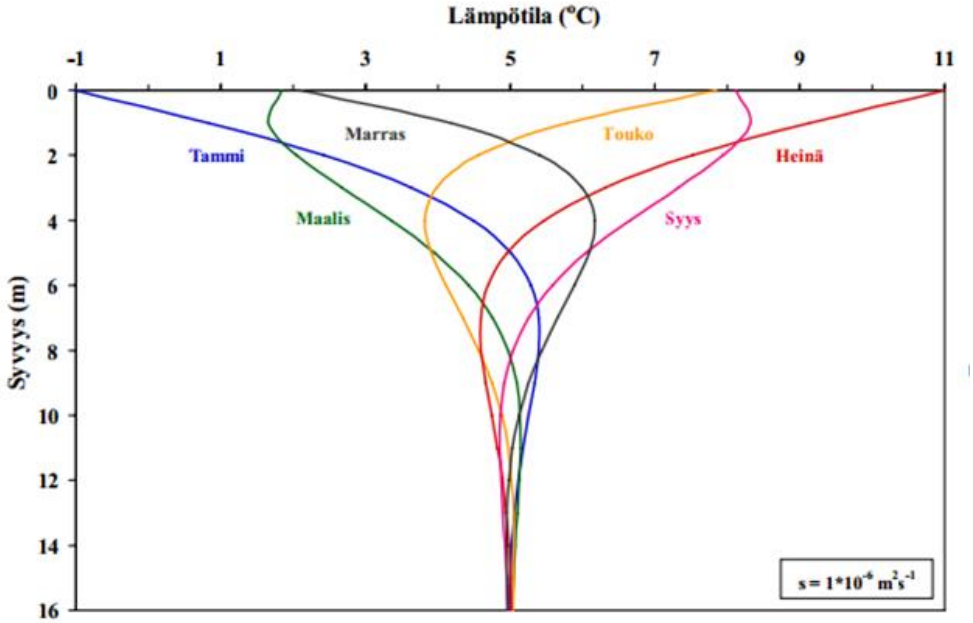

Figure 1. Underground temperature variation (GTK, 2010)

Cichong Liu
400079
cichong@aalto.fi

The underground thermal energy storage has a 50-year history which first developed in China with cold storage in aquifers in 1960s. During 1980s, the technology has attracted enormous attentions from worldwide. Table 1 lists some important cases of underground thermal energy storage (Sanner & Nordell, 1998).

Table 1. Typical cases of underground thermal energy storage system (Sanner & Nordell, 1998)

Year	Name	Remarks
since mid 1960s	several huge ATES plants in China	(Shanghai, Changzou)
1976	Auburn Univ., Mobile Al., USA	Aquifer experiment, abandoned
1981	"Sunclay", school, Kungsbacka, SE	BHE, solar coll., diesel engine heat pumps
1981	12 houses, Cortaillod, CH	BHE, solar collectors, heat pump
1982	"SPEOS", Lausanne-Dorigny, CH	ATES experiment, waste heat, abandoned
1982	Yamagata Univ., Yonezawa, JAP	ATES experiment
1982	Waste Incineration, Hørsholm, DK	High temp. ATES experiment, abandoned
1982	Univ. Minnesota, St. Paul, USA	High temp. ATES experiment, abandoned
1982	Hokkaido Rehabily, Sapporo, JAP	ATES, heat storage
1982	Univ. Alabama, Tuscaloosa, USA	ATES, cooling
1983	Lulevärme, Luleå, SE	Boreholes, high temp., operat. suspended
1983	224 flats, Aulnay-sous-bois, FR	ATES, with heat pumps
1984	CSHPSS, Groningen, NL	BHE, solar heat
1985	Scarborough Centre, Toronto, CAN	ATES, heating and cooling, heat pumps
1987	Le Plaisir, Thiverval-Grignon, FR	High temp. ATES experiment, abandoned
1987	Head Office SAS, Frösundavik, S	ATES, heating and cooling, heat pumps
1987	Perscombinatie, Amsterdam, NL	ATES, cooling
1989	Jean Sieber SA, Geneva-Meyrin, CH	BHE, solar coll., gas-engine heat pump
1991	Utrecht Univ., Utrecht, NL	High Temperature ATES, waste heat

ATES: Aquifer Thermal Energy Storage
BHE: Borehole Heat Exchangers

1.1.2 Types of the underground thermal energy storage systems

Underground thermal energy storage system can be generally divided into two types: Borehole thermal energy storage and aquifer thermal energy storage. They are classified based on the storage media. Basically, borehole thermal energy storage utilizes ground/soil as storage media while aquifer thermal energy storage utilizing gravel water as storage media.

In this project, underground thermal energy storage system is used for storing excess heat during summer periods and extracts it for the use in winter periods and borehole thermal energy storage system is applied.

Cichong Liu
400079
cichong@aalto.fi

In borehole thermal energy storage, boreholes are typically 50-200 m in depth (Gao et al., 2009) and 150-200 mm in diameter (Saljnikov et al., 2006). The inserting tubes, so-called borehole heat exchangers (Saljnikov et al., 2006) in some literatures, are used as heat exchangers, the ground/soil serves as the storage medium while the water is the energy transferring fluid. In many cases, borehole heat exchangers are also combined with heat pumps for significantly improving efficiency when low-temperature heat is extracted from the soil. As shown in Figure 2, the general construction of borehole tube typically consists of borehole wall, U-pipes (single-U and double-U) and grouting materials. 2(b) and 2(c) represent the cross-section area of the installed borehole heat exchanger with single U-tube and double U-tube respectively.

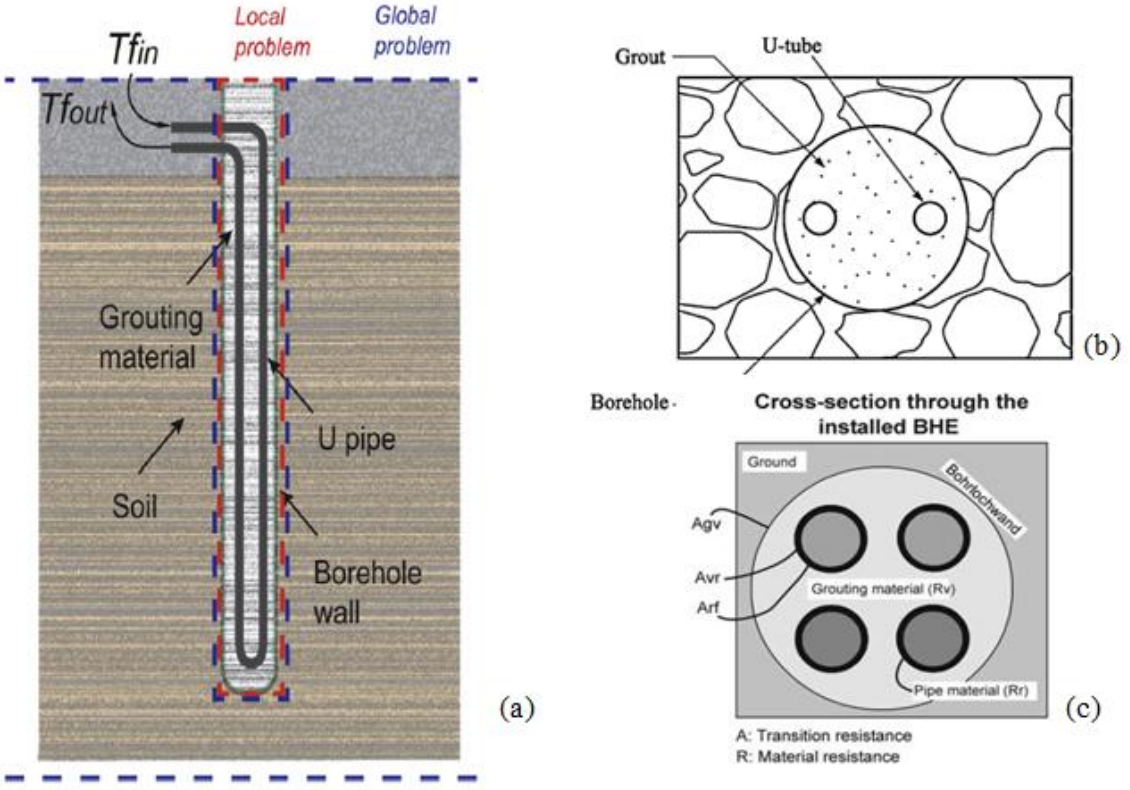

Figure 2. General construction of borehole heat exchanger (Sanner et al., 2003; Lazzarotto, 2014; Lee, 2013)

Usually, high density polyethylene is applied as U-pipe material and for grouting material, multiple choices exist. Grouting material is required to have high performance of heat transfer with the surrounding soil so high thermal conductivity of grouting material is essential to conduct heat. Bentonite, high solids composite (such as 9% of Blast Furnace Cement, 9% of Portland cement, 32%

Cichong Liu
400079
cichong@aalto.fi

fine silica sand and 50% water) (DLSC, 2014), water alone (Gustafsson et al., 2010) and 5%wt of graphite (Delaleux et al., 2012) have been studied as grouting material in multiple experiments while the latest one, 5%wt of graphite as grouting material reaches 5 W/mK of conductivity, highly reducing the thermal borehole resistance. Besides grouting material, also many other factors could influence the efficiencies of the storage system, for instance, ground temperature, operational temperature of the storage, thermal properties of the ground, etc. There is also a concern related with the distance the installed boreholes which also significantly influences the thermal interference effect. Normally, a distance of between 8-10 m can be an appropriate range to reduce the performance loss (Ahmet Gultekin et al., 2014) (U. Desideri et al., 2011).

The working mechanism of the borehole thermal energy storage system is to store excess heat into the ground during summer time by circulation hot water through borehole heat exchangers from the center to the edge of the storage. In this way, heat is transferred to surrounding soil by heat conduction. When winter comes, the flow direction is reversed and in this way, the heat stored in the soil is transferred back to the cold water and the hot water is circulated inversely for heating purposes.

1.1.3 Advantages and Disadvantages of the underground thermal energy storage systems

1.1.3.1 Advantages:

There are multiple advantages of utilizing the underground thermal energy storage systems and they can be concluded as following (Saljnikov et al., 2006):

- Underground thermal energy storage system could store enormous amounts of energy in the nature and the stored part can be used in future for multiple purposes;
- Little operational costs are required and in the long term, it can make large profits. (As reported, reduction of electricity costs for operation of cooling machines and plants is nearly 75%, the period of time during which the additional investment costs paid off is shorter than 5 years);
- The storage system itself doesn't have any pollution to the environment and by utilizing seasonal energy storage, large amount of energy is saved thus the environmental pollution caused by corresponding energy production is reduced in this manner;
- Possible utilization of the abandoned boreholes that were drilled for different purposes (Boreholes and aquifer thermal energy storage and choice of thermal response test method)

Cichong Liu
400079
cichong@aalto.fi

1.1.3.2 Disadvantages:

Besides all the advantages of the underground thermal energy storage system mentioned above, there are various challenges when deciding to build the project:

- Underground thermal energy storage system usually has a big size which requires a large space and multiple requirements for the soil in order to have a good heat transfer between ground and borehole heat exchanger are necessary thus it would be a task to select right location;
- Building borehole heat exchangers usually requires drilling holes underground for hundreds meters which means a large investment cost is required initially;
- In the heat transfer process, ground temperature is varying all the time therefore this system is not able to deliver or store heat at a constant temperature.

1.1.4 Parallel & Series connections of borehole heat exchangers

There are two methods to connect borehole heat exchangers underground: parallel connected or series connected as shown in Figure 3. Upper scheme is the series connection while the lower one is the parallel connection. Both systems have their own pros and cons (Geothermal heat pump systems, 2014).

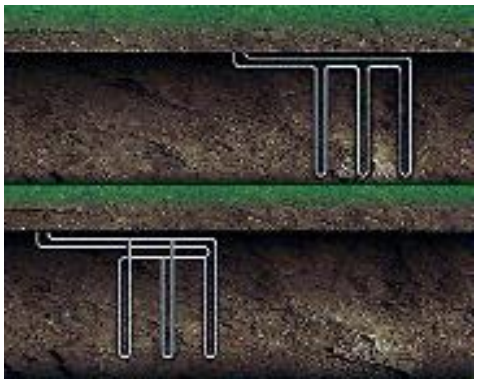

Figure 3. Series and parallel connections of borehole heat exchangers (Geothermal heat pump systems, 2014)

A series system, commonly has a larger diameter pipe. The system takes advantage of single path and pipe size and it has slightly higher thermal performance compared to the parallel structure. However, larger water or antifreeze volume is required for larger pipe size and higher cost is required for pipe material and the total length of such a system is limited due to fluid pressure drop and pumping costs.

On the contrary, a parallel structure is constructed with smaller diameter pipe thus lower cost of pipe material is needed and less antifreeze volume is required. Nevertheless, special attention needs to

Cichong Liu
400079
cichong@aalto.fi

be taken in order to assure that all the air is out of the piping loop and balancing of flow in each parallel pipe requires additional care.

1.1.5 Typical case realized

1.1.5.1 DLSC project in Canada

Figure 4 is an example of combined solar energy with borehole seasonal thermal storage system built by DLSC (Drake Landing Solar Community) which currently run in Okotoks, Alberta in Canada. This project is built to supply 52 houses' space and water heating with solar energy.

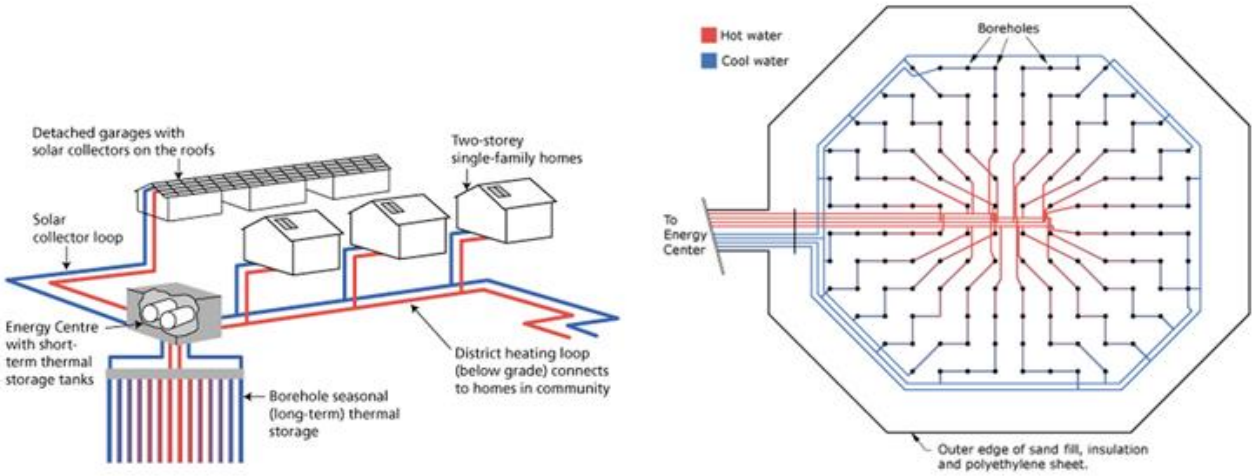

Figure 4. Combined solar energy with borehole seasonal thermal storage system (DLSC, 2014)

As shown in Figure 4, the project consists of solar panels, short term storage water tank, borehole heat exchangers and district heating loop.

800 solar panels are located on garage roofs absorbing solar energy and heating a glycol solution. The glycol solution loop travels along the loop arriving the short-term storage tank, the heat is transferred to the water stored in the tank and glycol solution goes back to the solar panel. In this manner, 1.5 MW of thermal power can be generated in a sunny day. Hot water continues to travel from the short term storage tank to series connected borehole heat exchangers. 144 boreholes are drilled in this project covering an area of 35 meters in diameter and each borehole is 37-meter deep (DLSC, 2014). As reported, the temperature of the ground is increased to 80˚C by the end of summer.

And when the winter comes, the hot water in the boreholes passes back to the short-term storage tank and is distributed to the houses through the district heating loop.

Cichong Liu
400079
cichong@aalto.fi

1.1.5.2 Greenhouse project in China

Figure 5 shows a greenhouse project realized in Shanghai, China. It is a system combining solar energy with borehole thermal energy storage. This project is built to supply heat to a 2304 m^2 greenhouse in order to provide a suitable micro-climate for various crops and keep them from variable outdoor weather conditions.

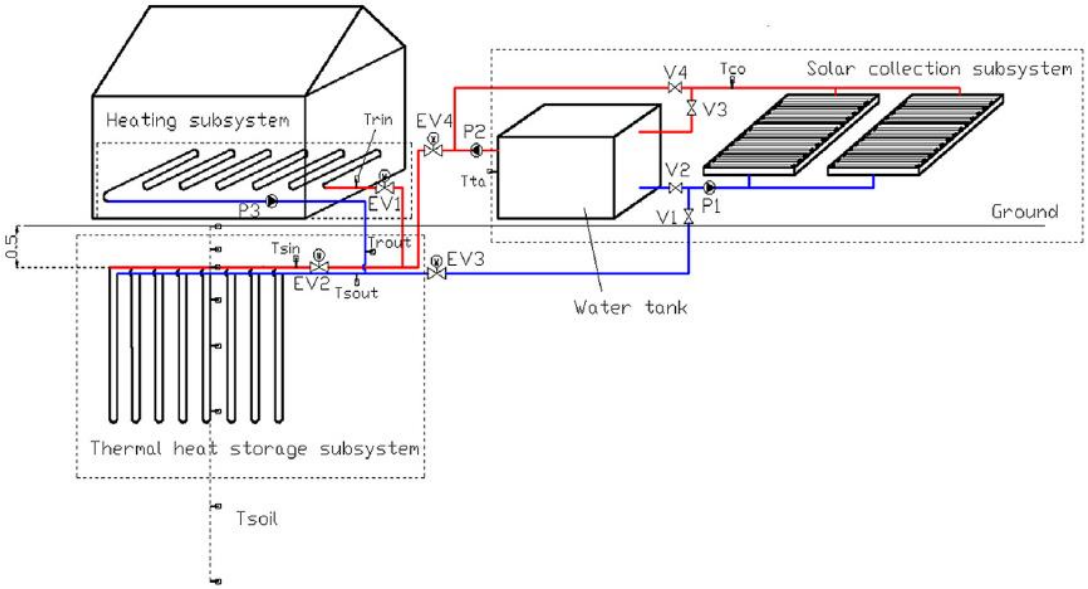

Figure 5. Greenhouse project scheme (Xu et al., 2014)

As shown in Figure 5, the system is constructed similar to DLSC project, consisting of three components: solar collectors, short term water storage tank, borehole thermal storage system (130 boreholes with depth of 10 m covering an area of 497 m^2) and the heat distribution pipe. The working principles are similar to DLSC project. During non-heating season (Mar. –Nov. in Shanghai), solar energy is captured and carried by hot water going through U-tubes to heat up the ground and during heating season, the process is reversed (Xu et al., 2014). The hot water stored underground travels back and go through the heat distribution pipe to the green house. Different to DLSC project, borehole heat exchangers in this project is connected in parallel.

Figure 6 shows ground temperature evolution of the underground thermal energy storage system with three different operating stages: A indicates the process before charging, B indicates the charging process and C indicates the discharging process. #1 shows the temperature variation in a running borehole heat exchanger while #2 shows the temperature variation of an observation well of

Cichong Liu
400079
cichong@aalto.fi

non-storage area. In period A, the ground temperature remains constant (18 ˚C) under 5m. When the charging period is started, the ground temperature starts increasing in the same pace regardless of the depth and it reaches approximately 40 ˚C until the end of the charging period (after 8 months) and started to decrease. After three months of discharging, the temperature goes back to 25˚C roughly.

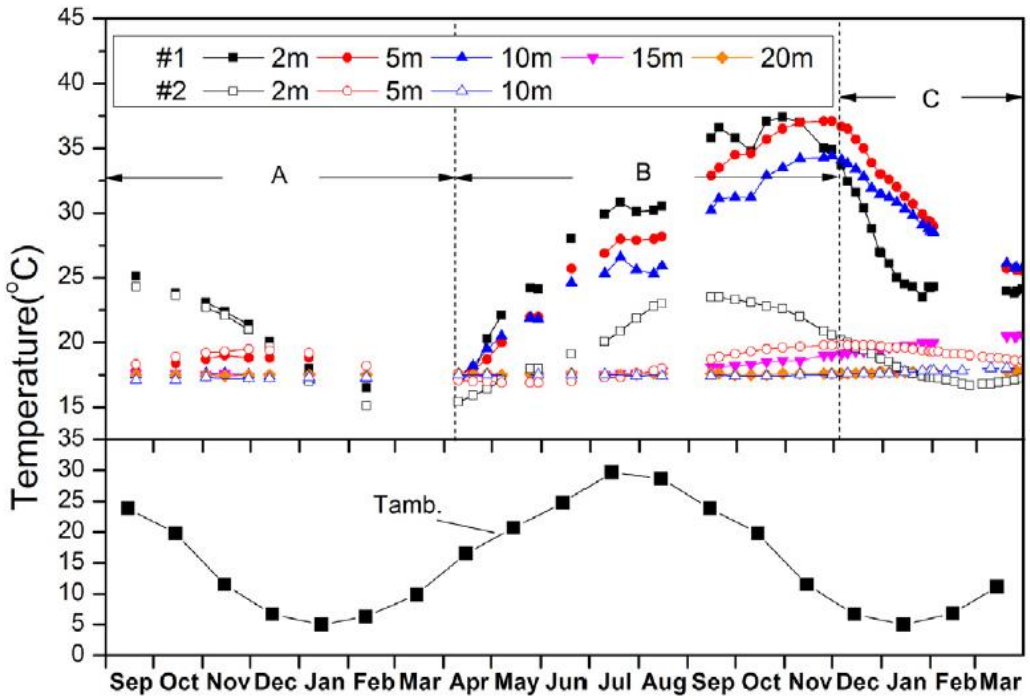

Figure 6. Ground temperature evolution during different time periods (Xu et al., 2014)

1.1.6 Aim of the new system combining district heating with underground thermal energy storage

In this project, instead of combining with a solar system, underground thermal energy storage is combined with district heating.

Figure 7 shows a typical heat demand vs CHP heat production curve for one normal community. During summer time, CHP will produce larger amount of heat than is actually consumed in winter, a heat deficit is existing between the heat demand and CHP heat production.

This new system is aimed for storing heat surplus in summer and to compensate the heat deficit in winter.

Cichong Liu
400079
cichong@aalto.fi

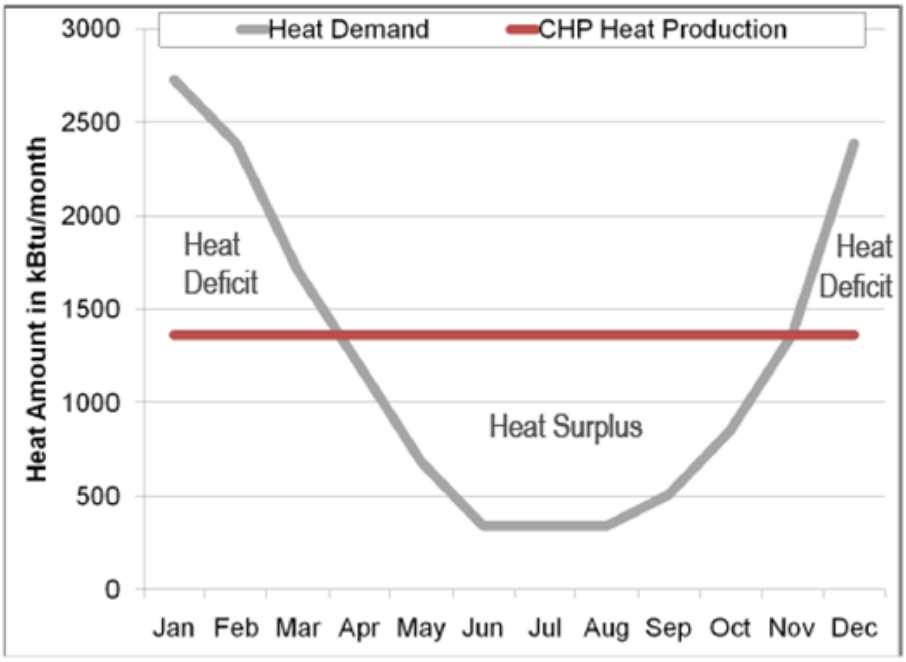

Figure 7. Heat Demand vs. CHP Heat Production curve (REHAU, 2014)

1.1.7 Cost of the underground thermal energy storage

It is relative hard to estimate the investment cost of the underground thermal energy storage system since multiple components are needed to be taken into consideration. Luo et al. (2013) concluded the capital cost of borehole heat exchangers can be categorized in following groups: drilling boreholes, buried pipe, spacer, grouting, heat pump and accessories, while accessories contain water circulation pumps, connection pipes, air pressure tank and buffer storage tank.

Blum et al. found that the distribution of the capital cost for studied borehole heat exchangers shows a normal distribution curve, thus they made a table to roughly estimate the capital cost of building borehole heat exchangers and heat pumps as indicated in Table 2. And in this project, a unit capital cost of 2161 €/kW per heating demand is used.

Cichong Liu
400079
cichong@aalto.fi

Table 2. Arithmetic means and standard deviations for costs of all studied technical and economical parameters including the best fitted statistical distributions (Blum et al., 2011)

Parameter	Number of valid values	**Arithmetic mean** and *standard deviation*	Best fitted statistical distribution
Heated area [m^2]	1047	**190** *57*	Lognormal
Number of BHE [-]	1091	**2** *0.8*	–
Total length of the BHE [m]	1109	**180** *90*	Normal
Depth of one BHE [m]	1104	**95** *34*	Lognormal
Heating demand [kW]	1113	**11** *3*	Log-normal
Costs for drilling and BHE [€]	899	**11,997** *3,881*	Normal
Cost for heat pump [€]	894	**11,649** *3,886*	Normal
Total capital cost [€]	931	**23,460** *6,754*	Normal
Specific heat extraction rate [Wm^{-1}]	1093	**48** *10*	Normal
Costs for drilling and BHE per unit length of the BHE [€ m^{-1}]	885	**67** *21*	Lognormal
Costs for drilling and BHE per unit heating demand [€ kW^{-1}]	893	**1,052** *336*	Lognormal
Heat pump costs per unit heating demand [€ kW^{-1}]	895	**1,039** *394*	Lognormal
Unit capital cost per heating demand [€ kW^{-1}]	925	**2,161** *693*	Lognormal

Cichong Liu
400079
cichong@aalto.fi

1.2 Introduction to the project

Figure 8 shows the basic flow scheme of the underground thermal energy storage system combined with district heating system to provide heating for a small community of 12 apartments.

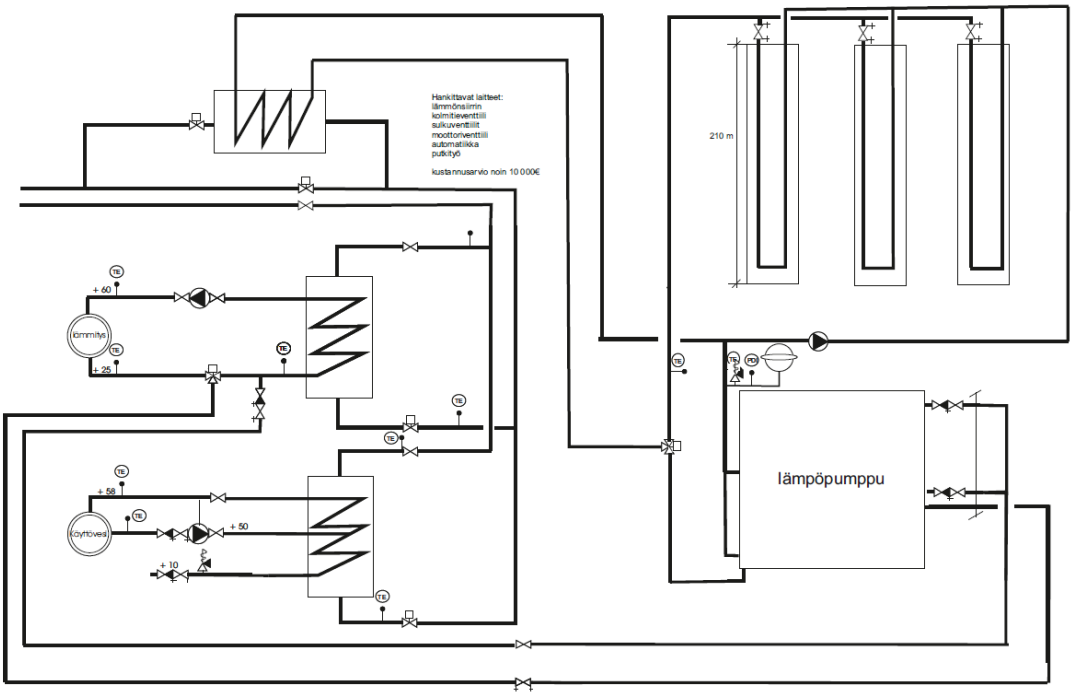

Figure 8. Scheme of the new system combining district heating with underground thermal energy storage

As introduced in previous chapter, underground thermal energy storage system is a long-term heat storage system which is used to store the waste heat in summer time and utilize the heat in winter. As the figure shows, during summer time, the district heat supply is connected to the underground thermal energy storage system through a heat exchanger. Summer heat is stored underground in this way and during the winter time, the heating of the building is not only supplied by the district heating system but also by the heat storage combined with a heat pump. To utilize the heat stored in summer from underground, it is necessary to utilize a heat pump in order to increase the temperature level of the circulating water to the expected temperature, around 60 degree in this case.

In this project, Helsinki is taken as a study example and following data is applied in the calculations.

1. Outdoor temperature profile

Cichong Liu
400079
cichong@aalto.fi

Figure 9 shows an hourly weather data in Finnish southern area with Finnish test reference years (ILMATIETEEN LAITOS, 2014).

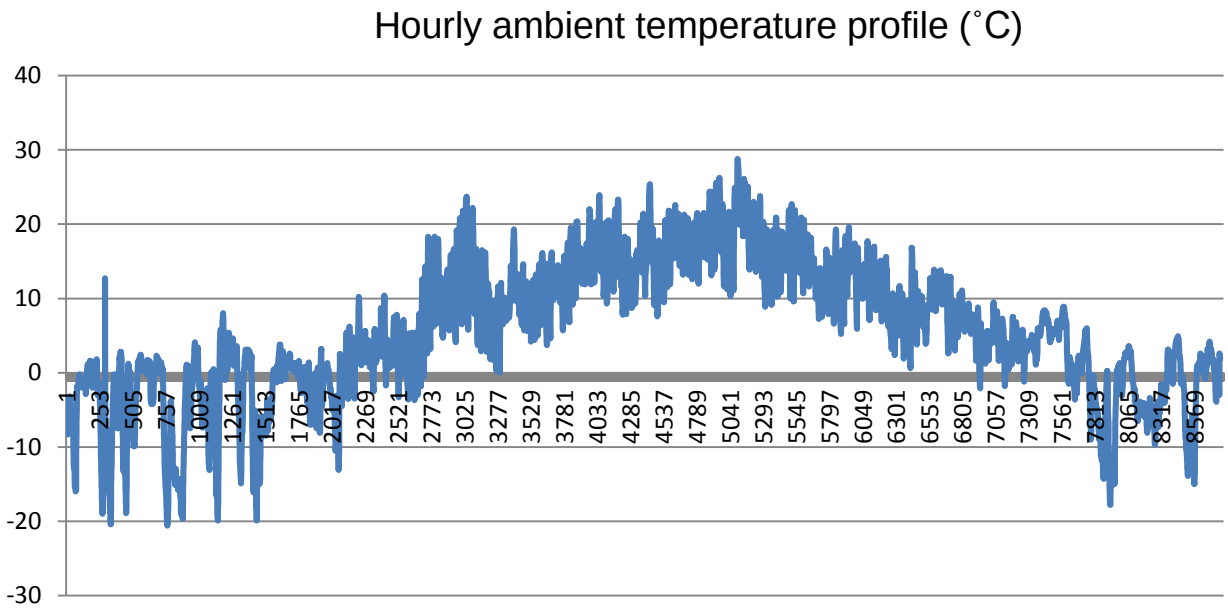

Figure 9. Hourly ambient temperature in Helsinki

2. Heat demand profile

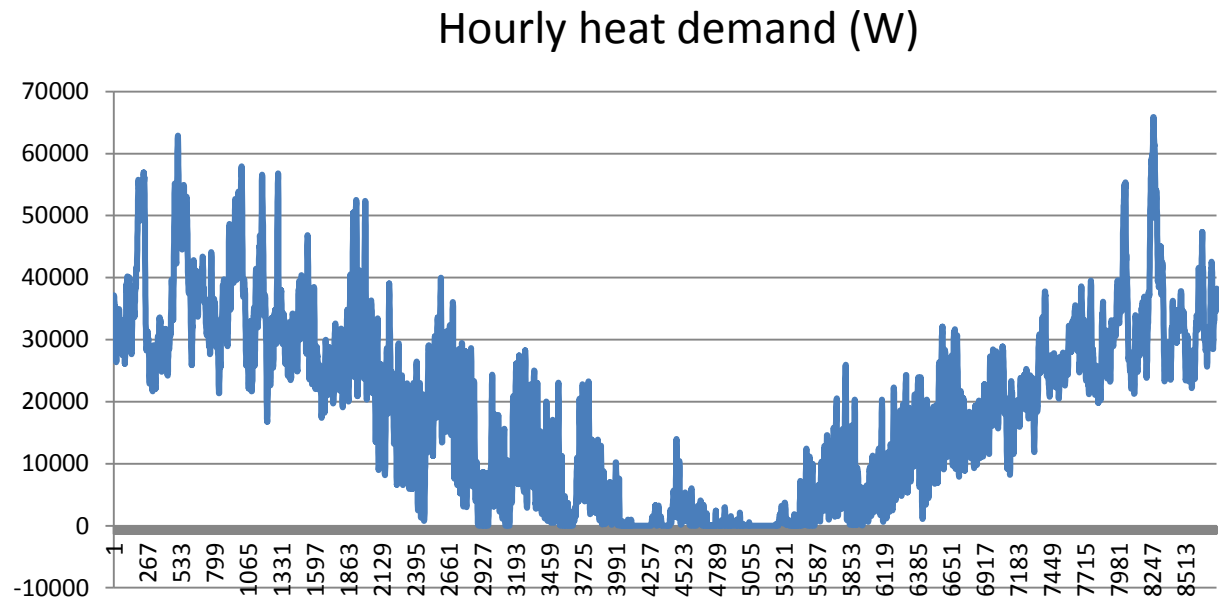

Figure 10. Hourly heat demand for the specific community

Cichong Liu
400079
cichong@aalto.fi

Figure 10 shows an hourly heat demand for the small community of 12 apartments and the data is calculated using IDA-ICE 4.5 and TRNSYS 17 by Laitinen et al. (2014).

3. Heat exchanger efficiency

The efficiencies of all the heat exchangers shown in Figure 8 are assumed to be 0.9 in all project calculations.

Cichong Liu
400079
cichong@aalto.fi

1.3 Purpose of the project

The main purpose of the project is to calculate the economic feasibility of building a new system combining underground thermal energy storage with district heating system. A heat transfer model of the borehole heat exchanger will be built first. Based on the heat transfer model, various scenarios will be built to analyze the payback years of the new system. The influencing parameters include the capacity and the total storage volume of the underground thermal energy storage system, COP of the connected heat pump, mass flow rates of the circulating fluid inside U-tubes, and the costs of summer heat etc.

By calculating the savings made by the community per year with different scenarios and comparing with the investment cost, payback years can be calculated out thus a conclusion can be drawn if the underground thermal energy storage system is economically feasible or not. Meanwhile, results of this project also provide the most optimal way to charge and discharge the underground thermal energy storage system.

Cichong Liu
400079
cichong@aalto.fi

2 Heat transfer model of the UTES

2.1 Short introduction of the heat transfer models for calculating heat exchange of the UTES

To analysis the economic feasibility of the UTES combined with DH system, it is important to realize the performance of the borehole heat exchangers.

In the underground thermal energy storage systems, the ground heat exchangers may include up to hundreds of boreholes depending on the size of the storage system. Each heat exchanger is composed of single or double U-tubes through which the fluid is circulated. Normally, the U-tubes have a diameter in the range of 20-40 mm and each borehole is around 60-200 m deep with a diameter of 100-200 mm.

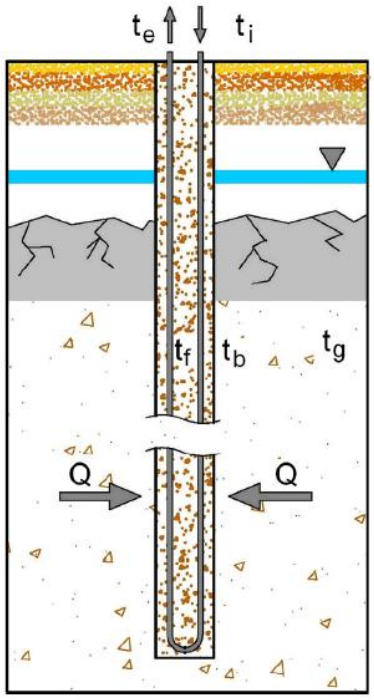

Figure 11. Scheme of a vertical grouted borehole with single U-tube (Sabu et al., 2014)

Figure 11 shows the schematics of a vertical grouted borehole with single U-tube construction.

To analyze the energy balance of the borehole heat exchangers, two aspects need to be considered: heat transfer outside boreholes and heat transfer inside boreholes.

Cichong Liu
400079
cichong@aalto.fi

2.1.1 Heat transfer outside borehole

The heat transfer outside boreholes is carried out in conduction mode. Several simulation models of the heat conduction outside boreholes have been reported. Kelvin's line model is the earliest approach to solve the heat transfer between boreholes and ground. In Kelvin's mode, the borehole has been assumed to be an infinite line source with an initial uniform temperature while the heat transfer in vertical direction has been ignored (Yang et al., 2010). Of course, under above assumptions, the model became relative simple and it can save a lot of the calculation time (Eskilson, 1987). However, the limitation of the model is also obvious. Eskilson (1987) and Fang et al. (2002) concluded that the model can only be applicable with small pipes and limited time range. Based on Kelvin's model, Hart and Couvillion (1986) developed more accurate model. In 1946, Carslaw and Jaeger discovered a new method called cylindrical source model. This model is a solution to the buried infinite cylindrical pipe with either a constant pipe surface temperature or a constant heat transfer rate between the boreholes and the ground. In this case, the final solution is only a function of time and distance from the borehole center, regardless of the depth of the borehole (Carslaw and Jaeger, 1946).

In 1987, an impressive progress was made by Eskilson to account the length of the boreholes which offset the limitations of Kelvin and Cylindrical models. Similar to cylindrical source model, the ground is assumed to be homogeneous and the thermal capacitance of the borehole elements is neglected (Eskilson, 1987). However, this approach is time consuming and includes an interpolation function which may lead to some computing errors (Yang et al., 2010).

The newest model was built based on Eskilson's model by Zeng et al. with following basic assumptions (Zeng et al., 2002):

The ground is regarded as a homogeneous semi-infinite medium, and its thermophysical properties do not change with temperature.

The medium has a uniform initial temperature, T_o.

The boundary of the medium-the ground surface has a constant temperature throughout the period considered.

The radial dimension of the borehole is neglected so that it may be approximated as a line source stretching from the boundary to a certain depth, H.

Cichong Liu
400079
cichong@aalto.fi

As a basis case of study, the heating rate per length of the source, q_l, is constant since the starting instant, τ=0.

Different from above mentioned models, finite line-source model developed by Zeng et al. (2002) took the influences of the finite length of borehole and the ground surface as a boundary into consideration. By comparing calculated results with numerical solutions in references, (Eskilson (1987) and Zeng et al. (2002)) a perfect match when $\alpha \frac{\tau}{r_b^2} \geq 5$ is shown (Zeng et al., 2002). The model was given by Zeng et al. as shown in equation (1).

$$T - T_o = \frac{q_l}{4k_{ground}\pi} \int_0^H \left\{ \frac{\operatorname{erfc}\left(\frac{\sqrt{r^2 + (z-h)^2}}{2\sqrt{a\tau}}\right)}{\sqrt{r^2 + (z-h)^2}} - \frac{\operatorname{erfc}\left(\frac{\sqrt{r^2 + (z+h)^2}}{2\sqrt{a\tau}}\right)}{\sqrt{r^2 + (z+h)^2}} \right\} dh \quad (1)$$

Where r represents the horizontal distance to the center of borehole, z represents the vertical distance to the ground surface, τ represents time, T_o is the initial starting temperature, q_l is the heating rate per length of the source, r_b represents the borehole radius, k_{ground} is the thermal conductivity of the soil and α denotes the thermal diffusivity of the soil.

Some other models including short time-step model developed by Yavuzturk and Spitler (1999), transient finite-element model developed by Muraya (1996), a finite difference model by Rottmayer et al.(1997) and a three-dimensional unstructured finite volume model by Li and Zheng (2009) have also been developed based on necessary assumptions. In this project, Zeng's model will be applied to analysis the heat exchange outside borehole systems.

2.1.2 Heat transfer inside boreholes

The heat transfer inside boreholes is mainly carried out by conduction and convection modes. The thermal resistance inside borehole is primarily determined by the thermal properties of the grouting materials. Besides, the U-tube materials, mass flow rate of the circulating fluid and thermal properties of the thermal fluid also have influences on the thermal resistance. Several models with varying degrees of complexity have been developed to describe the heat transfer inside the ground heat exchange boreholes including 1-D, 2-D and 3-D models. One-dimensional model was relatively easy by assuming the heat transfer process to be one-dimension and steady state. It was simple and convenient but it is not capable to deal with dynamic reaction of the borehole (Yang et al., 2010). In

Cichong Liu
400079
cichong@aalto.fi

1991, two-dimensional model was developed by Hellstrom. In this model, both resistances between circulating fluid in each pipe and borehole wall, R_{11} and R_{12}, and the resistance between the two pipes, R_{12}, are included. As shown in Figure 12, the configuration of U-tube in the borehole is symmetric thus it is reasonable to assume the thermal resistances between circulating fluid and the borehole wall in both sides are equal.

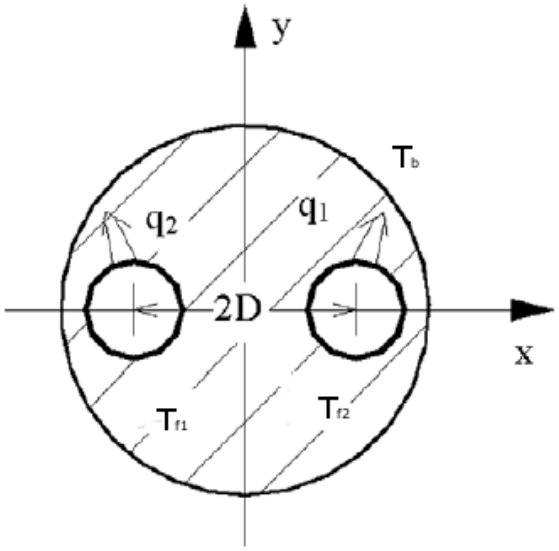

Figure 12. Configuration of U-tube in the borehole

$$\text{Pipe to borehole wall: } R_{11} = \frac{1}{2\pi k_b}\left[\ln\left(\frac{r_b}{r_{ext}}\right) + \frac{k_b - k_{ground}}{k_b + k_{ground}} \cdot \ln\left(\frac{r_b^2}{r_b^2 - D^2}\right)\right] + R_p \quad (2)$$

$$\text{Pipe to pipe: } R_{12} = \frac{1}{2\pi k_b}\left[\ln\left(\frac{r_b}{2D}\right) + \frac{k_b - k_{ground}}{k_b + k_{ground}} \cdot \ln\left(\frac{r_b^2}{r_b^2 + D^2}\right)\right] \quad (3)$$

$$R_{22} = R_{11} \quad (4)$$

$$\text{Resistance inside the tube: } R_p = \frac{1}{2\pi k_U}\ln\left(\frac{r_{ext}}{r_{int}}\right) + \frac{1}{2\pi r_{int} h} \quad (5)$$

Where r_b, r_{ext}, r_{int} are the radius of the borehole, outer radius of the U-tube and inner radius of the U-tube respectively, D represents half distance between two legs of the U-tube, k_{ground}, k_b, k_U are the thermal conductivities of the soil, grouting material and U-tube material and h represents the thermal convection coefficient between the circulating fluid and inner U-tube wall which is influenced by the flow condition of the circulating fluid. In normal cases, it can be calculated using equations (6), (7) and (8).

Cichong Liu
400079
cichong@aalto.fi

For turbulent flow:

$$\mathrm{Nu} = 0.023\mathrm{Re}^{0.8}\,\mathrm{Pr}^{1/3}\left(\frac{\mu}{\mu_w}\right)^{0.14} \quad (\mathrm{Re} > 10000) \quad (6)$$

For slightly turbulent flow:

$$\mathrm{Nu} = 0.116\left(\mathrm{Re}^{\frac{2}{3}} - 125\right)\mathrm{Pr}^{1/3}\left[1 + \left(\frac{d_i}{l}\right)^{\frac{2}{3}}\right]\left(\frac{\mu}{\mu_w}\right)^{0.14} \quad (2200 < Re < 10000) \quad (7)$$

For laminar flow:

$$\mathrm{Nu} = 1.86\mathrm{Re}^{\frac{1}{3}}\mathrm{Pr}^{\frac{1}{3}}\left(\frac{d_i}{l}\right)^{\frac{1}{3}}\left(\frac{\mu}{\mu_w}\right)^{0.14} \quad (\mathrm{Re} < 2200) \quad (8)$$

However, in 2-D model, the heat transfer is considered only under steady state condition and in this model, the axial heat transfer is not taken into account in which case T_{f1}=T_{f2}=T_f is assumed. While in reality, the temperatures of the fluid circulating through different legs of U-tubes are different.

In quasi-three-dimensional model which was proposed by Zeng et al. in 2003, the effects of up-flow and down-flow are taken into consideration by building the energy equilibrium equations for both flows as shown in equation (9)

$$\left.\begin{aligned} -\dot{m}c\frac{dT_{f1}}{dz} &= \frac{T_{f1} - T_b}{R_{11}} + \frac{T_{f1} - T_{f2}}{R_{12}} \\ \dot{m}c\frac{dT_{f2}}{dz} &= \frac{T_{f2} - T_b}{R_{22}} + \frac{T_{f2} - T_{f1}}{R_{12}} \end{aligned}\right\} \quad (0 \le z \le H) \quad (9)$$

$\dot{m}$ represents the mass flow rate inside the U-tube and c represents the specific heat capacity of the circulating fluid.

Two boundary conditions are applied in order to solve the equations:

$$\left.\begin{aligned} z = 0, T_{f1} &= T_{in} \\ z = H, T_{f2} &= T_{exit} \end{aligned}\right\} \quad (10)$$

T_{f1}, T_{f2} represent the fluid temperatures inside two legs of U-tubes, T_{in} and T_{exit} represent the entering and exiting fluid temperature from the U-tube and T_b represents the borehole wall temperature.

By applying Laplace transformation to the above equation, solutions of the entering and exiting temperatures of the circulating fluid can be found from equation (11) and (12).

Cichong Liu
400079
cichong@aalto.fi

$$\theta(Z) = \cosh(\beta Z) - \frac{1}{\sqrt{1-P^2}}\left[1 - P\frac{\cosh(\beta) - \sqrt{\frac{1-P}{1+P}} * \sinh(\beta Z)}{\cosh(\beta) + \sqrt{\frac{1-P}{1+P}} * \sinh(\beta)}\right] \cdot \sinh(\beta Z) \quad (11)$$

$$\theta(Z) = \frac{\cosh(\beta) - \sqrt{\frac{1-P}{1+P}} * \sinh(\beta)}{\cosh(\beta) + \sqrt{\frac{1-P}{1+P}} * \sinh(\beta)} \cosh(\beta Z) + \frac{1}{\sqrt{1-P^2}}\left[\frac{\cosh(\beta) - \sqrt{\frac{1-P}{1+P}} * \sinh(\beta)}{\cosh(\beta) + \sqrt{\frac{1-P}{1+P}} * \sinh(\beta)} - P\right] \cdot \sinh(\beta Z) \quad (12)$$

$$\theta = \frac{T_f(z) - T_b}{T_{in} - T_b}, Z = \frac{z}{H}, P = \frac{R_{11}}{R_{12}}$$

$$\beta = \frac{H}{\dot{m}c\sqrt{(R_{11} + R_{12})(R_{11} - R_{12})}}$$

Cichong Liu
400079
cichong@aalto.fi

2.2 Matlab programming

As illustrated in previous chapters, the main function of the new system is to store the waste heat during summer time and use it during winter. Thus it is reasonable to divide the whole year into two parts: summer (non-heating periods) and winter (heating periods). In this case, from May to September will be summer time (total 3762 hours), no space heating required while the other months will be winter time and space heating is required.

To simplify the program, firstly, a rearrangement is assigned to the known hourly data. The new data is displayed in a matrix Q_{heat} in the order of May to September, October to December and January to April and in this order, a time interval 1-3672 represents summer time and 3673-8671 represents winter time.

A complete heat transfer model of the borehole thermal energy storage system is built by connecting the models of the heat transfer outside boreholes with heat transfer inside boreholes. As illustrated above, the finite line-source model (the heat transfer model outside boreholes) was used to estimate the temperature of ground by assuming the borehole as a finite line source, thus it is reasonable to assume while $r=r_b$ (borehole wall radius), the ground temperature T calculated using equation (1) is the borehole wall temperature T_b. Figure 13 shows calculated results of borehole wall temperatures at different depth with varying heating rate of the boreholes after 30 days. The results are calculated based on the following assumptions: the length of the borehole is H=100 m, the radius of the borehole is r_b = 0.057 m, the initial temperature of the ground is 5 degree, the thermal conductivity of the ground is 3 W/mK and the thermal diffusivity of the ground is assumed to be $1.43 \cdot 10^{-6}$ m^2/s (Lanini et al., 2014).

Cichong Liu
400079
cichong@aalto.fi

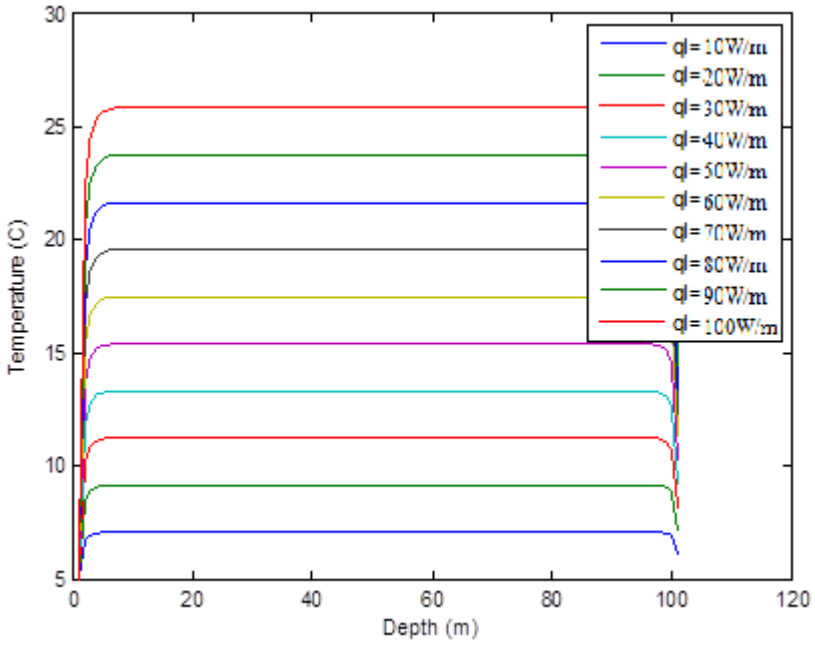

Figure 13. Borehole wall temperature variation with depth and heating rate

At the depth of 0 (the surface of the ground), temperatures is 5 degree Celsius because of the previous assumed boundary condition. And at the depth of 100 m, at the bottom of the borehole, the temperature also has a rapid drop due to a large heat transfer in the borehole axis direction to the deeper ground. Despite of two ends of the borehole, the borehole wall temperature remains constant along the vertical distance from the surface. Thus it is reasonable to assume the borehole wall temperature to be the temperature at $z = \frac{1}{2}H$.

Observed from the figure 13, the heating rate per length q_l has a large influence on the borehole wall temperatures and q_l can be calculated from the following equation:

$$q_l = \frac{(T_{in} - T_{exit})\dot{m}c}{H} \quad (13)$$

In equation (13), T_{in}, T_{exit} represent the entering and exiting U-tube temperatures of the circulating fluid which needed to be calculated from Zeng's quasi-three-dimensional model (heat transfer model outside boreholes) using equations (11) and (12) at z=0. Thus an iterating process is needed between these two models in order to obtain an appropriate q_l value.

Cichong Liu
400079
cichong@aalto.fi

For purpose of analyzing the influences of mass flow rates exerting on the borehole heat transfer behaviors, five scenarios were established based on the same borehole heat exchanger which is a typical construction example for boreholes and the construction details are listed in Table 3. The circulating fluid inlet temperatures are assumed to be 60 (Same as the hot water supplying temperature) in summer time ($T_{insummer}$) and 2 (Mean seawater temperature during the winter (Seatemperature, 2014)) ($T_{inwinter}$) in winter time as displayed in Table 3. And the circulating fluid mass flow rates for different scenarios can be found in Table 4.

Table 3. Basic sets-up for borehole heat exchanger

r_{ext} (m)	0.016	T_{in_summer} (˚C)	60
r_{int} (m)	0.013	T_{in_winter} (˚C)	2
D (m)	0.0285	k_{ground} (W/mK)	3
H (m)	100	k_U (W/mK)	0.6
r_b (m)	0.057	k_b (W/mK)	1.5
T_o (˚C)	5		

Table 4. Circulating fluid mass flow rates for different scenarios

Scenario No.	**0**	**1**	**2**	**3**	**4**
Mass flow rates in summer (kg/s)	0.5	0.1	1	0.5	0.5
Mass flow rates in winter (kg/s)	0.5	0.5	0.5	0.1	1

2.2.1 Baseline Scenario (Scenario 0)

2.2.1.1 Summer time (Non-heating periods)

During summer time, the iterating procedure is relatively simple and the heating rate q_l will only varies with summer day i. The iterating procedure is presented in Flow Chart 1. To be noticed, Zeng's model calculates only the instant temperature which means the exiting temperature varies every second resulting in a varying heating rate per length (q_l), thus in the iterating procedure, it is necessary to calculate the mean exiting temperature and mean heating rate per length during the assumed heating

Cichong Liu
400079
cichong@aalto.fi

period. And since q_l doesn't vary a lot within a day, to save the computation procedure, the mean exiting temperature and mean heating rate per length is averaged based on daily results.

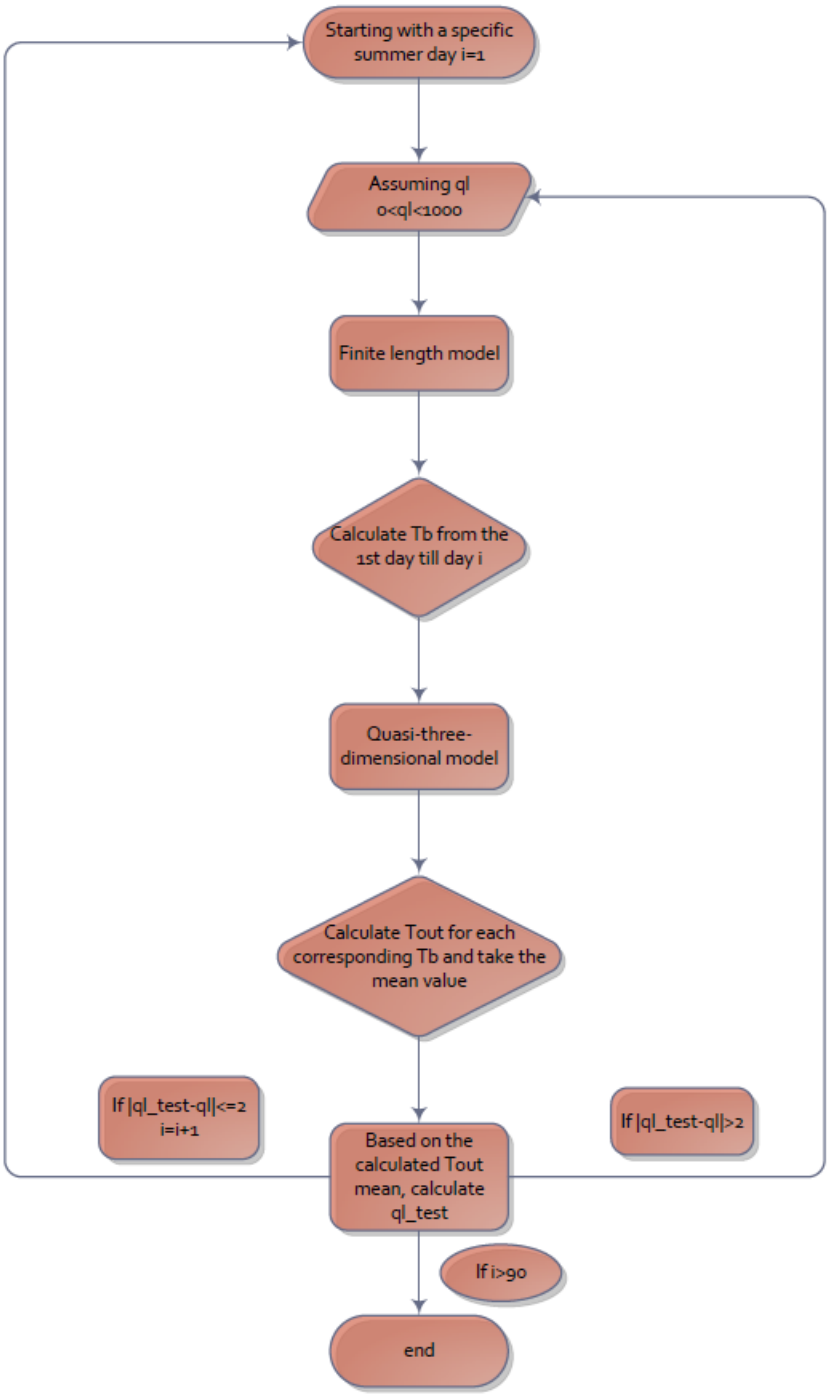

Flow Chart 1. Iterating procedure for summer time

Cichong Liu
400079
cichong@aalto.fi

Figure 14 shows the results how the mean heating rate per length and mean exiting fluid temperature varies with time for baseline scenario.

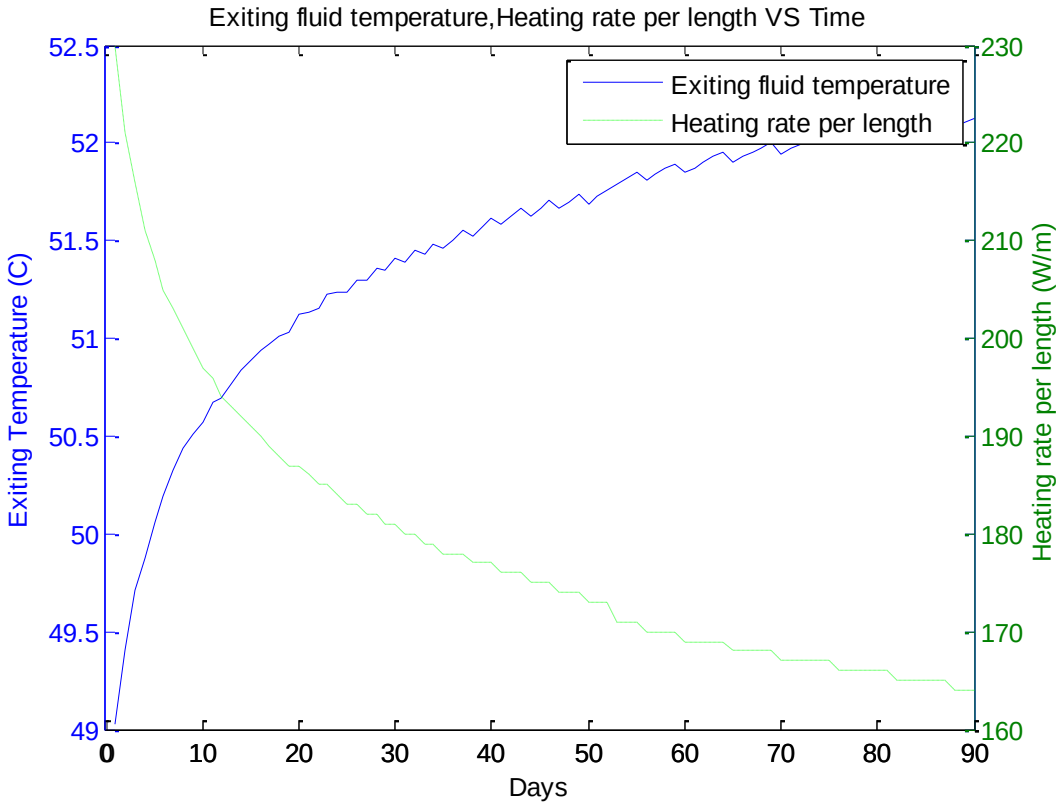

Figure 14. Mean exiting fluid temperature, Mean heating rate per length V.S. Time

As Figure 14 shows, the mean exiting fluid temperature increases and the heating rate per length decreases with time. It is quite rational because while the temperature of the soil increases with time, it slows down the heat transfer procedure which is the cause of the increase in the exiting fluid temperature and the decrease in the heating rate per length. The small drops (less than 0.1 degree) shown on the figure are due to the program convenience made in the Matlab program. In order to activate the iterating procedure, the tested q_l is set to be an integral number which has small difference from the real case resulting in some negligible errors (<0.1˚C) in the results.

With the help of Excel, it is possible to fit functions for heating rate per length and exiting temperature with the variable time. The fitting of the curves is presented in equation 14. Equation (14) shows the mean exiting fluid temperature as a function of time and Equation (15) shows the mean heating rate per length as a function of time.

Cichong Liu
400079
cichong@aalto.fi

$$T_{exit}\,[°C] = 0.7138 \ln\left(\frac{Sh\,[h]}{24}\right) + 48.946 \quad (14)$$

$$q_l[W/m] = 236.6 * \left(\frac{Sh\,[h]}{24}\right)^{-0.081} \quad (15)$$

where Sh represents time in hours [h] ranging from 1 to 3672.

Figure 15 below shows the temperature variation of the ground after 1, 30, 60, 90 days respectively at the reference depth of z=1/2*H.

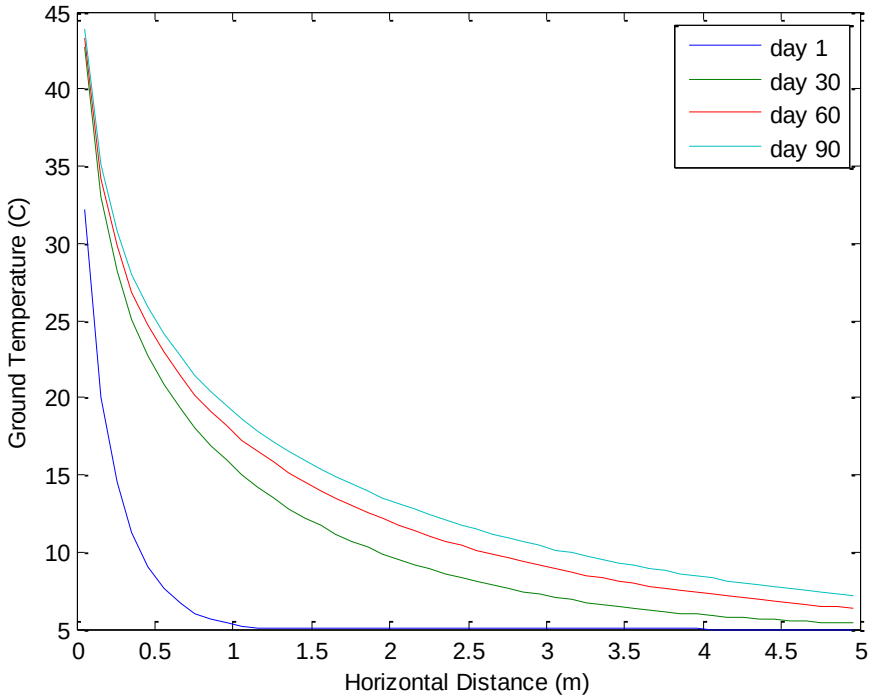

Figure 15. Ground temperature distribution around the borehole

Observed from the figure above, outside the borehole 5 m away, the maximum ground temperature doesn't exceed 8 degrees and according to Gultekin et al. (2014) and Desideri et al. (2011)'s studies, the optimal distance between borehole heat exchangers is in the range of 8-10 meters away so it is reasonable to assume that borehole heat exchangers don't influence each other's behavior.

2.2.1.2 Winter time (Heating periods)

The behaviors of the borehole heat exchangers during summer time (charging process) are analyzed in previous section and in winter, the basic models are the same. However, unlike the charging process, the ground temperature initially is non-uniformly distributed in the beginning of

Cichong Liu
400079
cichong@aalto.fi

winter time. After the charging process, the ground temperature is distributed in a degrading trend from the center of borehole as shown in Figure 15. Besides, in the winter time, the borehole heat exchanger is a heat sink instead of a heat source, thus the heating rate per length will be a negative value which is regarded as cooling rate per length in the following discussion.

To fit in the heat transfer model, the ground temperature is assumed to have an initial value $T_{owinter}$. As discussed in previous chapter, the mean exiting fluid temperature and the cooling rate per length are connected to the heat transfer outside borehole by the borehole wall temperature, thus it is not reasonable to assume an initial ground temperature by averaging the ground temperature for 5m area which would be too low to predict accurate values. What is done here is dividing the 5m area to two different parts: 0-2m part and 2m-5m part and taking the mean temperature for these two areas separately as shown in figure 16. An initial temperature $T_{owinter}$ was assumed according to the mean temperature of the first 2m area part. This assumption was made based on two facts: As shown in the summer case, the temperature of the ground in the area 2m-5m part doesn't vary a lot with the heat transfer procedure and the same can be extended to winter time. Additionally, for long time period, the mean ground temperature will be quite near the mean ground temperature of first 2m part.

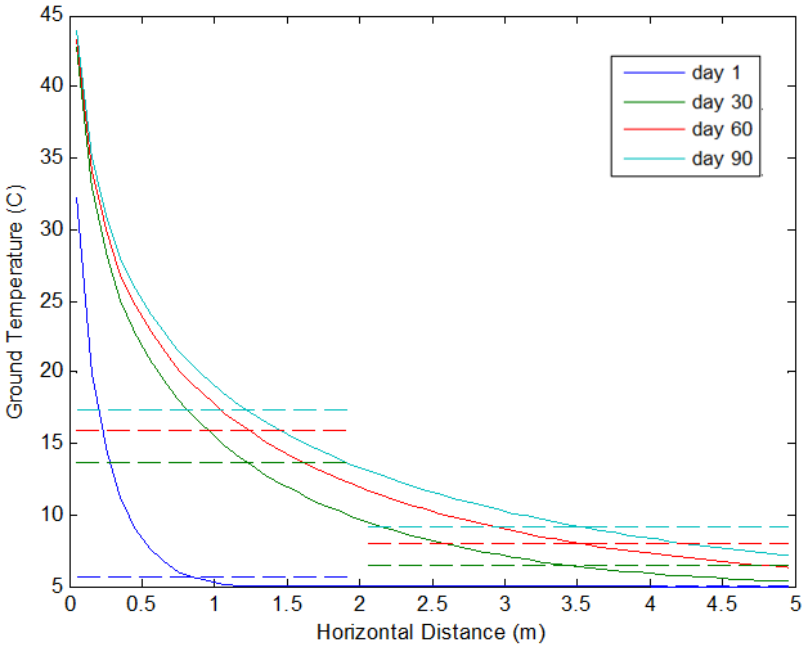

Figure 16. Mean Average temperature of the first 2m part and the second 3m part

Cichong Liu
400079
cichong@aalto.fi

Similar to the summer time, an iterating process as shown in Flow Chart 2 is required to find a suitable heating rate per length in order to predict the heat transfer in the winter time and the procedure can be found in the following flow chart. To be different from the summer process, the cooling rate per length is a function of both total charging time in summer and discharging time during winter since in the function, initial ground temperature is a varied factor which is influenced by the total charging time in summer. And so is the mean exiting fluid temperature from the U-tube.

Cichong Liu
400079
cichong@aalto.fi

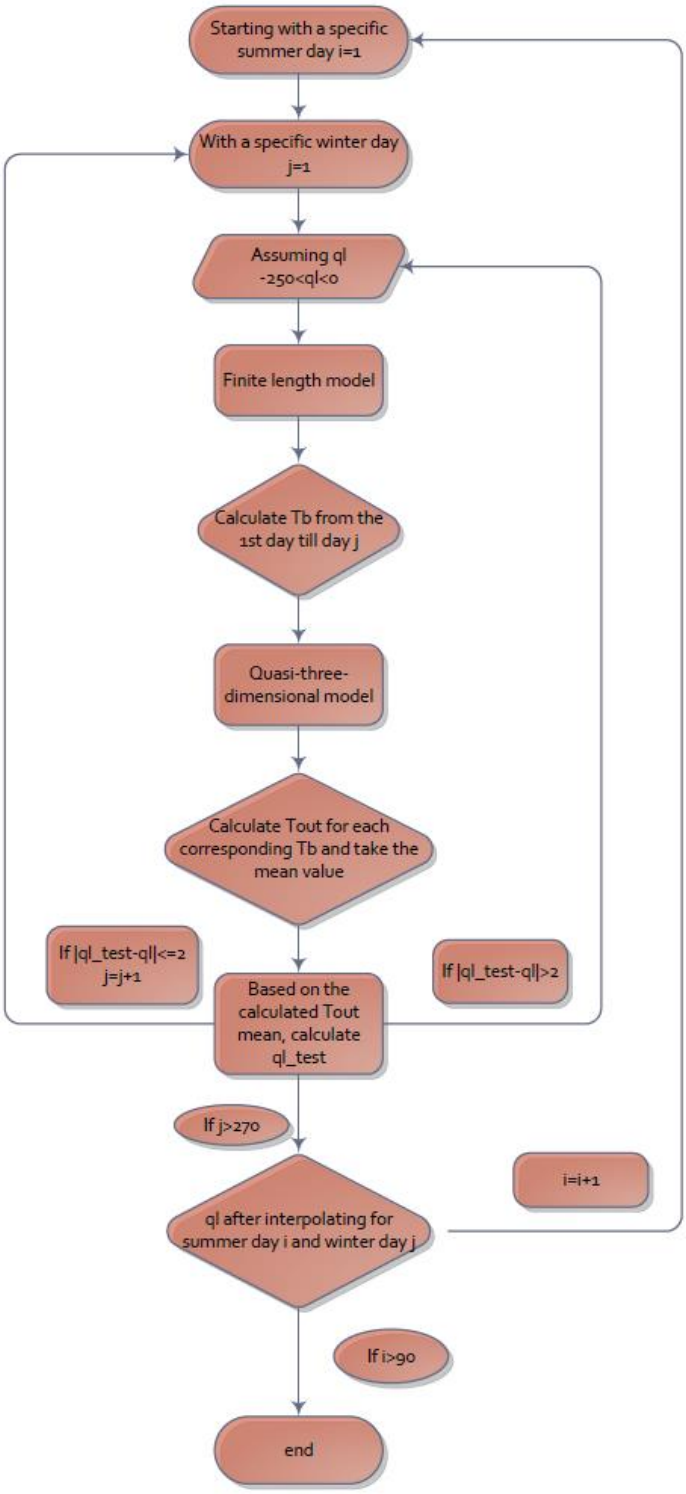

Flow Chart 2

Cichong Liu
400079
cichong@aalto.fi

The calculated results for the cooling rate per length q_l during winter time can be found in the Table 5 below, and a minus sign indicates a heat transfer flow from the soil to the borehole heat exchanger.

Table 5. Cooling rate per length as a function of summer and winter time (SD stands for Summer Day and WD stands for Winter Day)

	SD1	SD10	SD20	SD30	SD40	SD50	SD60	SD70	SD80	SD90
WD1	-16	-34	-43	-49	-53	-56	-58	-61	-63	-64
WD2	-15	-32	-42	-47	-51	-54	-56	-58	-60	-61
WD3	-15	-31	-40	-46	-50	-53	-54	-57	-59	-60
WD4	-14	-31	-40	-45	-49	-52	-54	-56	-57	-59
WD5	-14	-30	-39	-44	-48	-51	-53	-55	-57	-58
WD6	-14	-30	-39	-44	-48	-50	-52	-54	-56	-57
WD7	-14	-30	-38	-43	-47	-50	-52	-54	-55	-57
WD8	-14	-30	-38	-43	-47	-49	-51	-53	-55	-56
WD9	-14	-29	-38	-43	-46	-49	-51	-53	-54	-56
WD10	-14	-29	-37	-42	-46	-49	-50	-52	-54	-55
WD15	-13	-28	-36	-41	-45	-47	-49	-51	-53	-54
WD20	-13	-28	-36	-40	-44	-46	-48	-50	-51	-53
WD25	-13	-27	-35	-40	-43	-46	-47	-49	-51	-52
WD30	-13	-27	-35	-39	-43	-45	-47	-48	-50	-51
WD40	-12	-26	-34	-38	-42	-44	-46	-47	-49	-50
WD50	-12	-26	-33	-38	-41	-43	-45	-46	-48	-49
WD60	-12	-26	-33	-37	-40	-43	-44	-46	-47	-48
WD80	-12	-25	-32	-36	-39	-42	-43	-45	-46	-47
WD100	-12	-24	-31	-36	-39	-41	-42	-44	-45	-46
WD120	-11	-24	-31	-35	-38	-40	-42	-43	-45	-46
WD150	-11	-24	-30	-35	-37	-40	-41	-42	-44	-45
WD180	-11	-23	-30	-34	-37	-39	-40	-42	-43	-44
WD210	-11	-23	-30	-34	-36	-38	-40	-41	-43	-44
WD240	-11	-23	-29	-33	-36	-38	-39	-41	-42	-43
WD270	-11	-23	-29	-33	-36	-38	-39	-40	-42	-43

Table 6 shows mean ground temperature values for the first 2m part after winter discharging period.

Table 6. Mean ground temperature for the first 2m part

	SD1	SD10	SD20	SD30	SD40	SD50	SD60	SD70	SD80	SD90
WD1	5.58	9.86	12.17	13.57	14.57	15.28	15.79	16.29	16.78	17.12
WD10	5.27	9.22	11.36	12.65	13.56	14.20	14.69	15.15	15.59	15.91
WD40	4.97	8.52	10.43	11.62	12.41	13.02	13.42	13.88	14.26	14.55
WD90	4.73	8.08	9.89	11.01	11.79	12.36	12.73	13.16	13.50	13.77

Cichong Liu
400079
cichong@aalto.fi

WD150	4.66	7.84	9.65	10.63	11.46	11.91	12.34	12.76	13.08	13.33
WD210	4.56	7.73	9.39	10.42	11.23	11.76	12.08	12.49	12.79	13.04
WD270	4.49	7.58	9.30	10.30	11.00	11.51	11.92	12.33	12.61	12.85

Table 7 below shows the exiting fluid temperature for some selected conditions.

Table 7. Mean exiting fluid temperature in winter time as a function of summer and winter time (SD stands for Summer Day and WD stands for Winter Day)

	SD1	SD10	SD20	SD30	SD40	SD50	SD60	SD70	SD80	SD90
WD1	2.72	3.58	4.08	4.36	4.57	4.71	4.82	4.88	4.98	5.07
WD2	2.72	3.57	3.98	4.29	4.48	4.61	4.72	4.82	4.91	4.94
WD3	2.68	3.48	3.93	4.22	4.41	4.53	4.63	4.72	4.81	4.89
WD4	2.71	3.48	3.90	4.18	4.36	4.48	4.57	4.66	4.74	4.82
WD5	2.69	3.43	3.89	4.11	4.33	4.45	4.54	4.62	4.70	4.78
WD6	2.67	3.44	3.84	4.10	4.27	4.43	4.52	4.60	4.68	4.76
WD7	2.65	3.40	3.85	4.05	4.27	4.37	4.45	4.54	4.67	4.69
WD8	2.64	3.43	3.81	4.06	4.22	4.38	4.46	4.54	4.61	4.68
WD9	2.63	3.40	3.77	4.02	4.23	4.33	4.41	4.49	4.62	4.63
WD10	2.61	3.38	3.80	4.04	4.19	4.28	4.42	4.50	4.57	4.64
WD15	2.61	3.36	3.75	3.98	4.12	4.24	4.34	4.44	4.51	4.58
WD20	2.60	3.34	3.71	3.92	4.04	4.19	4.25	4.38	4.44	4.51
WD25	2.58	3.29	3.68	3.88	4.03	4.14	4.24	4.33	4.38	4.45
WD30	2.55	3.24	3.65	3.84	4.02	4.09	4.22	4.27	4.32	4.38
WD40	2.60	3.24	3.56	3.81	3.98	4.04	4.16	4.21	4.33	4.32
WD50	2.57	3.19	3.56	3.81	3.89	4.02	4.14	4.19	4.23	4.29
WD60	2.55	3.22	3.50	3.74	3.90	4.02	4.07	4.19	4.22	4.28
WD80	2.52	3.15	3.49	3.72	3.87	3.99	4.03	4.14	4.17	4.22
WD100	2.50	3.18	3.51	3.64	3.78	3.90	4.01	4.05	4.15	4.20
WD120	2.56	3.14	3.45	3.66	3.80	3.91	3.94	4.05	4.07	4.12
WD150	2.54	3.09	3.47	3.59	3.80	3.91	3.93	4.05	4.06	4.11
WD180	2.52	3.13	3.42	3.61	3.74	3.84	3.91	3.97	4.07	4.12
WD210	2.50	3.10	3.37	3.56	3.68	3.78	3.89	4.00	4.01	4.05
WD240	2.49	3.07	3.43	3.61	3.72	3.82	3.84	3.94	4.04	4.08
WD270	2.48	3.04	3.39	3.57	3.68	3.77	3.88	3.89	3.99	4.03

The next step is to develop a function to predict the cooling rate per length with variables of winter time and summer time and this has been done in two steps.

Firstly, for each summer day, the cooling rate per length will be a function of winter time as shown in equation (16), a and b are assumed constants.

$$q_l[\mathrm{W/m}] = a \ln\left(\frac{\mathrm{Wh\ [h]} - 3672}{24}\right) + b \quad (16)$$

Cichong Liu
400079
cichong@aalto.fi

The next step is plotting all a and b values versus summer time as shown in figure 17, it is easy to conclude that a and b are functions of summer time. With the help of Matlab curve fitting tool, the functions of a and b with a variable summer time are developed as shown in equation (17) and (18).

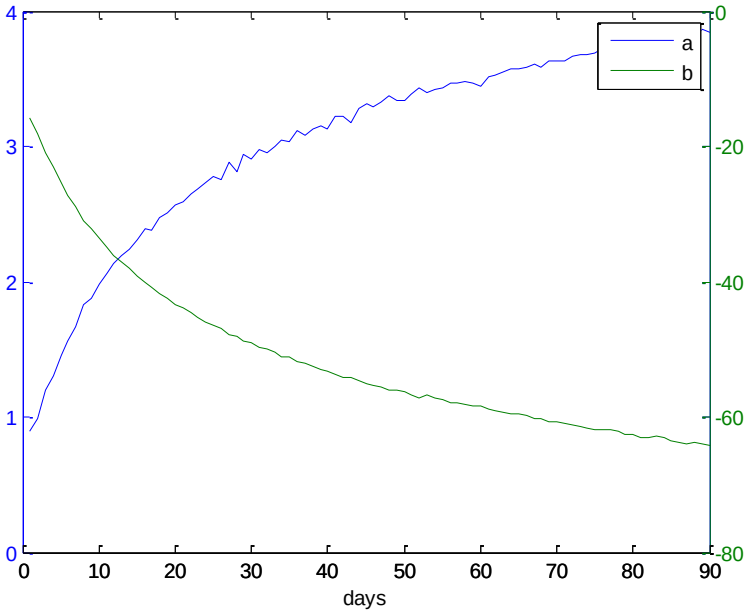

Figure 17. a and b vs. summer time

$$a = 0.7839 \ln\left(\frac{\text{Sh [h]}}{24}\right) + 0.2781 \quad (17)$$

$$b = -12.7809 \ln\left(\frac{\text{Sh [h]}}{24}\right) - 6.0357 \quad (18)$$

By combining equations (16), (17) and (18), it is possible to deduce the model for predicting the cooling rate per length as shown in equation (19).

$$q_l[\text{W/m}] = \left(0.7839 \ln\left(\frac{\text{Sh [h]}}{24}\right) + 0.2781\right) \cdot \ln\left(\frac{\text{Wh [h]} - 3672}{24}\right) - 12.7809 \ln\left(\frac{\text{Sh [h]}}{24}\right) - 6.0357 \quad (19)$$

Where Sh represents the summer hour [h], in the range of 1 to 3762 and Wh represents the winter hour [h], in the range of 3673 to 8761.

Same discipline applied to the exiting fluid temperature, the model for predicting the exiting fluid temperature is built as shown in equation (20).

Cichong Liu
400079
cichong@aalto.fi

$$T_{exit}\,[℃] = \left(-0.0375\ln\left(\frac{Sh\,[h]}{24}\right) - 0.0179\right)\cdot\ln\left(\frac{Wh\,[h] - 3672}{24}\right) + 0.6106\ln\left(\frac{Sh\,[h]}{24}\right) + 2.2929 \quad (20)$$

Another thing needed to be noticed is the cooling rate per length in winter time, which is not as large as the heating rate in summer time for the same borehole heat exchanger. This means it may take longer time in winter to take same amount of heat charged into ground out of the ground during summer time.

2.2.2 Other scenarios analysis

Mass flow rate of the circulating fluid can be a key parameter influencing the heat transfer of the borehole heat exchanger. As indicated in equation (5) and (9), the convective heat transfer rate and the mass flow rate itself both have significant effects on the heat transfer rate. The increase in mass flow rate will lead to an increase in the convective heat transfer which enhances the heat transfer between the borehole and the soil. Based on the equation (6), (7) and (8), the convective heat transfer coefficients can be calculated based on different mass flow rates of the circulating fluid as indicated in the following table (all the water properties are taken from Microelectronics Heat Transfer Laboratory (1997)).

Table 8. Convective heat transfer coefficients for different mass flow rates at different temperature conditions

	m=0.1 kg/s	**m=0.5 kg/s**	**m=1 kg/s**
h at 50 ˚C	853	3316	5773
h at 4 ˚C	540	2636	4589

Though an increase in the convective heat transfer rate will be observed if mass flow rate is increased, a larger mass flow rate will result in a smaller heating rate transfer per unit mass of the water and four different scenarios have been going through in order to discover the influences on the heat transfer brought by changing the mass flow rate conditions.

Table 9 displays the mass flow rates conditions of 4 different scenarios and corresponding predicted equations for heating/cooling rate per length and exiting fluid temperatures in summer and winter time by applying the same calculation methods as baseline scenario.

Cichong Liu
400079
cichong@aalto.fi

Table 9. Mass flow rates of 4 different scenarios and corresponding predicted equations for heat/cooling rate per length and exiting fluid temperature

Scenario		Mass flow rates (kg/s)	Heating/Cooling rate per length (W/m) Exiting Fluid Temperature (°C)
1	Summer	m=0.1	$q_l[W/m] = 145.34\left(\frac{Sh\,[h]}{24}\right)^{-0.053}$ $T_{exit}[°C] = 1.5631\ln\left(\frac{Sh\,[h]}{24}\right) + 25.6514$
	Winter	m=0.5	$q_l[W/m] = \left(0.5566\ln\left(\frac{Sh\,[h]}{24}\right) + 0.3375\right)\cdot\ln\left(\frac{Wh\,[h]-3672}{24}\right) - 9.1006\ln\left(\frac{Sh\,[h]}{24}\right) - 6.9330$ $T_{exit}[°C] = \left(-0.0269\ln\left(\frac{Sh\,[h]}{24}\right) - 0.0201\right)\cdot\ln\left(\frac{Wh\,[h]-3672}{24}\right) + 0.4357\ln\left(\frac{Sh\,[h]}{24}\right) + 2.3323$
2	Summer	m=1	$q_l[W/m] = 248.55\left(\frac{Sh\,[h]}{24}\right)^{-0.082}$ $T_{exit}[°C] = 0.3865\ln\left(\frac{Sh\,[h]}{24}\right) + 54.1685$
	Winter	m=0.5	$q_l[W/m] = \left(0.8150\ln\left(\frac{Sh\,[h]}{24}\right) + 0.2713\right)\cdot\ln\left(\frac{Wh\,[h]-3672}{24}\right) - 13.3214\ln\left(\frac{Sh\,[h]}{24}\right) - 4.7938$ $T_{exit}[°C] = \left(-0.0393\ln\left(\frac{Sh\,[h]}{24}\right) - 4.7938\right)\cdot\ln\left(\frac{Wh\,[h]-3672}{24}\right) + 0.6382\ln\left(\frac{Sh\,[h]}{24}\right) + 2.2746$
3	Summer	m=0.5	Same as Baseline Scenario
	Winter	m=0.1	$q_l[W/m] = \left(0.3537\ln\left(\frac{Sh\,[h]}{24}\right) + 0.0892\right)\cdot\ln\left(\frac{Wh\,[h]-3672}{24}\right) - 7.9872\ln\left(\frac{Sh\,[h]}{24}\right) - 2.56$ $T_{exit}[°C] = \left(-0.0842\ln\left(\frac{Sh\,[h]}{24}\right) - 0.0325\right)\cdot\ln\left(\frac{Wh\,[h]-3672}{24}\right) + 1.9070\ln\left(\frac{Sh\,[h]}{24}\right) + 2.9290$
4	Summer	m=0.5	Same as Baseline Scenario
	Winter	m=1	$q_l[W/m] = \left(0.8639\ln\left(\frac{Sh[h]}{24}\right) + 0.3198\right)\cdot\ln\left(\frac{Wh\,[h]-3672}{24}\right) - 13.5712\ln\left(\frac{Sh\,[h]}{24}\right) - 5.4638$ $T_{exit}[°C] = \left(-0.0208\ln\left(\frac{Sh[h]}{24}\right) - 0.0099\right)\cdot\ln\left(\frac{Wh[h]-3672}{24}\right) + 0.3246\ln\left(\frac{Sh[h]}{24}\right) + 2.1541$

More detailed results for these 4 scenarios can be found in Appendix.

Cichong Liu
400079
cichong@aalto.fi

2.2.3 Scenarios comparison

By comparing results among these five scenarios, it is possible to find out that an increase in the mass flow rate in summer time will bring a great increase in the heating rate and an obvious increase in the exiting fluid temperature. Meanwhile the ground will be heated up to a higher degree which indicates that a greater amount of heat will be transferred to the soil via borehole heat exchanger and vice versa. Figure 18 shows heating rate, exiting fluid temperature and ground temperature comparisons among scenario 0, 1 and 2 for summer time.

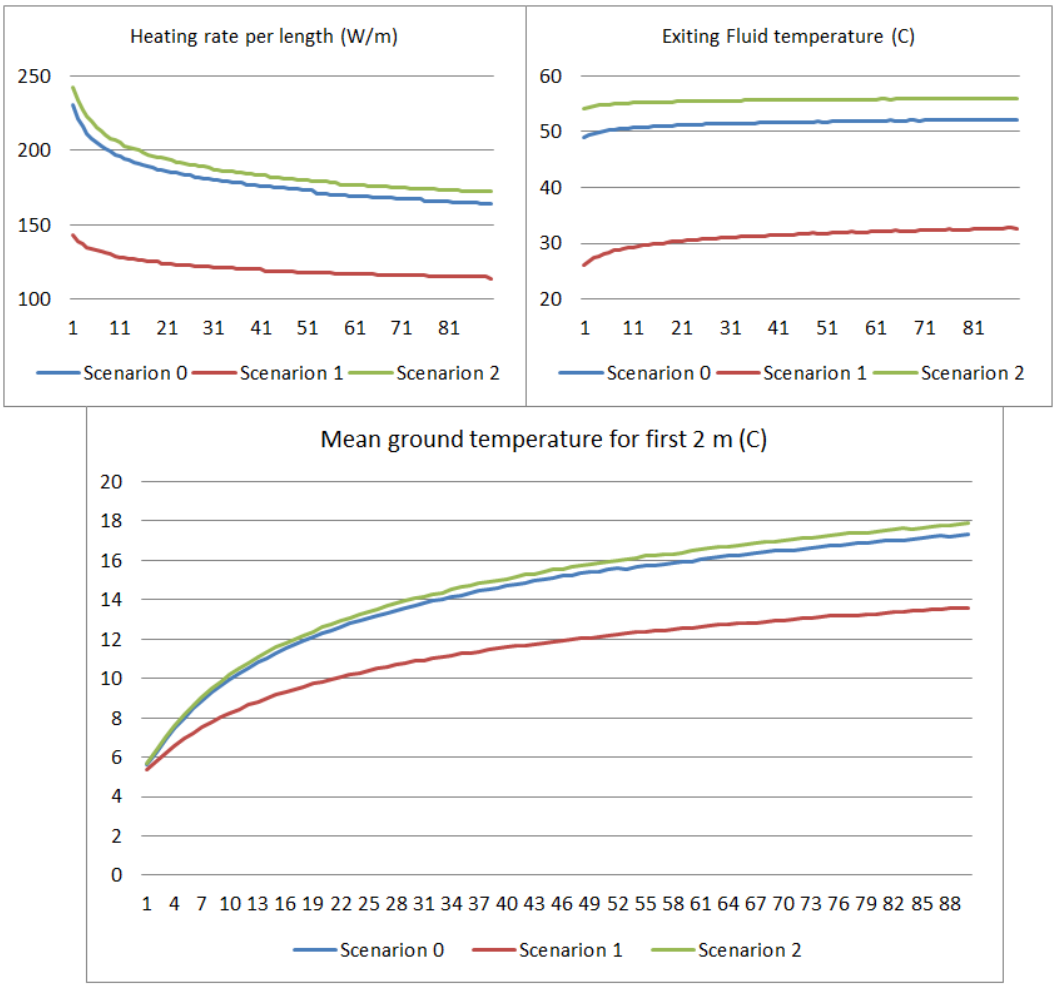

Figure 18. Comparisons of scenarios 0,1 and 2 in summer time

However, a decreasing mass flow rate in summer time will bring a decrease in the exiting fluid temperature in winter time and a decreasing cooling rate (absolute value), though it doesn't vary a lot.

Cichong Liu
400079
cichong@aalto.fi

Table 10 and Table 11 show the exiting fluid temperature and cooling rate per length for selected days in Scenarios 0, 1 and 2.

Table 10. Cooling rate per length (W/m) comparisons among scenario 0, 1 and 2

	Scenario 0	Scenario 1	Scenario 2
SD 30 WD 90	-36	-28	-36
SD 30 WD 180	-34	-26	-35
SD 30 WD 270	-33	-25	-33
SD 60 WD 90	-43	-33	-44
SD 60 WD 180	-40	-31	-41
SD 60 WD 270	-39	-30	-39
SD 90 WD 90	-48	-36	-48
SD 90 WD 180	-44	-34	-45
SD 90 WD 270	-43	-32	-43

Table 11. Exiting fluid temperature (˚C) comparisons among scenario 0, 1 and 2

	Scenario 0	Scenario 1	Scenario 2
SD 30 WD 90	3.68	3.3	3.74
SD 30 WD 180	3.61	3.09	3.65
SD 30 WD 270	3.57	2.98	3.61
SD 60 WD 90	3.96	3.51	4.1
SD 60 WD 180	3.91	3.44	3.97
SD 60 WD 270	3.88	3.41	3.9
SD 90 WD 90	4.21	3.66	4.29
SD 90 WD 180	4.12	3.55	4.17
SD 90 WD 270	4.03	3.51	4.08

Cichong Liu
400079
cichong@aalto.fi

While the summer mass flow rate was kept constant and the winter mass flow was adjusted, there will be no effects on the heat transfer model in summer time. However, the effects of mass flow rate on the heat transfer model during winter time are enormous. Table 12 and 13 show the comparisons of the cooling rate per length and exiting fluid temperature among scenario 0, 3 and 4. With the increase in mass flow rate in winter, a small increase in cooling rate per length can be observed but it will result in a large decrease in the exiting fluid temperature and vice versa.

Table 12. Cooling rate per length (W/m) comparisons among scenario 0, 3 and 4

	Scenario 0	Scenario 3	Scenario 4
SD 30 WD 90	-36	-21	-37
SD 30 WD 180	-34	-20	-35
SD 30 WD 270	-33	-20	-33
SD 60 WD 90	-43	-29	-44
SD 60 WD 180	-40	-27	-41
SD 60 WD 270	-39	-27	-40
SD 90 WD 90	-48	-31	-49
SD 90 WD 180	-44	-30	-45
SD 90 WD 270	-43	-29	-43

Table 13. Exiting fluid temperature (˚C) comparisons among scenario 0, 3 and 4

	Scenario 0	Scenario 3	Scenario 4
SD 30 WD 90	3.68	7.88	2.89
SD 30 WD 180	3.61	7.7	2.81
SD 30 WD 270	3.57	7.69	2.79
SD 60 WD 90	3.96	9.08	3.06
SD 60 WD 180	3.91	8.87	3.01
SD 60 WD 270	3.88	8.61	2.96

Cichong Liu
400079
cichong@aalto.fi

SD 90 WD 90	4.21	9.74	3.17
SD 90 WD 180	4.12	9.45	3.1
SD 90 WD 270	4.03	9.38	3.05

Cichong Liu
400079
cichong@aalto.fi

3 The analysis of heat pump connected with underground thermal energy storage

Figure 21 shows the working principle of a normal heat pump which is a reversed Carnot thermodynamic cycle. In this project, the heat pump is used in winter to increase the temperature level of the water delivered by the borehole heat exchanger to the desired temperature level of space heating. The evaporator side is connected with the borehole heat exchanger while the condenser side is connected with space heating networks.

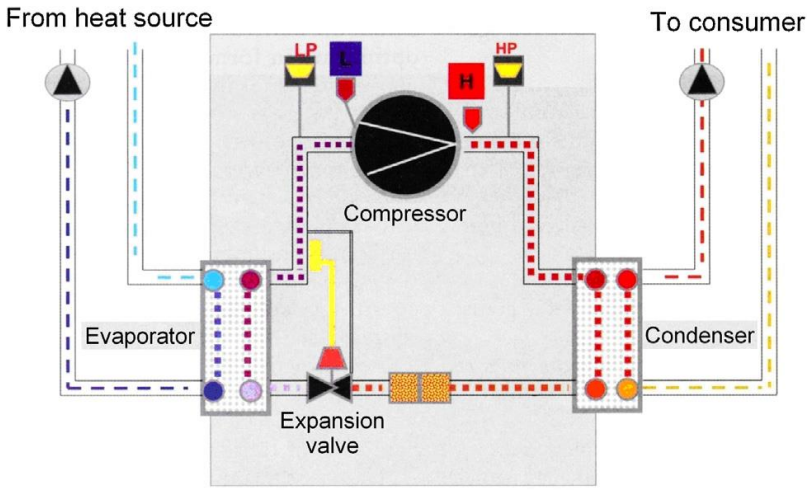

Figure 19. Heat pump working scheme (Sarbu & Sebarchievici, 2014)

The coefficient of performance (COP) of the heat pump is defined by a ratio between the useful thermal energy (Q_h) and power consumed in running the compressor (P) as shown in equation (21).

$$\mathrm{COP} = \frac{Q_h}{P} \quad (21)$$

Based on the Carnot principle, the ideal COP value of the heat pump can be estimated with known high temperature and low temperature levels as shown in equation (22).

$$\mathrm{COP}_{ideal} = \frac{T_h}{T_h - T_l} \quad (22)$$

where the units of temperatures are K

The evaporator side water temperature ranges from 2 to 12 degree as indicated from results above and the condenser side water temperature should reach the desired temperature level of space heating (in this case is 60 degree), thus the ideal COP ranges from 5.74 to 6.93.

Cichong Liu
400079
cichong@aalto.fi

In the real case, the COP will be smaller than the ideal COP value. As reported by Sanner et al.(2003), a maximum COP of existing ground source heat pumps is around 4.5 and their mean COP, regarded as 'Seasonal Performance Factor' during operation is lower, in the range of 3.0 to 3.8 only. Figure 22 shows the values of COP for brine/water heat pumps (as typically used heat pumps connected with borehole heat exchangers).

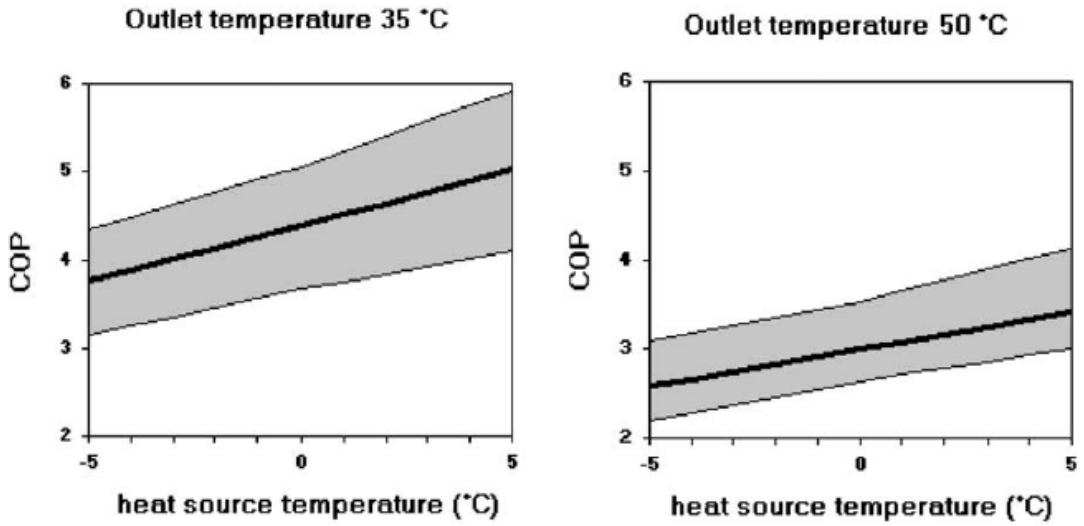

Figure 20. COP values for brine/water heat pumps connected with borehole heat exchangers (Sanner et al., 2003)

To simplify the program, the COP is assumed to be fixed for a range of exiting fluid temperatures. Based on figure 22, the corresponding COP values for different exiting fluid temperature ranges are assumed as listed in Table 14.

Table 14. Assumed COP Versus exiting fluid temperature

Exiting Fluid temperature intervals (°C)	COP
Under 2	2.8
2-4	3
4-6	3.3
6-8	3.6
8-10	3.9
10-12	4.2

Cichong Liu
400079
cichong@aalto.fi

4 Economic Analysis of the new system

Payback time of the new system is the key factor to evaluate if the underground thermal energy storage is worthy to be built. Based on the heat transfer analysis presented in previous sections and the general costs data as shown in Table 15, the payback time of five different scenarios are calculated and analyzed. The detailed methods of economic analysis are presented in the following section, taking baseline scenario as an example.

Table 15. Cost data

Summer heat cost (C_{summer} [€/MWh])	30
Winter heat cost ((C_{winter} [€/MWh])	110
Electricity cost ($C_{electricity}$ [€/MWh])	88

4.1 Baseline Scenario (Scenario 0)

4.1.1 Matlab programming

To compute in Matlab, the hourly heat demand data Q_{heat} of the community is divided into two matrixes $Q_{heat_{summer}}$ (= Q_{heat} (1:3762)) and $Q_{heat_{winter}}$ (= Q_{heat} (3763:8761)).

For optimizing the system getting the minimum payback time, there are three variables to control: charging hours in summer, discharging hours in winter and the number of borehole heat exchangers which is proportional to capacity of the new system.

The maximum heating demand during the whole year is 0.98 MW, thus the capacity of the CHP (producer) of this community assumed to be 1 MW and during the summer time, minimum heating demand (for hot water) is 4.48 kW.

In summer, the total money paid for the summer heat can be calculated using following equations:

$$\text{Extra costs in Summer} = \sum [\frac{C_{summer}}{10^6} * n_{used} * \dot{m} * c * (T_{supply} - T_{return})] \quad (23)$$

$$n_{used} = \frac{q_{summer}}{q_{l_{summer}} * H} \quad (24)$$

Cichong Liu
400079
cichong@aalto.fi

$$q_{summer} = \min\left(n * q_{l_{summer}} * H, 10^6 - Q_{heat_{summer}}\right) \quad (25)$$

Where n is the number of borehole heat exchangers being built, n_{used} is rounded based on the equation presented above and it is a 3762*1 matrix with each element representing the number of borehole heat exchanger used hourly during summer time, $\dot{m}$ represents the mass flow rate of one tube which is kept constant $\dot{m}$=0.5 kg/s for baseline scenario and varying with different scenarios (see Table 4), C_{summer} represents the cost of summer heat, $q_{lsummer}$ representing the heating rate per length in summer which is calculated based on equation (15) and q_{summer} is also a 3762*1 matrix with each element standing on heat capacity charged to the soil hourly.

q_{summer} represents the actual heat injected to the boreholes. It takes the minimum number of $q_{lsummer}$*n*H and (10^6-$Q_{heatsummer}$) in case of the capacity of the charged heat plus the heat demand in this hour exceeds 1 MW which is assumed to be the maximum output capacity from the producer. Here $q_{lsummer}$*n*H represents the heat flow which is limited by the heat transfer ability of U-tube heat exchangers. (10^6-$Q_{heatsummer}$) represents the heat flow delivered by the district heat producer minus the heat which is actually consumed in the buildings.

T_{supply} and T_{return} represent the supply and return temperatures of the district heating loops from the producers, in our case, 60 and 40 are assumed.

In winter, the total money saved from utilizing the stored heat from summer time can be calculated from following equations:

$$\text{Saved money in Winter} = \sum\left(q_{winter} * \frac{C_{winter}}{10^6} - q_{winter} * \frac{1}{COP} * \frac{C_{electricity}}{10^6}\right) \quad (26)$$

$$q_{winter} = \min\left(Q_{heat_{winter}}, q_{l_{winter}} * n * \frac{COP}{COP - 1} * H\right) \quad (27)$$

C_{winter} represents the cost of winter heat and $C_{electricity}$ represents the cost of electricity, $q_{lwinter}$ is calculated by applying equation (19) and q_{winter} takes the smaller number of $q_{lwinter}$*n*COP/(COP-1) and $Q_{heatwinter}$ in the case of the output heat is larger than the real heat demand required.

And the total profit made for one year will be:

$$\text{Money} = \text{Saved money in Winter} - \text{Extra cost in Summer} \quad (28)$$

Cichong Liu
400079
cichong@aalto.fi

The program is set to run for three loops corresponding to three control variables: number of boreholes installed (n), summer charging hours (SH) and winter discharging hours (WH) and the program will automatically pick up one largest profit for a corresponding n and record respective summer charging hours and winter discharging hours. The results for baseline scenario can be found in the following section.

4.1.2 Results

Table 16 below presents the profits made per year for baseline scenario where n indicates the number of boreholes to be built.

Table 16. Profits made per year for baseline scenario (€) for corresponding numbers of boreholes to be built

n	1	2	3	4	5	6	7	8	9	10
€	1.49E+03	2.98E+03	4.47E+03	5.96E+03	7.45E+03	8.94E+03	1.11E+04	1.19E+04	1.34E+04	1.49E+04
n	11	12	13	14	15	16	17	18	19	20
€	1.64E+04	1.78E+04	1.93E+04	2.14E+04	2.29E+04	2.38E+04	2.52E+04	2.67E+04	2.82E+04	2.96E+04
n	21	22	23	24	25	26	27	28	29	30
€	3.11E+04	3.26E+04	3.40E+04	3.55E+04	3.69E+04	3.84E+04	4.04E+04	4.19E+04	4.33E+04	4.47E+04
n	31	32	33	34	35	36	37	38	39	40
€	4.62E+04	4.70E+04	4.85E+04	4.99E+04	5.13E+04	5.28E+04	5.43E+04	5.58E+04	5.73E+04	5.87E+04
n	41	42	43	44	45	46	47	48	49	50
€	6.03E+04	6.18E+04	6.33E+04	6.48E+04	6.64E+04	6.80E+04	6.96E+04	7.12E+04	7.29E+04	7.46E+04

The profits made per year is increasing with the increase of the number of borehole heat exchangers which makes sense the larger amount of heat stored resulting in a larger profit.

Table 17 shows the corresponding summer charging hours and winter discharging hours for the largest profit.

Table 17. Corresponding summer charging hours and winter discharging hour for largest profit corresponding to different number of boreholes to be built

n	1	2	3	4	5	6	7	8	9	10
SH/ WH	473/ 8761	473/ 8761	473/ 8761	473/ 8761	473/ 8761	472/ 8761	553/ 8761	472/ 8761	472/ 8761	471/ 8761
n	11	12	13	14	15	16	17	18	19	20
SH/ WH	471/ 8761	470/ 8761	470/ 8761	469/ 8761	469/ 8761	469/ 8761	469/ 8761	468/ 8761	468/ 8761	468/ 8761
n	21	22	23	24	25	26	27	28	29	30
SH/ WH	467/ 8761	467/ 8761	466/ 8761	465/ 8761	464/ 8761	464/ 8761	476/ 8761	479/ 8761	476/ 8761	467/ 8761
n	31	32	33	34	35	36	37	38	39	40
SH/ WH	476/ 8761	457/ 8761	456/ 8761	462/ 8761	462/ 8761	462/ 8761	463/ 8761	463/ 8761	464/ 8761	464/ 8761
n	41	42	43	44	45	46	47	48	49	50
SH/ WH	464/ 8761	464/ 8761	464/ 8761	464/ 8761	465/ 8761	465/ 8761	465/ 8761	465/ 8761	465/ 8761	465/ 8761

Cichong Liu
400079
cichong@aalto.fi

To calculate the payback years of the underground thermal energy storage, another necessary step is to estimate the investment cost.

In Philipp et al.'s (2011) study, they summarize 1091 borehole heat exchanger projects and calculated an arithmetic mean investment cost for drilling and BHE per unit heating demand is 1052 £/kW and the heat pump costs per heating demand is 1039 £/kW, so the unit capital cost per heating demand is 2161 £/kW.

Thus equation (29) expressed the equation to calculate the investment cost for the underground thermal energy storage combined with heat pumps.

$$\text{Investment} = 2.161 * n * q_{l_{summer}} * H \quad (29)$$

And payback years can be calculated by dividing the investment cost by total profits made in one year as shown in equation (30).

$$\text{Pay back years} = \frac{\text{Investment}}{\text{Money}} \quad (30)$$

Table 18 shows the payback years for different numbers of the borehole heat exchangers.

Table 18. The shortest payback years for corresponding number of boreholes to be built

n	1	2	3	4	5	6	7	8	9	10
Years	26.98	26.98	26.98	26.98	26.99	27.00	25.14	27.02	27.03	27.04
n	11	12	13	14	15	16	17	18	19	20
Years	27.05	27.06	27.07	26.17	26.24	27.12	27.13	27.15	27.16	27.17
n	21	22	23	24	25	26	27	28	29	30
Years	27.19	27.20	27.22	27.24	27.27	27.28	26.85	26.87	26.92	27.00
n	31	32	33	34	35	36	37	38	39	40
Years	26.99	27.45	27.47	27.46	27.47	27.47	27.47	27.46	27.45	27.43
n	41	42	43	44	45	46	47	48	49	50
Years	27.42	27.39	27.37	27.34	27.30	27.26	27.20	27.14	27.08	27.00

So based on the specified borehole heat exchanger as stated in Table 3 and a fixed flowing rate of the circulating fluid 0.5 kg/s in both summer and winter time, the minimum payback year is 25 years when 7 borehole heat exchangers are built. And to make the best profits, the summer charging hours will be 553 hours and the winter discharging will last for the whole heating period. However, another fact to be noticed is that the payback year doesn't vary a lot with the number of borehole heat exchanger and this can be explained by the proportional increase of the profits made per year with the number of borehole heat exchangers.

Cichong Liu
400079
cichong@aalto.fi

4.1.3 How the cost of heat in summer affects the results

Above results present payback time of building the new system based on a fixed summer heat cost of 30€/MWh, following discussions provide the results calculated based on varied summer heat costs, providing a reference for the investors a relation between payback years and cost of summer heat. Table 19 shows how the payback years vary with the cost of summer heat. With the increase of summer heat cost, the payback years are also increasing, with the yellow shading

Table 19. Payback years influenced by summer heat cost

No	1	2	3	4	5	6	7	8	9	10
C=10	17.25	17.25	17.25	17.25	17.26	17.27	17.27	17.28	17.29	17.30s
C=30	26.98	26.98	26.98	26.98	26.99	27.00	25.14	27.02	27.03	27.04
C=80	47.76	47.76	47.43	47.76	47.76	47.77	42.94	47.79	47.81	47.82
No	11	12	13	14	15	16	17	18	19	20
C=10	17.31	17.32	17.34	17.35	16.95	17.37	17.38	17.40	17.41	17.43
C=30	27.05	27.06	27.07	26.17	26.24	27.12	27.13	27.15	27.16	27.17
C=80	47.83	47.84	45.21	45.37	45.60	47.91	47.93	47.94	47.96	47.98
No	21	22	23	24	25	26	27	28	29	30
C=10	17.45	17.47	17.49	17.51	17.54	17.57	17.60	17.62	17.72	17.48
C=30	27.19	27.20	27.22	27.24	27.27	27.28	26.85	26.87	26.92	27.00
C=80	48.00	48.02	48.04	48.06	46.89	46.95	46.93	46.87	47.07	47.06
No	31	32	33	34	35	36	37	38	39	40
C=10	17.52	17.76	17.80	17.83	17.87	17.92	17.95	17.99	18.03	18.08
C=30	26.99	27.45	27.47	27.46	27.47	27.47	27.47	27.46	27.45	27.43
C=80	47.20	48.23	48.26	48.26	48.24	48.23	48.13	48.03	47.93	47.84
No	41	42	43	44	45	46	47	48	49	50
C=10	18.11	18.15	18.20	18.23	18.26	18.31	18.34	18.39	18.43	18.49
C=30	27.42	27.39	27.37	27.34	27.30	27.26	27.20	27.14	27.08	27.00
C=80	47.74	47.62	47.48	47.30	47.04	46.81	46.51	46.19	45.85	45.38

If the summer heat costs 10 €/MWh, the minimum pay back years will be 17 years and it is suggested to build 15 boreholes and charge 1501 hours in summer and discharge for the whole winter; if the summer heat cost 30 €/MWh, the minimum pay back years will 25 and it is suggested to build 7 boreholes and charge 553 hours in summer and discharge for the whole period and if the summer heat cost up to 80 €/MWh, the payback time is increased to 43 years and also 7 boreholes are suggested to be built, a charging period of 204 hours and the discharging period of the whole winter are proposed.

Cichong Liu
400079
cichong@aalto.fi

4.2 Other scenarios analysis

This chapter present the results evaluated based on other four scenarios with different circulating fluid mass flow rates in different seasons. Table 20 shows how the payback years calculated based on different scenarios

Table 20. Payback time calculated based on different scenarios

No	1	2	3	4	5	6	7	8	9	10
S0	26.98	26.98	26.98	26.98	26.99	27.00	25.14	27.02	27.03	27.04
S1	21.07	21.07	18.58	21.07	21.07	19.90	20.08	21.09	21.10	21.10
S2	40.06	40.06	35.52	40.06	40.07	38.16	36.25	40.11	40.12	40.13
S3	51.68	51.68	51.68	51.68	51.68	51.68	47.30	51.70	51.71	51.72
S4	26.54	26.54	26.54	26.54	26.55	26.56	24.70	26.58	26.58	26.59
No	11	12	13	14	15	16	17	18	19	20
S0	27.05	27.06	27.07	26.17	26.24	27.12	27.13	27.15	27.16	27.17
S1	20.49	20.55	20.60	20.64	20.70	21.17	21.18	21.19	21.20	21.21
S2	40.14	39.69	38.14	38.35	38.42	40.22	40.23	40.25	40.27	40.28
S3	51.73	51.74	50.11	49.57	49.72	51.77	51.78	51.79	51.80	51.82
S4	26.60	26.62	26.63	25.71	25.79	26.67	26.69	26.71	26.72	26.74
No	21	22	23	24	25	26	27	28	29	30
S0	27.19	27.20	27.22	27.24	27.27	27.28	26.85	26.87	26.92	27.00
S1	21.22	20.93	20.95	20.98	21.01	21.03	21.06	21.09	21.12	21.15
S2	40.30	40.33	40.35	40.63	39.26	39.35	39.45	39.50	39.56	39.65
S3	51.83	51.84	51.86	51.87	51.90	51.16	50.78	50.87	50.91	50.99
S4	26.75	26.77	26.79	26.81	26.83	26.85	26.44	26.46	26.48	26.53
No	31	32	33	34	35	36	37	38	39	40
S0	26.99	27.45	27.47	27.46	27.47	27.47	27.47	27.46	27.45	27.43
S1	21.17	21.42	21.45	21.48	21.50	21.53	21.56	21.59	21.62	21.66
S2	39.67	40.54	40.56	40.58	40.58	40.61	40.63	40.58	40.52	40.45
S3	51.08	52.00	52.01	52.01	51.77	51.74	51.70	51.62	51.55	51.47
S4	26.56	27.02	27.05	27.08	27.09	27.12	27.12	27.12	27.11	27.10
No	41	42	43	44	45	46	47	48	49	50
S0	27.42	27.39	27.37	27.34	27.30	27.26	27.20	27.14	27.08	27.00
S1	21.69	21.73	21.60	21.64	21.68	21.73	21.77	21.82	21.86	21.91
S2	40.39	40.33	40.19	40.03	39.86	39.66	39.42	39.12	38.78	38.21
S3	51.36	51.25	51.14	51.01	50.61	50.40	50.17	49.91	49.65	49.34
S4	27.08	27.06	27.04	27.01	26.98	26.94	26.88	26.83	26.66	26.58

According to the results, the sets-up in Scenario 1 will bring the minimum pay back years which is the mass flow rate in summer = 0.1 kg/s and the mass flow rate in winter = 0.5 kg/s. In this manner, the minimum payback time will be 18 years and 3 boreholes are preferred to be built. The suggested combination for charging and discharging processes is 1554 hours charging during summer and discharging for the whole period.

Cichong Liu
400079
cichong@aalto.fi

5 Case in Turku

5.1 New system

In Turku, a similar system was built except in summer, the borehole and district heating system is serially connected which means the borehole heat exchangers are charged at a lower temperature level which brings a lower heating rate. However, no money will be charged for summer heat and in the best case, the return temperature will be cooled down which maximize the electrical efficiency of the power plant, so it is a large possibility that the CHP power plant will agree to charge less for electricity.

Another thing to be noticed is that if the system is serially connected, the heat cannot be supplied as much as possible which largely depends on the heat demand hourly. The minimum heat demand in summer is 4.4791 kW and based on supply and return temperatures of the district heating networks, in our case, they are 60 and 40 ℃ respectively, it corresponds to 0.053 kg/s mass flow rate of hot water. Thus in the following calculation, the charging mass flow rate in summer is assumed to be 0.05 kg/s. And the same borehole construction is applied except changing the borehole length from 100m to 180m as Turku Heat Company required. Detail sets-up of borehole heat exchanger applied in Turku case can be found in Table 21.

Table 21. Basic sets-up of borehole heat exchanger applied in Turku case

r_{ext} (m)	0.016	**T_{in_summer} (˚C)**	40
r_{int} (m)	0.013	**$\dot{m}$ (kg/s)**	0.05
D (m)	0.0285	**k_{ground} (W/mK)**	3
H (m)	180	**k_U (W/mK)**	0.6
r_b (m)	0.057	**k_b (W/mK)**	1.5
T_o (˚C)	5	**T_{in_winter} (˚C)**	-3

By applying the same methodology, it is possible to predict the heating rate per length and exiting fluid temperature versus time as shown in figure 41 and the prediction equations can be found in (31) and (32).

Cichong Liu
400079
cichong@aalto.fi

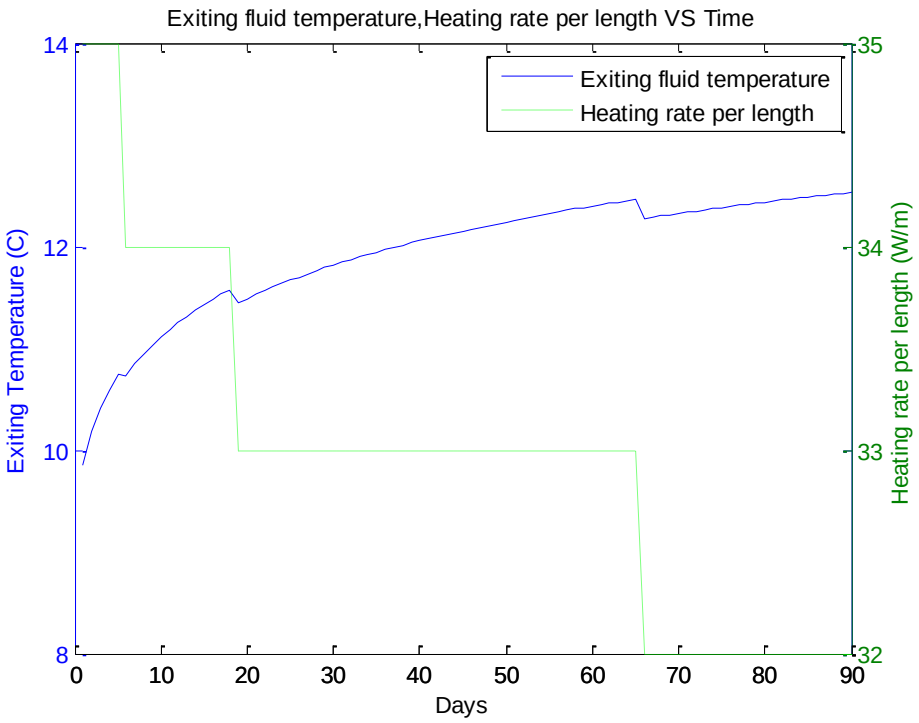

Figure 21. Mean exiting fluid temperature, Mean heating rate per length versus Time

$$T_{exit}[°C] = 0.6362 \ln\left(\frac{h\,[h]}{24}\right) + 9.6878 \quad (31)$$

$$q_l[W/m] = 35.88\left(\frac{h}{24}\right)^{-0.024} \quad (32)$$

Figure 24 below shows the ground temperature distribution after summer and the newly adjusted initial ground temperature for winter time.

Cichong Liu
400079
cichong@aalto.fi

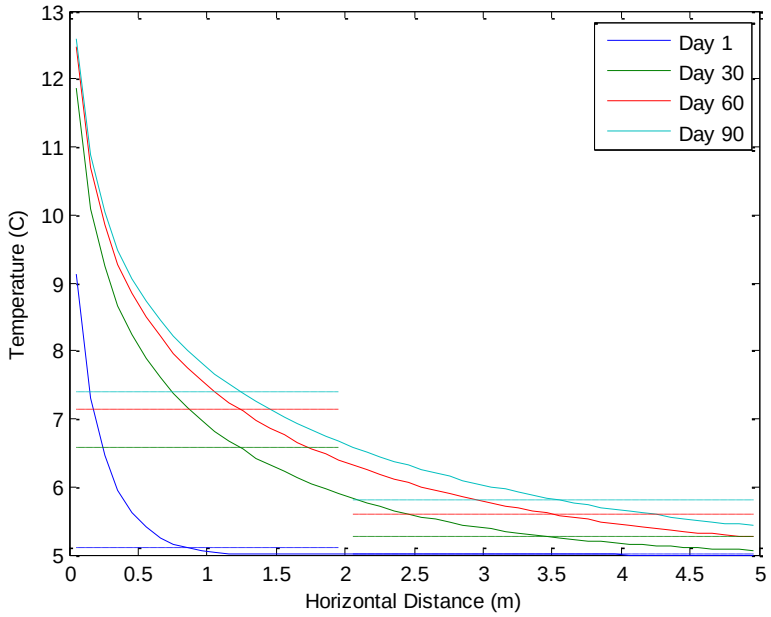

Figure 22. Ground temperature distribution around the boreholes and newly adjusted temperature

5.1.1 Winter mass flow rate = 0.5 kg/s

5.1.1.1 Winter heat transfer prediction

While in winter, different mass flow rates were tested in order to minimize the costs.

Table 22 and Table 23 show the cooling rate per length and the mean exiting temperature of the circulating fluid from the U-tube respectively and equation (33) and (34) present the predicting function for cooling rate per length and exiting fluid temperature with a winter circulating fluid mass flow rate of 0.5 kg/s.

$$q_l[W/m] = \left(0.1387 \ln\left(\frac{Sh\ [h]}{24}\right) + 1.5767\right) \cdot \ln\left(\frac{Wh\ [h] - 3672}{24}\right) - 2.3818 \ln\left(\frac{Sh\ [h]}{24}\right) - 27.8923 \quad (33)$$

$$T_{exit}[°C] = \left(-0.0117 \ln\left(\frac{Sh\ [h]}{24}\right) - 0.1433\right) \cdot \ln\left(\frac{Wh\ [h] - 3672}{24}\right) + 0.2032 \ln\left(\frac{Sh\ [h]}{24}\right) - 0.4974 \quad (34)$$

Table 22. Cooling rate per length as a function of summer and winter time (SD stands for Summer Day and WD stands for Winter Day)

	SD1	SD10	SD20	SD30	SD40	SD50	SD60	SD70	SD80	SD90
WD1	-30	-33	-35	-36	-37	-37	-38	-38	-38	-39
WD2	-29	-32	-33	-35	-35	-36	-37	-37	-37	-37
WD3	-28	-31	-33	-34	-34	-35	-36	-36	-36	-36

Cichong Liu
400079
cichong@aalto.fi

WD4	-28	-30	-32	-33	-34	-34	-35	-35	-35	-36
WD5	-27	-30	-32	-33	-33	-34	-35	-35	-35	-35
WD6	-27	-30	-31	-32	-33	-33	-34	-34	-34	-35
WD7	-27	-29	-31	-32	-33	-33	-34	-34	-34	-35
WD8	-26	-29	-31	-32	-32	-33	-33	-34	-34	-34
WD9	-26	-29	-30	-31	-32	-33	-33	-33	-34	-34
WD10	-26	-29	-30	-31	-32	-32	-33	-33	-33	-34
WD15	-25	-28	-29	-30	-31	-32	-32	-32	-32	-33
WD20	-25	-27	-29	-30	-30	-31	-31	-32	-32	-32
WD25	-25	-27	-28	-29	-30	-30	-31	-31	-31	-32
WD30	-24	-27	-28	-29	-30	-30	-31	-31	-31	-31
WD40	-24	-26	-27	-28	-29	-29	-30	-30	-30	-31
WD50	-23	-26	-27	-28	-28	-29	-29	-30	-30	-30
WD60	-23	-25	-27	-28	-28	-29	-29	-29	-29	-30
WD80	-23	-25	-26	-27	-27	-28	-28	-29	-29	-29
WD100	-22	-24	-26	-26	-27	-28	-28	-28	-28	-29
WD120	-22	-24	-25	-26	-27	-27	-28	-28	-28	-28
WD150	-22	-24	-25	-26	-26	-27	-27	-27	-27	-28
WD180	-21	-23	-24	-25	-26	-26	-27	-27	-27	-27
WD210	-21	-23	-24	-25	-25	-26	-26	-26	-27	-27
WD240	-21	-23	-24	-25	-25	-26	-26	-26	-26	-27
WD270	-21	-22	-24	-24	-25	-25	-26	-26	-26	-27

Table 23. Mean exiting fluid temperature as a function of summer and winter time (SD stands for Summer Day and WD stands for Winter Day)

	SD1	SD10	SD20	SD30	SD40	SD50	SD60	SD70	SD80	SD90
WD1	-0.32	-0.08	0.03	0.14	0.20	0.31	0.33	0.36	0.42	0.41
WD2	-0.41	-0.18	0.00	0.02	0.16	0.19	0.20	0.23	0.30	0.35
WD3	-0.44	-0.23	-0.13	-0.03	0.02	0.12	0.13	0.17	0.23	0.21
WD4	-0.53	-0.32	-0.15	-0.06	-0.01	0.02	0.10	0.14	0.12	0.18
WD5	-0.51	-0.32	-0.23	-0.14	-0.01	0.01	0.01	0.05	0.11	0.17
WD6	-0.57	-0.38	-0.22	-0.13	-0.08	-0.06	0.03	0.06	0.04	0.09
WD7	-0.62	-0.35	-0.27	-0.19	-0.14	-0.04	-0.04	0.00	0.06	0.03
WD8	-0.67	-0.40	-0.33	-0.24	-0.11	-0.09	-0.01	-0.06	0.00	0.06
WD9	-0.62	-0.44	-0.28	-0.20	-0.16	-0.14	-0.06	-0.02	-0.05	0.01
WD10	-0.65	-0.48	-0.32	-0.24	-0.20	-0.10	-0.10	-0.07	0.00	-0.04
WD15	-0.70	-0.54	-0.39	-0.31	-0.28	-0.17	-0.18	-0.15	-0.08	-0.13
WD20	-0.80	-0.55	-0.50	-0.43	-0.30	-0.30	-0.21	-0.17	-0.21	-0.16
WD25	-0.77	-0.64	-0.49	-0.42	-0.39	-0.29	-0.31	-0.27	-0.21	-0.26
WD30	-0.83	-0.60	-0.56	-0.50	-0.36	-0.37	-0.28	-0.35	-0.29	-0.23
WD40	-0.93	-0.71	-0.57	-0.50	-0.49	-0.38	-0.41	-0.37	-0.31	-0.25

Cichong Liu
400079
cichong@aalto.fi

WD50	-0.90	-0.68	-0.66	-0.60	-0.47	-0.48	-0.39	-0.35	-0.41	-0.35
WD60	-0.96	-0.75	-0.61	-0.55	-0.54	-0.44	-0.47	-0.43	-0.37	-0.43
WD80	-0.94	-0.86	-0.73	-0.67	-0.54	-0.56	-0.47	-0.44	-0.50	-0.44
WD100	-1.01	-0.82	-0.69	-0.64	-0.63	-0.53	-0.57	-0.53	-0.47	-0.54
WD120	-1.07	-0.88	-0.76	-0.71	-0.71	-0.60	-0.51	-0.61	-0.55	-0.49
WD150	-1.15	-0.96	-0.84	-0.80	-0.67	-0.69	-0.61	-0.57	-0.51	-0.59
WD180	-1.07	-0.90	-0.78	-0.74	-0.74	-0.63	-0.68	-0.65	-0.58	-0.53
WD210	-1.12	-0.95	-0.83	-0.79	-0.80	-0.70	-0.61	-0.71	-0.65	-0.59
WD240	-1.17	-1.00	-0.88	-0.85	-0.71	-0.75	-0.66	-0.63	-0.70	-0.65
WD270	-1.20	-1.04	-0.93	-0.89	-0.76	-0.80	-0.71	-0.67	-0.61	-0.70

5.1.1.2 Economic analysis

Unlike parallel construction, the mass flow rate in summer depends on the heat demand during summer time and so is the heat amount to be charged into ground. Besides, the heat in summer is the waste heat from hot water usage which is free in Turku case. Thus the economy of the new system is needed to be calculated utilizing a new methodology.

Similar to parallel construction, the number of the boreholes is still a key factor to define in order to minimize the cost. Unlike parallel case, the mass flow rate in summer cannot be as large as the system designed; it largely depends on the hourly heat demand in summer, so the number of boreholes to be run hourly can be decided by following equation:

$$n = \frac{Q_{heat_{summer}}}{(T_{supply} - T_{return}) * m * c} \quad (35)$$

n is a 3762*1 matrix which indicates how many boreholes can possibly run hourly. Utilizing find function in Matlab, it is possible to count the frequency of the number of boreholes and figure 26 shows how many boreholes need to work for specific working hours. E.g., 1 borehole needs to run for more than 1000 hours, 2 boreholes need to run around 200 hours and so on. The next step is numbering the boreholes and count the maximum running hours during the summer for every borehole and figure 27 shows for one borehole, how many hours it needs to be operated during summer time. For instance, if only one borehole was installed, it needs to operate for the whole summer and if there are two boreholes installed, there will be one borehole need to work for the whole summer and the other borehole is only possibly to run for around 2700 hours during the whole summer.

Cichong Liu
400079
cichong@aalto.fi

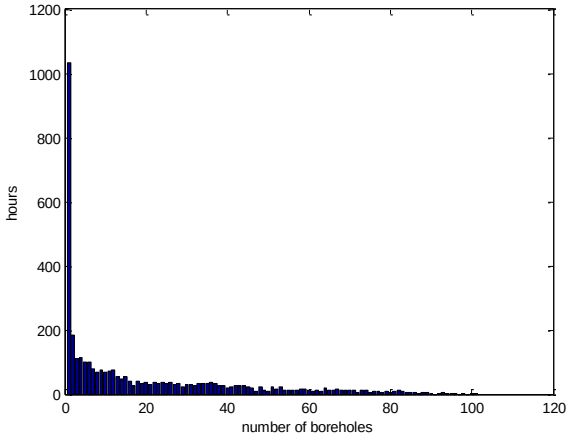

Figure 23. Frequency of number of boreholes

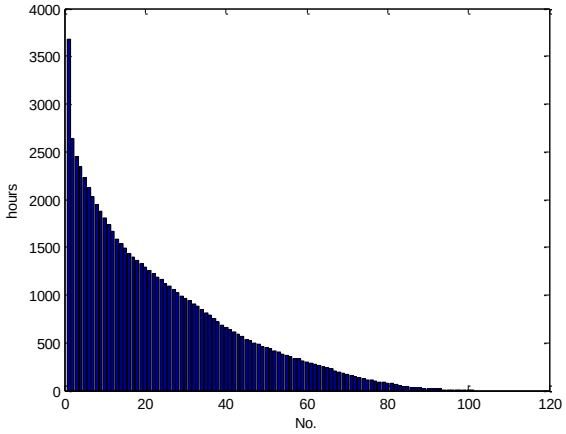

Figure 24. Operating hours for Numbering boreholes

As shown figure 21, when loading heat to the ground in summer time, the heating rate per length doesn't vary a lot with time, since summer heat doesn't cost anything, maximizing the heating hours in summer will be the best option.

In winter, the calculation steps are similar to previous cases, the Matlab program automatically picks up the highest profits made by building different number of boreholes and the results are shown in Table below.

Table 24. Profits made per year for baseline scenario (€) corresponding to number of boreholes to be built

No	1	2	3	4	5	6	7	8	9	10
€	3.49E+03	6.91E+03	1.03E+04	1.37E+04	1.71E+04	2.05E+04	2.39E+04	2.72E+04	3.06E+04	3.38E+04
No	11	12	13	14	15	16	17	18	19	20
€	3.71E+04	4.04E+04	4.37E+04	4.70E+04	5.02E+04	5.35E+04	5.67E+04	5.99E+04	6.31E+04	6.62E+04
No	21	22	23	24	25	26	27	28	29	30
€	6.94E+04	7.25E+04	7.56E+04	7.87E+04	8.18E+04	8.48E+04	8.79E+04	9.09E+04	9.38E+04	9.68E+04
No	31	32	33	34	35	36	37	38	39	40
€	9.97E+04	1.03E+05	1.05E+05	1.08E+05	1.11E+05	1.14E+05	1.17E+05	1.19E+05	1.22E+05	1.25E+05
No	41	42	43	44	45	46	47	48	49	50
€	1.27E+05	1.30E+05	1.32E+05	1.35E+05	1.37E+05	1.40E+05	1.42E+05	1.44E+05	1.47E+05	1.49E+05

Table 25. The shortest payback years for corresponding number of boreholes to be built (calculated based on investment cost of 10000€/3 boreholes)

No	1	2	3	4	5	6	7	8	9	10
Years	3.54	3.59	3.61	3.63	3.64	3.65	3.66	3.67	3.68	3.69
No	11	12	13	14	15	16	17	18	19	20
Years	3.70	3.71	3.72	3.72	3.73	3.74	3.75	3.76	3.76	3.77
No	21	22	23	24	25	26	27	28	29	30

Cichong Liu
400079
cichong@aalto.fi

Years	3.78	3.78	3.79	3.80	3.80	3.81	3.82	3.82	3.83	3.84
No	31	32	33	34	35	36	37	38	39	40
Years	3.85	3.85	3.86	3.87	3.88	3.88	3.89	3.90	3.91	3.92
No	41	42	43	44	45	46	47	48	49	50
Years	3.93	3.94	3.94	3.95	3.96	3.97	3.98	3.99	4.00	4.01

The program computes the minimum payback time which is 3.54 years when building one borehole. The results shown in table 25 above indicate that increasing the number of boreholes, the payback years extend and this can be explained by Figure 26 and 27. By building more boreholes, the investment is larger and the spare time of the extra boreholes will be longer.

5.1.2 Winter mass flow rate = 0.25 kg/s

5.1.2.1 Winter heat transfer prediction

Table 26 and Table 27 show the cooling rate per length and the mean exiting temperature of the circulating fluid from the U-tube respectively and equation (36) and (37) present the predicting function for cooling rate per length and exiting fluid temperature with a mass flow rate of 0.25 kg/s.

$$q_l[\mathrm{W/m}] = \left(0.0946 \ln\left(\frac{\mathrm{Sh\ [h]}}{24}\right) + 1.0861\right) \cdot \ln\left(\frac{\mathrm{Wh\ [h]} - 3672}{24}\right) - 1.9132 \ln\left(\frac{\mathrm{Sh\ [h]}}{24}\right) - 22.2714 \quad (36)$$

$$T_{exit}[°\mathrm{C}] = \left(-0.0207 \ln\left(\frac{\mathrm{Sh\ [h]}}{24}\right) - 0.1795\right) \cdot \ln\left(\frac{\mathrm{Wh\ [h]} - 3672}{24}\right) + 0.33 \ln\left(\frac{\mathrm{Sh\ [h]}}{24}\right) - 1.0093 \quad (37)$$

Table 26. Cooling rate per length as a function of summer and winter time (SD stands for Summer Day and WD stands for Winter Day)

	SD1	SD10	SD20	SD30	SD40	SD50	SD60	SD70	SD80	SD90
WD1	-24	-26	-28	-29	-29	-30	-30	-30	-31	-31
WD2	-23	-25	-27	-28	-28	-29	-29	-29	-30	-30
WD3	-23	-25	-26	-27	-28	-28	-29	-29	-29	-29
WD4	-22	-25	-26	-27	-27	-28	-28	-28	-29	-29
WD5	-22	-24	-26	-26	-27	-28	-28	-28	-28	-29
WD6	-22	-24	-25	-26	-27	-27	-28	-28	-28	-28
WD7	-22	-24	-25	-26	-26	-27	-27	-27	-28	-28
WD8	-22	-24	-25	-26	-26	-27	-27	-27	-28	-28
WD9	-21	-23	-25	-25	-26	-27	-27	-27	-28	-28
WD10	-21	-23	-25	-25	-26	-26	-27	-27	-27	-28
WD15	-21	-23	-24	-25	-25	-26	-26	-26	-27	-27
WD20	-20	-22	-24	-24	-25	-25	-26	-26	-26	-27
WD25	-20	-22	-23	-24	-25	-25	-25	-26	-26	-26
WD30	-20	-22	-23	-24	-24	-25	-25	-25	-26	-26

Cichong Liu
400079
cichong@aalto.fi

WD40	-20	-22	-23	-23	-24	-24	-25	-25	-25	-26
WD50	-19	-21	-22	-23	-24	-24	-24	-25	-25	-25
WD60	-19	-21	-22	-23	-23	-24	-24	-24	-25	-25
WD80	-19	-21	-22	-22	-23	-23	-24	-24	-24	-24
WD100	-19	-20	-21	-22	-23	-23	-23	-24	-24	-24
WD120	-18	-20	-21	-22	-22	-23	-23	-23	-24	-24
WD150	-18	-20	-21	-22	-22	-22	-23	-23	-23	-23
WD180	-18	-20	-21	-21	-22	-22	-23	-23	-23	-23
WD210	-18	-19	-20	-21	-22	-22	-22	-22	-23	-23
WD240	-18	-19	-20	-21	-21	-22	-22	-22	-23	-23
WD270	-18	-19	-20	-21	-21	-22	-22	-22	-22	-23

Table 27. Mean exiting fluid temperature as a function of summer and winter time (SD stands for Summer Day and WD stands for Winter Day)

	SD1	SD10	SD20	SD30	SD40	SD50	SD60	SD70	SD80	SD90
WD1	1.31	1.74	1.90	2.14	2.23	2.28	2.40	2.45	2.44	2.52
WD2	1.23	1.64	1.79	1.93	2.12	2.16	2.28	2.33	2.31	2.39
WD3	1.11	1.51	1.75	1.89	1.96	2.11	2.12	2.17	2.26	2.22
WD4	1.12	1.40	1.64	1.77	1.96	1.99	2.11	2.16	2.13	2.21
WD5	1.04	1.43	1.55	1.80	1.86	1.89	2.01	2.06	2.15	2.11
WD6	0.98	1.36	1.59	1.72	1.78	1.93	1.93	1.98	2.06	2.14
WD7	0.92	1.30	1.53	1.65	1.71	1.86	1.98	1.90	1.99	2.07
WD8	0.87	1.24	1.47	1.59	1.77	1.79	1.91	1.96	1.92	2.00
WD9	0.95	1.19	1.42	1.53	1.72	1.74	1.86	1.91	1.87	1.94
WD10	0.91	1.27	1.37	1.61	1.67	1.81	1.81	1.85	1.94	1.89
WD15	0.75	1.10	1.32	1.43	1.61	1.62	1.74	1.79	1.74	1.81
WD20	0.78	1.11	1.18	1.43	1.47	1.62	1.59	1.64	1.73	1.81
WD25	0.69	1.02	1.22	1.32	1.36	1.50	1.63	1.53	1.61	1.69
WD30	0.62	0.94	1.14	1.23	1.42	1.41	1.53	1.58	1.52	1.60
WD40	0.50	0.81	1.00	1.25	1.28	1.42	1.39	1.44	1.52	1.60
WD50	0.57	0.87	1.06	1.15	1.17	1.31	1.43	1.32	1.41	1.49
WD60	0.50	0.79	0.98	1.06	1.24	1.22	1.34	1.39	1.31	1.39
WD80	0.40	0.66	0.84	1.09	1.10	1.25	1.20	1.25	1.33	1.41
WD100	0.40	0.74	0.92	0.99	1.00	1.14	1.26	1.13	1.22	1.30
WD120	0.40	0.66	0.84	0.90	1.09	1.05	1.17	1.22	1.13	1.21
WD150	0.38	0.57	0.74	0.80	0.98	1.13	1.06	1.11	1.20	1.28
WD180	0.38	0.49	0.65	0.90	0.90	1.04	0.98	1.02	1.11	1.19
WD210	0.38	0.43	0.78	0.83	0.82	0.97	1.09	0.95	1.03	1.11
WD240	0.38	0.56	0.72	0.77	0.95	0.91	1.03	1.08	0.97	1.05
WD270	0.38	0.51	0.67	0.72	0.90	0.85	0.97	1.02	1.11	0.99

Cichong Liu
400079
cichong@aalto.fi

5.1.2.2 Economic analysis

By applying the same method analyzing the economics of the case with a winter mass flow rate of 0.25 kg/s, the results can be found in table 28 and 29.

Table 28. Profits made per year for scenario with winter mass flow rate =0.25 kg/s (€) for corresponding numbers of boreholes to be built

No	1	2	3	4	5	6	7	8	9	10
€	2.96E+03	5.85E+03	8.74E+03	1.16E+04	1.45E+04	1.73E+04	2.02E+04	2.30E+04	2.58E+04	2.86E+04
No	11	12	13	14	15	16	17	18	19	20
€	3.14E+04	3.42E+04	3.70E+04	3.98E+04	4.25E+04	4.53E+04	4.80E+04	5.08E+04	5.35E+04	5.62E+04
No	21	22	23	24	25	26	27	28	29	30
€	5.89E+04	6.16E+04	6.43E+04	6.69E+04	6.96E+04	7.22E+04	7.48E+04	7.74E+04	8.00E+04	8.25E+04
No	31	32	33	34	35	36	37	38	39	40
€	8.51E+04	8.76E+04	9.01E+04	9.26E+04	9.51E+04	9.75E+04	1.00E+05	1.02E+05	1.05E+05	1.07E+05
No	41	42	43	44	45	46	47	48	49	50
€	1.09E+05	1.12E+05	1.14E+05	1.16E+05	1.19E+05	1.21E+05	1.23E+05	1.25E+05	1.27E+05	1.30E+05

Table 29. The shortest payback years for corresponding number of boreholes to be built

No	1	2	3	4	5	6	7	8	9	10
Years	4.22	4.28	4.31	4.33	4.34	4.36	4.37	4.38	4.39	4.40
No	11	12	13	14	15	16	17	18	19	20
Years	4.41	4.42	4.43	4.44	4.45	4.46	4.47	4.47	4.48	4.49
No	21	22	23	24	25	26	27	28	29	30
Years	4.50	4.51	4.51	4.52	4.53	4.54	4.55	4.55	4.56	4.57
No	31	32	33	34	35	36	37	38	39	40
Years	4.58	4.58	4.59	4.60	4.61	4.62	4.63	4.63	4.64	4.65
No	41	42	43	44	45	46	47	48	49	50
Years	4.66	4.67	4.68	4.69	4.70	4.71	4.72	4.73	4.74	4.75

As shown in the table above, the minimum payback time is 4.22 years when building one borehole with a winter mass flow rate = 0.25 kg/s.

Cichong Liu
400079
cichong@aalto.fi

5.2 Geothermal heat pump analysis

A geothermal heat pump system combines the borehole heat exchanger(s) with the heat pump and the construction looks pretty similar to the new system however the heat discharged in winter from the ground comes directly from the soil which means there is no heat charge into the ground in summer time. Thus in the following calculation, the initial ground temperature starts with five degree.

Applying the same borehole heat exchanger as stated in table 21 and with a winter mass flow of 0.5 kg/s, the winter heat transfer prediction and the economic analysis of the geothermal heat pump can be found in chapter 5.2.1 and 5.2.2 respectively.

5.2.1 Winter heat transfer prediction

Figure 29 shows the cooling rate per length and the mean exiting temperature of the circulating fluid from the U-tube respectively and equation (29) and (30) present the predicting function for cooling rate per length and exiting fluid temperature with a mass flow rate of 0.5 kg/s.

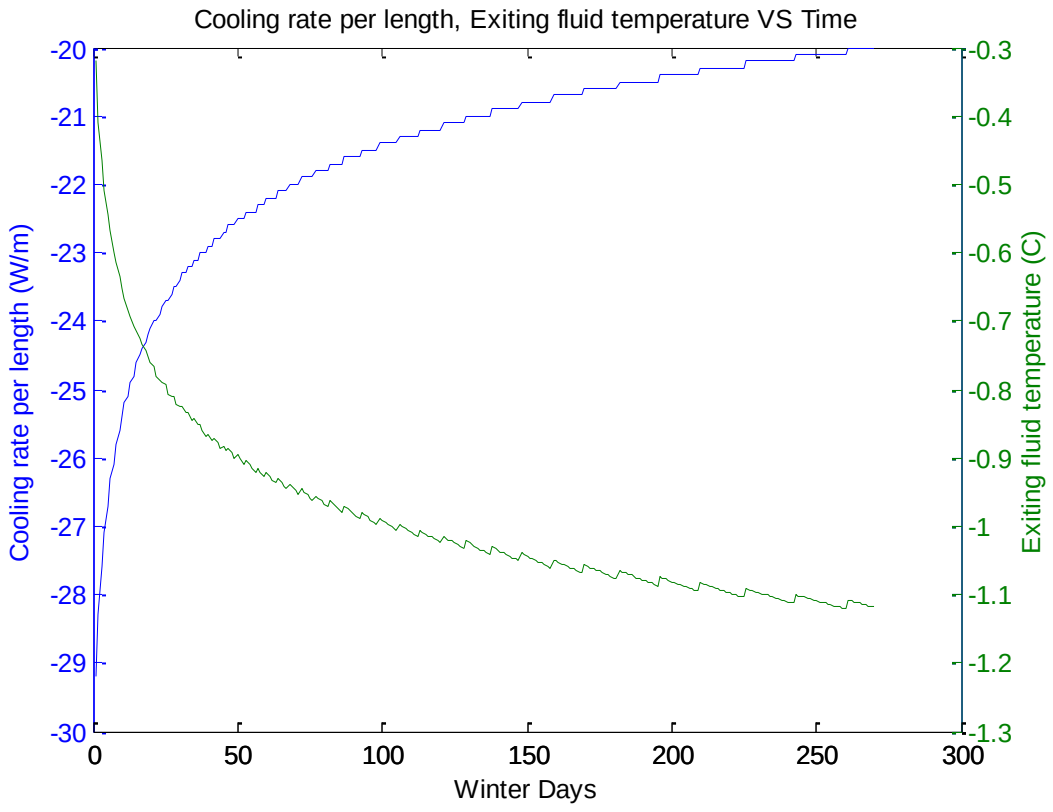

Figure 25. Cooling rate per length and exiting fluid temperatures versus winter days

Cichong Liu
400079
cichong@aalto.fi

$$q_l[W/m] = 1.6145\ln\left(\frac{Wh\ [h] - 3672}{24}\right) - 29.435 (38)$$

$$T_{exit}[°C] = -0.152\ln\left(\frac{Wh\ [h] - 3672}{24}\right) - 0.3532\ (39)$$

Figure 30 below shows the ground temperature distributions for selected conditions.

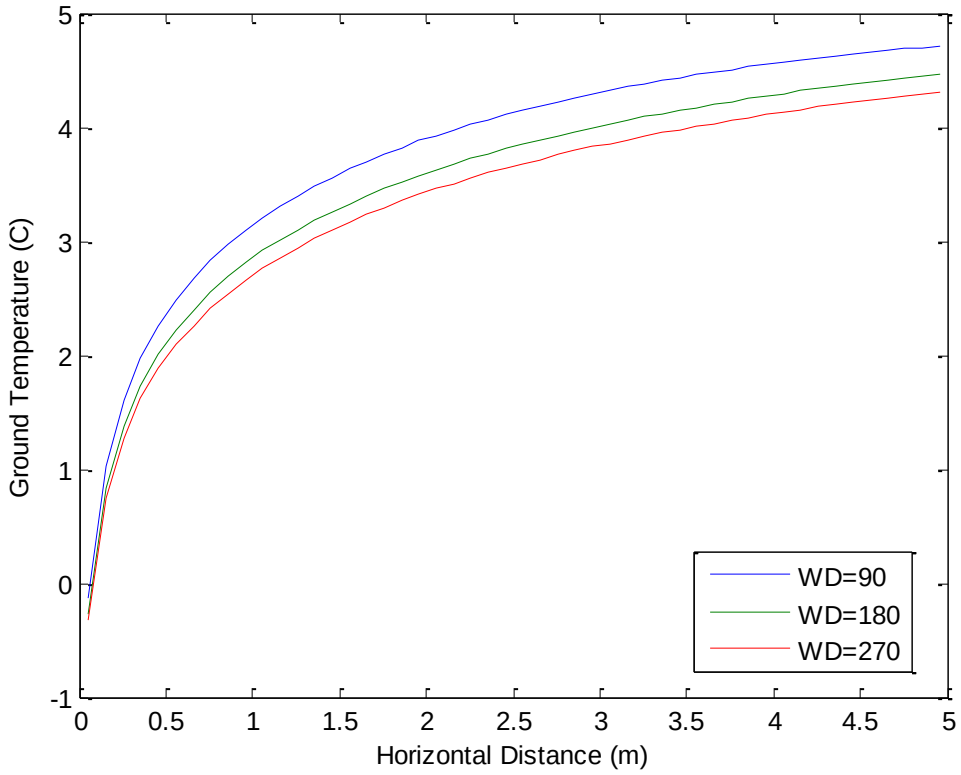

Figure 26. Ground temperature distribution for selected conditions

5.2.2 Economic analysis

The method to economically analyze geothermal heat pump is similar to previous cases except the evaluation for summer period is removed, the results can be found in table 30 and 31.

Table 30. Profits made per year for geothermal heat pump scenario (€) for corresponding numbers of boreholes to be built

No	1	2	3	4	5	6	7	8	9	10
€	2.62E+03	5.25E+03	7.87E+03	1.05E+04	1.31E+04	1.57E+04	1.83E+04	2.10E+04	2.36E+04	2.62E+04
No	11	12	13	14	15	16	17	18	19	20
€	2.88E+04	3.14E+04	3.40E+04	3.66E+04	3.92E+04	4.18E+04	4.44E+04	4.69E+04	4.95E+04	5.21E+04
No	21	22	23	24	25	26	27	28	29	30
€	5.47E+04	5.72E+04	5.98E+04	6.23E+04	6.49E+04	6.74E+04	6.99E+04	7.24E+04	7.49E+04	7.74E+04
No	31	32	33	34	35	36	37	38	39	40

Cichong Liu
400079
cichong@aalto.fi

€	7.99E+04	8.24E+04	8.48E+04	8.73E+04	8.97E+04	9.22E+04	9.46E+04	9.70E+04	9.94E+04	1.02E+05
No	41	42	43	44	45	46	47	48	49	50
€	1.04E+05	1.06E+05	1.09E+05	1.11E+05	1.13E+05	1.16E+05	1.18E+05	1.20E+05	1.22E+05	1.25E+05

Table 31. The shortest payback years for corresponding number of boreholes to be built

No	1	2	3	4	5	6	7	8	9	10
Years	4.89	4.89	4.89	4.90	4.90	4.90	4.90	4.90	4.90	4.90
No	11	12	13	14	15	16	17	18	19	20
Years	4.91	4.91	4.91	4.91	4.91	4.92	4.92	4.92	4.92	4.93
No	21	22	23	24	25	26	27	28	29	30
Years	4.93	4.93	4.94	4.95	4.95	4.95	4.96	4.96	4.97	4.97
No	31	32	33	34	35	36	37	38	39	40
Years	4.98	4.99	4.99	5.00	5.01	5.01	5.02	5.03	5.04	5.05
No	41	42	43	44	45	46	47	48	49	50
Years	5.06	5.06	5.07	5.08	5.09	5.10	5.11	5.12	5.14	5.15

As shown in the table 31, the minimum payback time is 4.89 years by building geothermal heat pump with a winter mass flow rate = 0.5 kg/s.

Cichong Liu
400079
cichong@aalto.fi

6 Discussion

As shown above, the mass flow rate of the circulating fluid can have significant effects on both heat transfer and economics of the boreholes.

The mass flow rate of the circulating fluid in summer and winter will bring different effects on the final results. An increase in summer mass flow rate will increase the heat transfer in summer but also lead to an increase in the exiting fluid temperature. And in parallel connected case, the heat stored in soil during summer time is much more than the heat taken from the soil during the winter. Thus an increase in summer flow rate will bring an extra cost in summer and the increase in exiting fluid temperature will result in a great heat loss. Though the increase in the mass flow rate in summer will lead to a ground temperature increase which increases the heat transfer rate in winter, unless the summer heat is free, in parallel connected case, it is always beneficial to charge the borehole with a smaller mass flow rate. There's also a lower boundary for the summer flow rate, the minimum summer flow rate has to maintain the level when the whole cooling period ends, and the ground mean temperature can still be higher than the level of the initial ground temperature before summer time. Otherwise, it will bring a result with lower efficiency year by year of the boreholes which indicates a decreasing profit yearly.

In the same manner, an increase in the mass flow rate in winter will cause an increase in the cooling rate and a decrease in the exiting fluid temperature. Thus a larger mass flow rate in winter will cause larger usage of the stored heat in the soil; of course, a lower level of the exiting fluid temperature corresponds to a lower COP value of the heat pump. However, the influences brought by the COP are smaller comparing to the influences brought by the mass flow rate. Therefore, as long as the ground mean temperature is higher than the initial ground temperature, it is always economically better to increase the mass flow rate in winter both in parallel and serially connected cases.

To conclude, to maximize the profits, the system has to keep the summer mass flow rate as low as possible and to keep the winter mass flow rate as high as possible and meanwhile, the two mass flow rates have to reach a balance in order to make the ground mean temperature after the whole heating & cooling period goes back to the initial ground temperature. In Turku case, with a fixed summer flow rate 0.05 kg/s, the largest winter flow rate is approximately 0.5 kg/s and the mean ground temperature can go back to 5.3 degree after a whole year.

Cichong Liu
400079
cichong@aalto.fi

Another big influencing parameter on the economics is the number of boreholes to be built. In the result of the economic analysis, the shortest payback time is by building one borehole only and this is because one borehole can maximize the charging hours in summer while more boreholes are built, the longer spare time during summer of the boreholes is required. However, as the results indicated, the payback years don't vary too much by building more boreholes. Thus it is all depending on the customers to decide how many boreholes they want to build.

Comparing to a normal geothermal heat pump, the new system takes advantage of the waste summer heat. By storing the summer heat inside the ground, it raises the ground temperature level so that the winter cooling rate is increased and the exiting fluid temperature from the borehole is also increased which corresponding to an increase in the COP of the heat pump. As stated in the result section, the cooling rate in winter without charging procedure in summer is approximately 21 W/m comparing to 27 W/m cooling rate with summer charging process, while the exiting fluid temperature is -1.2 ^{o}C without charging comparing to the -0.7 ^{o}C with summer heat stored. By applying the economic analysis, the payback years of a normal borehole geothermal heat pump are approximately 4.8 years, longer than the new system (3.54 years).

And as mentioned in previous sections, by utilizing the waste heat in summer, this procedure lowers the return temperature level back to the power plant which increases the electrical efficiency of the power plant so if the community could reach a good deal with the power plant, for example, buying electricity in a lower price, it is possible to increase the economic profits thus the payback years can be shortened.

Cichong Liu
400079
cichong@aalto.fi

7 Conclusions

To conclude, regardless of the connection method of the new system, the profits can be maximized by minimizing the summer flow rate and maximizing the winter flow rate as long as they two reach a balance to make sure the ground temperature after a whole year is larger than the initial ground temperature.

For Turku case, the best option is to charge the borehole with 0.05 kg/s mass flow rate hot water and discharge the borehole with 0.5 kg/s mass flow rate and the COP of the connected heat pump ranges from 2.8 to 3.2 depending on the exiting fluid temperature. With only one borehole installed, the payback years are the shortest, 3.54 years. Though with more borehole installed, the payback years are longer but not varied too much so it is the customers' choice to decide how many borehole they want to build.

Cichong Liu
400079
cichong@aalto.fi

8 Acknowledgement

The author would like to thank Kari Saari for his guidance and Markku Lampinen and Kuosa Maunu for their supervision and all the data support.

Cichong Liu
400079
cichong@aalto.fi

9 References:

Blum, P., Campillo, G., & Kölbel, T. (2011). Techno-economic and spatial analysis of vertical ground source heat pump systems in Germany. Energy, 36(5), 3002-3011.

Carslaw HS, Jaeger JC. (1946). Conduction of heat in solids. Oxford UK: Claremore Press.

Zeng HY, Diao NR, Fang ZH. (2002) A finite line-source model for boreholes in geothermal heat exchangers. Heat Transfer Asian Res 31(7):558–67.

Delaleux, F., Py, X., Olives, R., Dominguez, R. (2012). Enhancement of geothermal borehole heat exchangers performances by improvement of bentonite grouts conductivity. Appl. Therm. Eng. 33–34, 92–99.

Desideri, U., Sorbi, N., Arcioni, L., & Leonardi, D. (2011). Feasibility study and numerical simulation of a ground source heat pump plant, applied to a residential building. Applied Thermal Engineering, 31(16), 3500-3511.

Drake Landing Solar Community. (2014). Borehole thermal energy storage (BTES). Available from: http://dlsc.ca, accessed 2014.03.20.

Eskilson P. Thermal analysis of heat extraction boreholes. (1987). Ph.D. thesis. Sweden:University of Lund.

Fang ZH, Diao NR, Cui P. (2002). Discontinuous operation of geothermal heat exchangers. Tsinghua Sci Technol, 7(2):194–7.

Gao, Q., Li, M., Yu, M., Spitler, J. D., & Yan, Y. Y. (2009). Review of development from GSHP to UTES in China and other countries. Renewable and Sustainable Energy Reviews, 13(6), 1383-1394.

Geothermal heat pump systems. (2014). Vertical loops, Geothermal heat pump systems reference, http://c03.apogee.net/contentplayer/?coursetype=geo&utilityid=oge&id=6848, accessed 2014.03.21

GTK. (2010). GTK:n geoenergiatutkimukset http://viestinta2.kpakk.fi/mine/uploads/pdf/kaivosseminaari_esitykset/perjantai/kallio/kokkola040610.pdf, page 9, accessed 2014.03.22.

Gultekin, A., Aydın, M., & Sisman, A. (2014). Determination of Optimal Distance between Boreholes. https://pangea.stanford.edu/ERE/pdf/IGAstandard/SGW/2014/Gultekin.pdf, accessed 2014.03.28.

Gustafsson, A.M., Westerlund, L., Hellstro¨m, G. (2010). CFD-modelling of natural convection in a groundwater-filled borehole heat exchanger. Appl. Therm. Eng. 30, 683–691.

Hart DP, Couvillion R. (1986). Earth coupled heat transfer. Publication of the National Water Well Association.

Hellstrom G. (1991). Ground heat storage: Thermal analyses of duct storage systems. Sweden: Department of Mathematical Physics University of Lund.

ILMATIETEEN LAITOS. (2014). Energialaskennan testivuosien tuntiaineisto, http://ilmatieteenlaitos.fi/c/document_library/get_file?uuid=10e5d4a5-72cc-4755-8cd3-1b60328dfce6&groupId=30106, accessed 2014.04.01.

Lanini, F. Delaleux, X. Py, D. Nguyen. (2014). Improvement of Borehole Thermal Energy Storage Design Based on Experimental and Modelling Results, Energy and Buildings.

Laitinen, A., Tuominen, P., Holopainen, R., Tupmaala, P., Jokisalo, J., Eskola, L., Siren, K. (2014). Renewable Energy Production of Finnish Heat pumps, Final Report of the SPF-project, VTT PUBLICATIONS.

Lazzarotto, A. (2014). A network-based methodology for the simulation of borehole heat storage systems, Renewable Energy Vol. 62, pp. 265-275.

Lee, K. S. (2013). Borehole Thermal Energy storage, Underground Thermal Energy Storage, Chapter 5, Green Energy and Technology, Springer London.

Li Zhongjian, Zheng Maoyu. (2009). Development of a numerical model for the simulation of vertical U-tube ground heat exchangers. Appl Therm Eng, 29(5-6):920–4.

Luo, J., Rohn, J., Bayer, M., & Priess, A. (2013). Thermal performance and economic evaluation of double U-tube borehole heat exchanger with three different borehole diameters. Energy and Buildings, 67, 217-224.

Microelectronics Heat Transfer Laboratory. (1997). http://www.mhtl.uwaterloo.ca/old/onlinetools/airprop/airprop.html, accessed 2014.04.22

Muraya NK, O'Neal DL, Heffington WM. (1996). Thermal interference of adjacent legs in a vertical U-tube heat exchanger for a ground-coupled heat pump. ASHRAE Trans, 102(2):12–21.

REHAU. (2014). Underground thermal energy storage, http://solarthermalworld.org/sites/gstec/files/100611-1030-b-christopher_fox_-_rehau_-_underground_thermal_energy_storage.pdf, accessed 2014.04.23.

Rottmayer SP, Beckman WA, Mitchell JW. (1997). Simulation of a single vertical Utube ground heat exchanger in an infinite medium. ASHRAE Trans, 103(2):651–9.

Saljnikov, A. L. E. K. S. A. N. D. A. R., Goričanec, D. A. R. K. O., Stipić, R., Krope, J., & Kozić, Đ. (2006). Borehole and Aquifer Thermal Energy Storage and Choice of Thermal Response Test Method. In Proceedings of the 4th WSEAS International Conference on Heat Transfer, Thermal Engineering and Environment (pp. 11-15).

Sanner, B., Karytsas, C., Mendrinos, D., & Rybach, L. (2003). Current status of ground source heat pumps and underground thermal energy storage in Europe. Geothermic, 32(4), 579-588.

Sanner, B., Nordell, B. (1998). Underground thermal energy storage with heat pumps, IEA Heat Pump Center Newsletter, Vol. 16, No.2, pp10-15.

Sarbu, I., & Sebarchievici, C. (2014). General review of ground-source heat pump systems for heating and cooling of buildings. Energy and Buildings, 70, 441-454.

Seatemperature. (2014). Västanfjärd Sea Temperature, http://www.seatemperature.org/europe/finland/vastanfjard.htm, accessed 2014.07.20.

Schmidt, T., Mangold, D., Mu¨ ller-Steinhagen, H. (2003). Seasonal thermal energy storage in Germany. In: ISES Solar World Congress, 14.-19. June, Go¨teborg, Schweden.

Xu, J., Wang, R.Z., Li, Y. (2013). A review of available technologies for seasonal thermal energy storage. Solar Energy, Vol 103, pp. 610-638.

Xu, J., Y. Li, R.Z. Wang, W. Liu. (2014). Performance investigation of a solar heating system with underground seasonal energy storage for greenhouse application, Energy, Volume 67, 1 April, Pages 63-73

Yang, H., Cui, P., & Fang, Z. (2010). Vertical-borehole ground-coupled heat pumps: a review of models and systems. Applied Energy, 87(1), 16-27.

Yavuzturk C, Spitler JD, Rees SJ. (1994). A Transient two-dimensional finite volume model for the simulation of vertical U-tube ground heat exchangers. ASHRAE Trans, 105(A):465–74.

Cichong Liu
400079
cichong@aalto.fi

Zeng HY, Diao NR, Fang ZH. (2003). Efficiency of vertical geothermal heat exchangers in ground source heat pump systems. J Therm Sci, 12(1):77–81.

Cichong Liu
400079
cichong@aalto.fi

10 Appendix

10.1 Matlab Code

10.1.1 Summer iterating

```
r_ext=0.016; %m
r_int=0.013; %m
r_b=0.057; %m
m=0.05; %kg/s
D=0.0285; %m the distance of U_tube center to borehole center
T_in=40; %C
h_HTF=500;
L=180; %m
cp=4185;
%tic
i=1;
delta=zeros(82,1);
delta(1)=1000;
ql_real=zeros(90,1);
T_out_mean=zeros(90,1);
ql_start=300;
for day=1:90
    %toc
    %tic
    %display(day)
    if day>2
    ql_start=ql_real(day-1)+1;
    end
for ql=ql_start:-1:0
    r=r_b;
    z=0.5*L;
    x=1;
    T_b=zeros(90,1);
    T_out=zeros(size(T_b));
    if delta(i)<=2
        ql_real(day)=ql;
        T_out_mean(day)=T_out_bar;
        break
    end
    for d=1:day %day
```

Cichong Liu
400079
cichong@aalto.fi

```
        t=d*3600*24;
        [T_ground_z_r_t]=groundtemperature_variate( r,z,t,ql,L );
        T_b(x)=T_ground_z_r_t;
        [T_fluid_z1,T_fluid_z2,R11,R12 ] = fluidtemperature(0,T_b(x),h_HTF,r_ext,r_int,r_b,m,L,D,T_in );
        T_out(x)=T_fluid_z2;
        x=x+1;
    end
    T_out_bar=mean(T_out(T_out>0));
    ql_test=(T_in-T_out_bar)*m*cp/L;
    delta(i+1)=abs(ql-ql_test);
    i=i+1;
end
delta=zeros(292,1);
delta(1)=1000;
i=1;
end
%toc

% figure;
% [AX,H1,H2]=plotyy(1:90,T_out_mean,1:90,ql_real,'plot');
% xlabel('Days');
% title('Exiting fluid temperature,Heating rate per length VS Time');
% set(get(AX(1),'Ylabel'),'String','Exiting Temperature (C)');
% set(get(AX(2),'Ylabel'),'String','Heating rate per length (W/m)');
% set(H2,'LineStyle',':','Color','Green');
% legend('Exiting fluid temperature','Heating rate per length')

Tout=fittype('a*log(x)+b');
heatrating=fittype('c*log(x)+d');
T_outex=fit([1:90].',T_out_mean,Tout,'StartPoint',[1,T_out_mean(1)]);
a=T_outex.a;
b=T_outex.b;
heatratingex=fit([1:90].',ql_real,heatrating,'StartPoint',[1,ql_real(1)]);
c=heatratingex.c;
d=heatratingex.d;
```

Published with MATLAB? R2013b

```
function [T_ground_z_r_t] = groundtemperature_variate( r,z,t,ql,L )
%heat transfer outside borehole
```

Cichong Liu
400079
cichong@aalto.fi

```
%   ground temperature function



lamda_ground=3; %W/m.k
alfa=1.43*(10^(-6)); %m2/s
T0=5;

fun=@(l,r,z,t)(erfc(sqrt(r^2+(z-l).^2)./(2*sqrt(alfa*t)))./(sqrt(r^2+(z-l).^2))-
(erfc(sqrt(r^2+(z+l).^2)./(2*sqrt(alfa*t)))./(sqrt(r^2+(z+l).^2));

T_ground_z_r_t=(ql/(4*pi*lamda_ground))*(integral(@(l)fun(l,r,z,t),0,L))+T0;



end
```

Published with MATLAB? R2013b

```
function [ T_fluid_z1,T_fluid_z2,R11,R12 ] = fluidtemperature( z,T_b,h_HTF,r_ext,r_int,r_b,m,L,D,T_in )
%heat transfer inside borehole
%   fluid temperature function



lamda_HDPE=0.6;%W/m.k
lamda_b=1.5; %W/m.k
lamda_ground=3; %W/m.k

cp=4185; %J/KG.K



R_p=(1/(2*pi*lamda_HDPE))*log(r_ext/r_int)+1/(2*pi*r_int*h_HTF);
delta=(lamda_b-lamda_ground)/(lamda_b+lamda_ground);
R11=(1/(2*pi*lamda_b))*(log(r_b/r_ext)+delta*log((r_b^2)/(r_b^2-D^2)))+R_p;
R12=(1/(2*pi*lamda_b))*(log(r_b/(2*D))+delta*log((r_b^2)/(r_b^2+D^2)));
Z=z/L;
P=R12/R11;
beta=L/(m*cp*sqrt((R11+R12)*(R11-R12)));
Theta=zeros(size(z,2),2);
Theta(:,1)=cosh(beta*Z)-(1/sqrt(1-P^2))*(1-P*(cosh(beta)-sqrt((1-P)/(1+P))*sinh(beta))/(cosh(beta)+sqrt((1-
P)/(1+P))*sinh(beta)))*sinh(beta*Z);
Theta(:,2)=((cosh(beta)-sqrt((1-P)/(1+P))*sinh(beta))/(cosh(beta)+sqrt((1-P)/(1+P))*sinh(beta)))*cosh(beta*Z)+(1/sqrt(1-
```

Cichong Liu
400079
cichong@aalto.fi

```
P^2))*((cosh(beta)-sqrt((1-P)/(1+P))*sinh(beta))/(cosh(beta)+sqrt((1-P)/(1+P))*sinh(beta))-P)*sinh(beta*Z);
T_fluid_z=Theta*(T_in-T_b)+T_b;
T_fluid_z1=T_fluid_z(:,1);
T_fluid_z2=T_fluid_z(:,2);


end
```

Published with MATLAB? R2013b

```
function [ h_HTF ] = convection( rho,m,r_int,mu,cp,k,L)
%function to calculate the convective heat transfer coefficient of the
%circulating fluid
%



mu_w=1.79*(10^(-3));
Re=rho*m*r_int*2/mu;
Pr=cp*mu/k;
di=r_int*2;
l=L;
if Re>10000
    Nu=0.023*(Re^0.8)*(Pr^(1/3))*(mu/mu_w);
else if Re<2200
        Nu=1.86*(Re^(1/3))*(Pr^(1/3))*((di/l)^(1/3))*((mu/mu_w)^0.14);
    else
        Nu=0.116*(((Re)^(2/3))-125)*(Pr^(1/3))*(1+((di/l)^(2/3)))*((mu/mu_w)^0.14);
    end
end
h_HTF=Nu*k/(r_int*2);
end
```

Published with MATLAB? R2013b

```
function [ T_mean,T_ground_r ] = meantemperature
%UNTITLED3 Summary of this function goes here
%   Detailed explanation goes here


tic
L=180; %m


z=0.5*L;
```

Cichong Liu
400079
cichong@aalto.fi

```
[dtq] = readql;
day=1:90;
dtq=dtq(round(day),3);
x=1;
y=1;
T_ground_r=zeros(size(0.057:0.1:4.957,2),90);
for day=1:90
    t=day*3600*24;
    for r=0.057:0.1:4.957
        [T] = groundtemperature_variate( r,z,t,dtq(y),L );
        T_ground_r(x,y)=T;
        x=x+1;
    end
    x=1;
    y=y+1;
end

area=zeros(50,1);
area(1)=0.057^2;
for i=2:50
    area(i)=(0.057+(i-1)*0.1)^2-(0.057+(i-2)*0.1)^2;
end

%  r_T=zeros(size(T_ground_r,1),size(T_ground_r,2)+1);
% r_T(:,1)=0.057:0.1:4.957;
% r_T(:,2:end)=T_ground_r;
T_total=zeros(2,size(T_ground_r,2));
T_mean=zeros(2,size(T_ground_r,2));
for j=1:90
 T_total(1,j)=sum(T_ground_r(1:20,j).*area(1:20));
 T_total(2,j)=sum(T_ground_r(21:50,j).*area(21:50));
end
 T_mean(1,:)=T_total(1,:)/(1.957^2);
 T_mean(2,:)=T_total(2,:)/(4.957^2-1.957^2);
 toc
end

%
plot(0.057:0.1:4.957,T_ground_r(:,1),0.057:0.1:4.957,T_ground_r(:,30),0.057:0.1:4.957,T_ground_r(:,60),0.057:0.1:4.957,T_gro
und_r(:,90));
```

Cichong Liu
400079
cichong@aalto.fi

```
% hold on
% y11(1:20)=T_mean(1,1);
% y21(1:30)=T_mean(2,1);
% y130(1:20)=T_mean(1,30);
% y230(1:30)=T_mean(2,30);
% y160(1:20)=T_mean(1,60);
% y260(1:30)=T_mean(2,60);
% y190(1:20)=T_mean(1,90);
% y290(1:30)=T_mean(2,90);
% x1=0.057:0.1:1.957;
% x2=2.057:0.1:4.957;
% plot(x1,y11,'--',x1,y130,'--',x1,y160,'--',x1,y190,'--')
% plot(x2,y21,'--',x2,y230,'--',x2,y260,'--',x2,y290,'--')
% xlabel('Horizontal Distance (m)')
% ylabel('Temperature (C)')
% legend('Day 1','Day 30', 'Day 60', 'Day 90')
```

Published with MATLAB? R2013b

```
function [output ] = readql
%UNTITLED2 Summary of this function goes here
%   Detailed explanation goes here

load('ql_real');
load('T_out_mean');
output=zeros(size(ql_real,1),3);
output(:,1)=1:90;
output(:,2)=T_out_mean;
output(:,3)=ql_real;
end
```

Published with MATLAB? R2013b

10.1.2 Winter iterating

```
r_ext=0.016; %m
r_int=0.013; %m
r_b=0.057; %m
m=0.5; %kg/s
D=0.0285; %m the distance of U_tube center to borehole center
T_in=-3; %C
h_HTF=2636;
```

Cichong Liu
400079
cichong@aalto.fi

```
L=180; %m
cp=4185;
z=0.5*L;
%[T_mean]=meantemperature;
x=1;
y=1;
delta=zeros(300,1);
ql_real=zeros(270,90);
T_out_mean=zeros(size(ql_real));
delta(1)=1000;
i=1;
ql_start=0;
tic
for summer_day=1:90
    %T0=T_mean(1,summer_day);
    T0=5;
    toc
    display(summer_day);
    tic
    for d=[1:9 10:5:30 40:10:270]
        if summer_day>=2
        ql_start=ql_real(d,summer_day-1)+1;
        end
        for ql=ql_start:-1:-2500
            T_out=zeros(d,1);
            j=1;

            x=1;
            for day1=1:d
                t=day1*3600*24;
                [T_b] = wintergroundtemperature( r_b,z,t,ql,L,T0 );
                if T_b <=T_in
                    break
                end
                [T_fluid_z1,T_fluid_z2,R11,R12 ] = winterfluidtemperature( 0,T_b,h_HTF,r_ext,r_int,r_b,m,L,D,T_in );
                T_out(day1)=T_fluid_z2;
                x=x+1;
                j=j+1;
            end
            T_out_bar=mean(T_out);%(T_out~=0));
```

Cichong Liu
400079
cichong@aalto.fi

```
            ql_test=(T_in-T_out_bar)*m*cp/L;
            delta(i+1)=abs(ql_test-ql);
            i=i+1;
            if delta(i)<=2
                ql_real(x-1,y)=ql;
                T_out_mean(x-1,y)=T_out_bar;
                break
            end
        end
        delta=zeros(300,1);
        delta(1)=1000;
        i=1;
    end
    y=y+1;
end
toc
```

Published with MATLAB? R2013b

```
function [T_ground_z_r_t] = wintergroundtemperature( r,z,t,ql,L,T0  )
%heat transfer outside borehole
%   ground temperature
lamda_ground=3; %W/m.k
alfa=1.43*(10^(-6)); %m2/s
% h=t_summer/3600;
% ql_summer=234.2*((h/24)^(-0.077));

fun=@(l,r,z,t)(erfc(sqrt(r^2+(z-l).^2)./(2*sqrt(alfa*t)))./(sqrt(r^2+(z-l).^2))-
(erfc(sqrt(r^2+(z+l).^2)./(2*sqrt(alfa*t)))./(sqrt(r^2+(z+l).^2));

T_ground_z_r_t=(ql/(4*pi*lamda_ground)).*(integral(@(l)fun(l,r,z,t),0,L))+T0;

end
```

Published with MATLAB? R2013b

```
function [ T_fluid_z1,T_fluid_z2,R11,R12 ] = winterfluidtemperature( z,T_b,h_HTF,r_ext,r_int,r_b,m,L,D,T_in )
%heat transfer inside borehole
%   fluid temperature inside U-tube
lamda_HDPE=0.6;%W/m.k
lamda_b=1.5; %W/m.k
lamda_ground=3; %W/m.k
```

Cichong Liu
400079
cichong@aalto.fi

```
cp=4185; %J/KG.K


R_p=(1/(2*pi*lamda_HDPE))*log(r_ext/r_int)+1/(2*pi*r_int*h_HTF);
delta=(lamda_b-lamda_ground)/(lamda_b+lamda_ground);
R11=(1/(2*pi*lamda_b))*(log(r_b/r_ext)+delta*log((r_b^2)/(r_b^2-D^2)))+R_p;
R12=(1/(2*pi*lamda_b))*(log(r_b/(2*D))+delta*log((r_b^2)/(r_b^2+D^2)));
Z=z/L;
P=R12/R11;
beta=L/(m*cp*sqrt((R11+R12)*(R11-R12)));
Theta=zeros(size(z,2),2);
Theta(:,1)=cosh(beta*Z)-(1/sqrt(1-P^2))*(1-P*(cosh(beta)-sqrt((1-P)/(1+P))*sinh(beta))/(cosh(beta)+sqrt((1-
P)/(1+P))*sinh(beta)))*sinh(beta*Z);
Theta(:,2)=((cosh(beta)-sqrt((1-P)/(1+P))*sinh(beta))/(cosh(beta)+sqrt((1-P)/(1+P))*sinh(beta)))*cosh(beta*Z)+(1/sqrt(1-
P^2))*((cosh(beta)-sqrt((1-P)/(1+P))*sinh(beta))/(cosh(beta)+sqrt((1-P)/(1+P))*sinh(beta))-P)*sinh(beta*Z);
T_fluid_z=T_b-Theta*(T_b-T_in);
T_fluid_z1=T_fluid_z(:,1);
T_fluid_z2=T_fluid_z(:,2);


end
```

Published with MATLAB? R2013b

```
a=zeros(90,1);
b=zeros(90,1);
c=zeros(90,1);
d=zeros(90,1);
ql_real_winter1=zeros(270,90);
T_out_winter1=zeros(270,90);
f=fittype('aa*log(x)+bb');
f2=fittype('cc*log(x)+dd');
x=[1:9 10:5:30 40:10:270].';
for i=1:90
    y=ql_real(ql_real(:,i)<0,i);
    g=fit(x,y,f,'StartPoint',[x(1) y(1)]);
    y2=T_out_mean(T_out_mean(:,i)~=0,i);
    g2=fit(x,y2,f2,'StartPoint',[x(1) y2(1)]);
    a(i)=g.aa;
    b(i)=g.bb;
    c(i)=g2.cc;
    d(i)=g2.dd;
```

Cichong Liu
400079
cichong@aalto.fi

```
    ql_real_winter1(:,i)=round(feval(g,1:270));
    T_out_winter1(:,i)=round(feval(g2,1:270));
end



% plotyy(1:90,a,1:90,b);

afit=fittype('a1*log(x)+a2');
fita=fit([1:90].',a,afit,'StartPoint',[1 a(1)]);
a1=fita.a1;
a2=fita.a2;
bfit=fittype('b1*log(x)+b2');
fitb=fit([1:90].',b,bfit,'StartPoint',[1 b(1)]);
b1=fitb.b1;
b2=fitb.b2;

cfit=fittype('c1*log(x)+c2');
fitc=fit([1:90].',c,cfit,'StartPoint',[1 c(1)]');
c1=fitc.c1;
c2=fitc.c2;
dfit=fittype('d1*log(x)+d2');
fitd=fit([1:90].',d,dfit,'StartPoint',[1 d(1)]');
d1=fitd.d1;
d2=fitd.d2;
```

Published with MATLAB? R2013b

```
load('winterinterpolating', 'ql_real_winter1');
tic
%load('T_out_mean');
L=180; %m
z=0.5*L; %m
T_ground=zeros(size(0.057:0.1:1.957,2),1);
T_ground_mean=zeros(270,90);
x=1;
[T_mean]=meantemperature;
area=zeros(20,1);
area(1)=0.057^2;
T_ground_record=zeros(9,50);
for s=2:20
```

Cichong Liu
400079
cichong@aalto.fi

```
    area(s)=(0.057+(s-1)*0.1)^2-(0.057+(s-2)*0.1)^2;
end
for i=1:270
    if rem(i,27)==0;
        toc
        display(i)
        tic
    end
    for j=1:90;
        ql=ql_real_winter1(i,j);
        t=i*3600*24;
        T0=T_mean(1,j);
        for r=0.057:0.1:1.957
        [T_ground(x)] = wintergroundtemperature( r,z,t,ql,L,T0 );
        x=x+1;
        end
        T_ground_mean(i,j)=(sum(T_ground.*area))/(1.957^2);
        x=1;
    end
end
q=1;
p=1;
for m=90:90:270
    for n=30:30:90
        ql=ql_real_winter1(m,n);
        t=m*3600*24;
        T0=T_mean(1,n);
        for r=0.057:0.1:4.957
            [T_ground_record(p,q)] = wintergroundtemperature( r,z,t,ql,L,T0 );
            q=q+1;
        end
        q=1;
        p=p+1; %1-90,30;2-90,60;3-90,90;4-180,30;5-180,60;6-180,90;7-270,30...
    end
end
y=zeros(50,3);
y(:,1)=T_mean(1,30);
y(:,2)=T_mean(1,60);
y(:,3)=T_mean(1,90);
figure;
```

Cichong Liu
400079
cichong@aalto.fi

```
s(1)=subplot(1,3,1);
plot(s(1),0.057:0.1:4.957,T_ground_record([1 4 7],:),0.057:0.1:4.957,y(:,1),'--');
title('SD 30');
ylabel('Ground Temperature (C)');
s(2)=subplot(1,3,2);
plot(s(2),0.057:0.1:4.957,T_ground_record([2 5 8],:),0.057:0.1:4.957,y(:,2),'--');
xlabel('Horizontal Distance (m)');
ylabel('Ground Temperature (C)');
title('SD 60');
s(3)=subplot(1,3,3);
plot(s(3),0.057:0.1:4.957,T_ground_record([3 6 9],:),0.057:0.1:4.957,y(:,3),'--');
ylabel('Ground Temperature (C)');
hleg=legend('WD 90','WD 180','WD 270','To');set(hleg,'Location','NorthEastOutside')
title('SD 90');
ql_real_ex=zeros(25,10);
ql_real_ex=ql_real_winter1([1:10 15:5:30 40:10:60 80:20:120 150:30:270],[1 10:10:90]);
T_out_mean_ex=zeros(size(ql_real_ex));
T_out_mean_ex=T_out_mean([1:10 15:5:30 40:10:60 80:20:120 150:30:270],[1 10:10:90]);
T_ground_mean_ex=zeros(7,10);
T_ground_mean_ex=T_ground_mean([1 10 40 90 150 210 270], [1 10:10:90]);


toc
```

Published with MATLAB? R2013b

10.1.3 Economic analysis

```
clear
load('Q_heat.mat')
Q_heat=Q_heat/1000000;
money_made=zeros(3673,5088);
money=zeros(50,1);
a=zeros(size(money));
b=zeros(size(money));
C_summer=0;
C_winter=120;
C_electricity=88;
%COP=3;
Q_heat_summer=Q_heat(1:3673);
Q_heat_winter=Q_heat(3674:8761);
m=0.5;
```

Cichong Liu
400079
cichong@aalto.fi

```
c=4185*(10^(-6));
T_in=60;
T_out=40;
tic
for n=1:50
    display(n)
    toc
    tic
    for t1=1:3673
%         display(t1)
        ql_summer=(35.88*(t1/24)^(-0.024))/10000; %
        Q_heat_summer_copy=Q_heat_summer(1:t1);
        q_heat_summer=zeros(1,0);
        q_heat_summer=ql_summer*n;
        q_heat_summer=min(q_heat_summer,1-Q_heat_summer_copy);
        nn=floor(q_heat_summer/ql_summer);
        paid=sum(C_summer*nn*m*c*(T_in-T_out));
        for t2=3674:8761
%             display(t2)
            %ql_winter=-((0.1387*log(t1/24)+1.5767)*log((t2-3673)/24)-2.3818*log(t1/24)-27.8923)/10000; %
            ql_winter=-(0.5251*log((t2-3673)/24)-10.134)/10000;
            Q_heat_winter_copy=Q_heat_winter(1:t2-3673);
            q_heat_winter=zeros(1,0);
            [COP]=COP_cal(t1,t2);
            q_heat_winter=ql_winter*n*(COP/(COP-1));
            q_heat_winter=min(q_heat_winter,Q_heat_winter_copy);
            paid_back=sum(q_heat_winter*C_winter-q_heat_winter*(1/COP)*C_electricity);
            money_made(t1,t2-3673)=paid_back-paid;
        end
    end
    [C,I]=max(money_made);
    [money(n),b(n)]=max(C);
    a(n)=I(b(n));
    money_made=zeros(3673,5088);
end
toc
year=zeros(size(money));
for i=1:size(year,1)
    %ql_summer=(234.2*((a(i)/24)^(-0.077)))/10000;
    ql_winter=-(0.5251*log((8761-3673)/24)-10.134)/10000;
```

Cichong Liu
400079
cichong@aalto.fi

```
    year(i)=2161000*i*ql_winter/money(i);
end
```

Published with MATLAB? R2013b

```
function [ COP ] = COP_cal( st,wt)
%COP calculation
% T_exit=(-0.0117*log(st/24)-0.1433)*log((wt-3673)/24)+0.2032*log(st/24)-0.4974;
T_exit=-0.032*log((wt-3673)/24)+2.5591;
if T_exit>=10
    COP=4.2;
else if T_exit>=8
        COP=3.9;
    else if T_exit>=6
            COP=3.6;
        else if T_exit>=4
                COP=3.3;
            else
                COP=3;
            end
        end
    end
end

end
```

Published with MATLAB? R2013b

10.1.4 Turku case analysis

```
clear
load('Q_heat.mat')
Q_heat=Q_heat/1000000;
money_made=zeros(5088,1);
% money=zeros(50,1);
% a=zeros(size(money));

C_summer=0;
C_winter=120;
C_electricity=88;
%COP=3;
Q_heat_summer=Q_heat(1:3673);
Q_heat_winter=Q_heat(3674:8761);
```

Cichong Liu
400079
cichong@aalto.fi

```
m=0.05;
c=4185*(10^(-6));
T_in=60;
T_out=40;
tic
% for n=1:50
%     display(n)
    toc
    tic
%     for t1=1:3673
%         display(t1)
%         ql_summer=(35.88*(t1/24)^(-0.024))/10000; %
        Q_heat_summer_copy=Q_heat_summer(1:3673);
%         q_heat_summer=zeros(1,0);
        num=round(Q_heat_summer_copy/((60-40)*c*m));
        num_max=max(num);
        borehole=zeros(num_max,1);
        q_heat_summer=zeros(size(borehole));
        summer_hour=zeros(size(borehole));
        money=zeros(num_max,1);
        b=zeros(size(money));
        for i=num_max:-1:1
        borehole(i)=size(find(num==i),1);
        summer_hour(i)=sum(borehole(i:num_max));
        %q_heat_summer(i)=(35.88*(summer_hour(i)/24)^(-0.024))/10000;
        end
%         q_heat_summer=ql_summer*num;
for n=1:num_max
    t1=summer_hour(1:n).';
    for t2=[4000:1000:8000 8761]
        %             display(t2)
        ql_winter=-((0.1387*log(t1/24)+1.5767)*log((t2-3673)/24)-2.3818*log(t1/24)-27.8923)/10000; %
        %             ql_winter=-(0.5251*log((t2-3673)/24)-10.134)/10000;
        Q_heat_winter_copy=Q_heat_winter(1:t2-3673);
%         q_heat_winter=zeros(1,0);
        %             [COP]=COP_cal(t1,t2);
        COP=2.8;
        q_heat_winter=sum(ql_winter*(COP/(COP-1)));
        q_heat_winter=min(q_heat_winter,Q_heat_winter_copy);
        paid_back=sum(q_heat_winter*C_winter-q_heat_winter*(1/COP)*C_electricity);
```

Cichong Liu
400079
cichong@aalto.fi

```
            money_made(t2-3673)=paid_back;
        end
        %       end
        [C,I]=max(money_made);
    %     [money(n),b(n)]=max(C);
    %     a(n)=I(b(n));
        b(n)=I;
        money(n)=C;
        money_made=zeros(5088,1);
    end
    year=zeros(size(money));
    q_heat_summer=zeros(1,1);
    for ii=1:size(year,1)
        q_heat_summer(1:ii)=(35.88*(summer_hour(1:ii)/24).^(-0.024))/10000;
        year(ii)=sum(2161000*q_heat_summer)/money(ii);
        q_heat_summer=zeros(ii+1,1);
    end
    % end
```

Published with MATLAB? R2013b

10.2 Scenario Results

10.2.1 Scenario 1 (mass flow rate in summer = 0.1kg/s, mass flow rate in winter =0.5 kg/s)

In Scenario 1, case for mass flow rate in summer =0.1kg/s and mass flow rate in winter still remaining 0.5 kg/s is analyzed.

Figure 27 shows the mean exiting fluid temperature and mean heating rate per length in summer time. And equation (40) and (41) show the equations predicting the mean exiting fluid temperature and mean heating rate per length in Scenario 1.

Cichong Liu
400079
cichong@aalto.fi

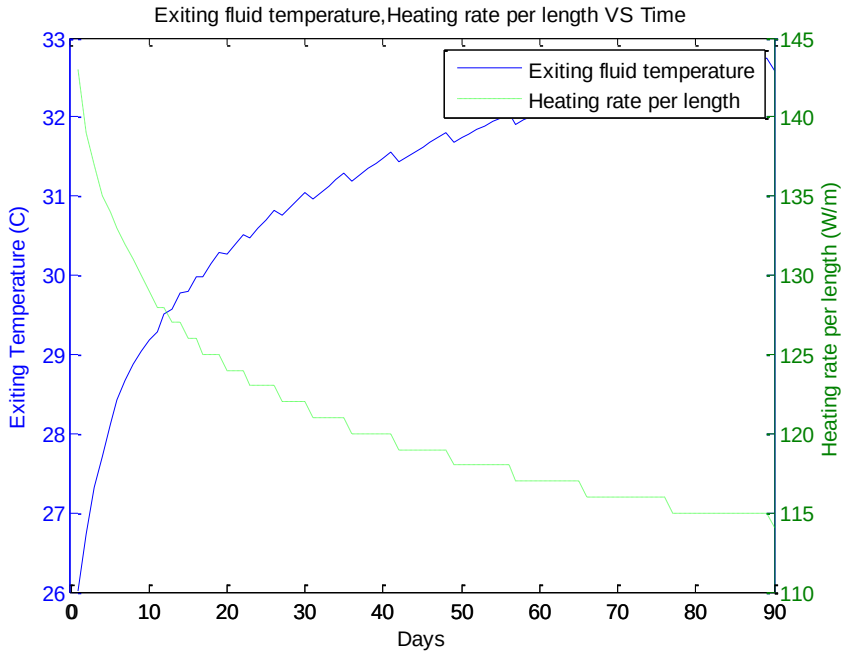

Figure 27. Mean exiting fluid temperature, Mean heating rate per length versus Time

$$T_{exit}\,[°C] = 1.5631 \ln\left(\frac{h\,[h]}{24}\right) + 25.6514 \quad (40)$$

$$q_l[W/m] = 145.34\left(\frac{h\,[h]}{24}\right)^{-0.053} \quad (41)$$

Cichong Liu
400079
cichong@aalto.fi

Figure 28 below shows the ground temperature distribution after summer and the newly adjusted initial ground temperature for winter time.

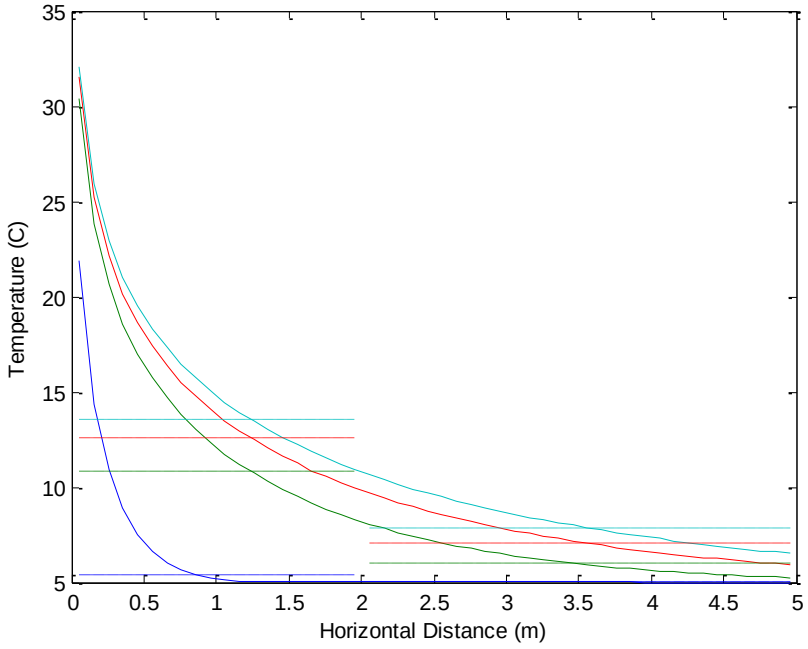

Figure 28. Ground temperature distribution around the boreholes and newly adjusted temperature

Table 32 and Table 33 show the cooling rate per length and the mean exiting temperature of the circulating fluid from the U-tube respectively and equation (42) and (43) present the predicting function for cooling rate per length and exiting fluid temperature.

$$q_l\,[W/m] = \left(0.5566 \ln\left(\frac{Sh\,[h]}{24}\right) + 0.3375\right) \cdot \ln\left(\frac{Wh\,[h] - 3672}{24}\right) - 9.1006 \ln\left(\frac{Sh\,[h]}{24}\right) - 6.9330 \quad (42)$$

$$T_{exit}\,[°C] = \left(-0.0269 \ln\left(\frac{Sh\,[h]}{24}\right) - 0.0201\right) \cdot \ln\left(\frac{Wh\,[h] - 3672}{24}\right) + 0.4357 \ln\left(\frac{Sh\,[h]}{24}\right) + \mathbf{2.3323} \quad (43)$$

Table 32. Cooling rate per length as a function of summer and winter time (SD stands for Summer Day and WD stands for Winter Day)

	SD1	SD10	SD20	SD30	SD40	SD50	SD60	SD70	SD80	SD90
W D 1	-15	-26	-33	-37	-40	-43	-44	-46	-48	-49
W D 2	-14	-25	-32	-36	-39	-41	-43	-44	-46	-47
W D 3	-14	-25	-31	-35	-38	-40	-41	-43	-44	-45
W D 4	-14	-24	-30	-34	-37	-39	-41	-42	-44	-45
W D 5	-13	-24	-30	-34	-36	-39	-40	-42	-43	-44

Cichong Liu
400079
cichong@aalto.fi

W D 6	-13	-24	-30	-33	-36	-38	-40	-41	-42	-43
W D 7	-13	-23	-29	-33	-36	-38	-39	-41	-42	-43
W D 8	-13	-23	-29	-33	-35	-37	-39	-40	-42	-43
W D 9	-13	-23	-29	-33	-35	-37	-39	-40	-41	-42
W D 10	-13	-23	-29	-32	-35	-37	-38	-40	-41	-42
W D 15	-12	-22	-28	-31	-34	-36	-37	-39	-40	-41
W D 20	-12	-22	-27	-31	-33	-35	-36	-38	-39	-40
W D 25	-12	-21	-27	-30	-33	-34	-36	-37	-38	-39
W D 30	-12	-21	-27	-30	-32	-34	-35	-37	-38	-39
W D 40	-12	-21	-26	-29	-32	-33	-35	-36	-37	-38
W D 50	-11	-20	-26	-29	-31	-33	-34	-35	-36	-37
W D 60	-11	-20	-25	-28	-31	-32	-34	-35	-36	-37
W D 80	-11	-20	-25	-28	-30	-32	-33	-34	-35	-36
WD100	-11	-19	-24	-27	-29	-31	-32	-33	-34	-35
WD120	-11	-19	-24	-27	-29	-31	-32	-33	-34	-35
WD150	-10	-19	-23	-26	-28	-30	-31	-32	-33	-34
WD180	-10	-18	-23	-26	-28	-29	-31	-32	-33	-34
WD210	-10	-18	-23	-26	-28	-29	-30	-31	-32	-33
WD240	-10	-18	-22	-25	-27	-29	-30	-31	-32	-33
WD270	-10	-18	-22	-25	-27	-28	-30	-31	-32	-32

Table 33. Mean exiting fluid temperature as a function of summer and winter time (SD stands for Summer Day and WD stands for Winter Day)

	SD1	SD10	SD20	SD30	SD40	SD50	SD60	SD70	SD80	SD90
W D 1	2.68	3.29	3.58	3.80	3.95	4.01	4.15	4.21	4.28	4.34
W D 2	2.68	3.20	3.52	3.73	3.86	3.96	4.05	4.14	4.17	4.22
W D 3	2.64	3.18	3.49	3.69	3.81	3.91	3.99	4.09	4.10	4.16
W D 4	2.62	3.19	3.43	3.67	3.79	3.89	3.96	4.05	4.07	4.12
W D 5	2.65	3.15	3.44	3.62	3.73	3.82	3.95	3.98	4.05	4.10
W D 6	2.63	3.12	3.39	3.57	3.73	3.83	3.89	3.98	4.05	4.10
W D 7	2.62	3.15	3.42	3.59	3.69	3.78	3.90	3.93	4.00	4.04
W D 8	2.61	3.12	3.39	3.55	3.71	3.80	3.86	3.95	3.95	4.00
W D 9	2.59	3.10	3.36	3.52	3.68	3.76	3.82	3.91	3.97	4.02
W D 10	2.58	3.08	3.33	3.55	3.65	3.73	3.85	3.87	3.94	3.98
W D 15	2.58	3.04	3.30	3.50	3.60	3.68	3.80	3.82	3.87	3.92
W D 20	2.58	3.01	3.29	3.42	3.57	3.64	3.75	3.77	3.82	3.86
W D 25	2.55	3.01	3.27	3.40	3.55	3.60	3.72	3.77	3.79	3.86
W D 30	2.53	3.00	3.26	3.38	3.52	3.58	3.69	3.77	3.75	3.85
W D 40	2.50	2.95	3.19	3.37	3.51	3.56	3.67	3.67	3.72	3.75
W D 50	2.56	2.98	3.22	3.31	3.44	3.57	3.60	3.67	3.72	3.74
W D 60	2.54	2.94	3.17	3.34	3.46	3.51	3.62	3.61	3.65	3.76
W D 80	2.51	2.89	3.19	3.32	3.38	3.51	3.52	3.59	3.63	3.66

Cichong Liu
400079
cichong@aalto.fi

WD100	2.49	2.93	3.13	3.29	3.40	3.44	3.50	3.60	3.64	3.66
WD120	2.47	2.90	3.09	3.24	3.35	3.47	3.48	3.54	3.58	3.60
WD150	2.45	2.86	3.13	3.27	3.37	3.40	3.50	3.56	3.59	3.61
WD180	2.52	2.82	3.09	3.22	3.32	3.35	3.44	3.50	3.53	3.55
WD210	2.50	2.89	3.05	3.18	3.28	3.40	3.39	3.45	3.58	3.59
WD240	2.49	2.86	3.02	3.24	3.34	3.36	3.45	3.50	3.53	3.54
WD270	2.48	2.84	2.98	3.21	3.31	3.32	3.41	3.47	3.50	3.51

10.2.2 Scenario 2 (mass flow rate in summer = 1 kg/s, mass flow rate in winter = 0.5 kg/s)

In Scenario 2, case for mass flow rate in summer =1 kg/s while mass flow rate in winter still remaining 0.5 kg/s is analyzed.

Figure 29 shows the mean exiting fluid temperature and mean heating rate per length in summer time. And equation (44) and (45) shows the equations predicting the mean exiting fluid temperature and mean heating rate per length in Scenario 2.

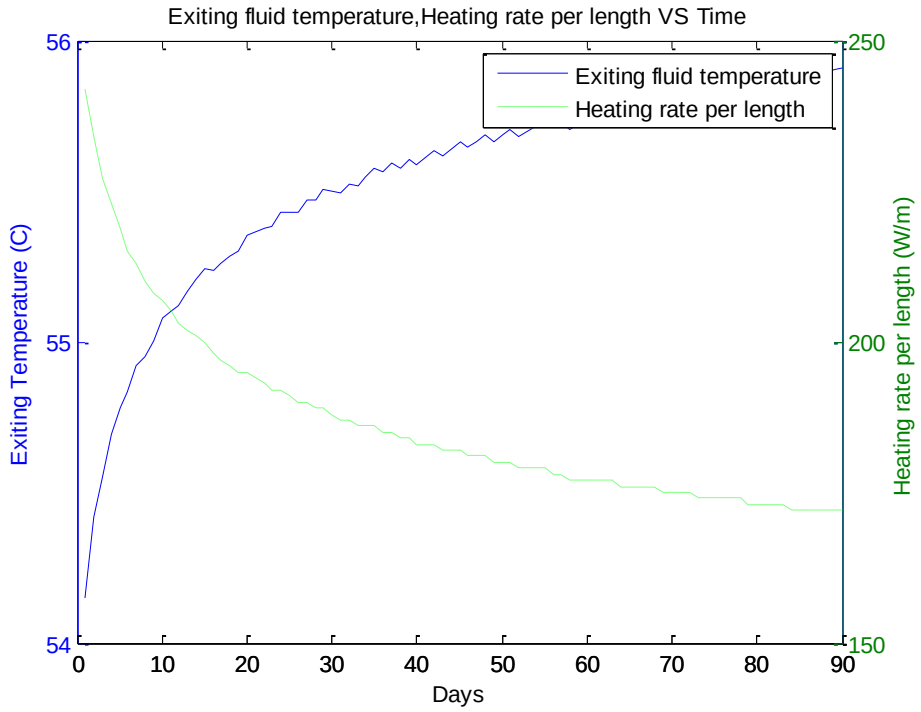

Figure 29. Mean exiting fluid temperature, Mean heating rate per length versus Time

$$T_{exit}\,[°C] = 0.3865 \ln\left(\frac{h\,[h]}{24}\right) + 54.1685 \quad (44)$$

$$q_l[W/m] = 248.55\left(\frac{h\,[h]}{24}\right)^{-0.082} \quad (45)$$

Cichong Liu
400079
cichong@aalto.fi

Figure 30 below shows the ground temperature distribution after summer and the newly adjusted initial ground temperature for winter time.

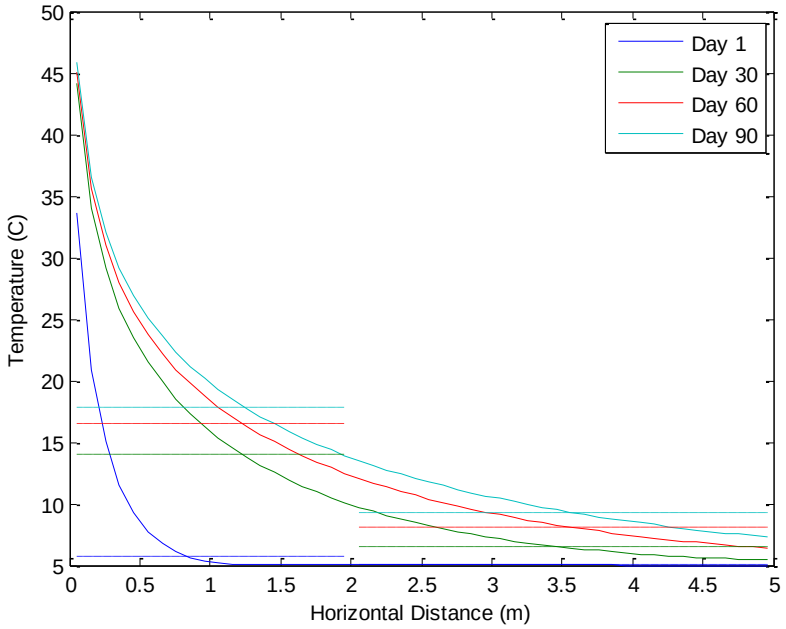

Figure 30. Ground temperature distribution around the boreholes and newly adjusted temperature

Table 34 and Table 35 show the cooling rate per length and the mean exiting temperature of the circulating fluid from the U-tube respectively and equation (46) and (47) present the predicting function for cooling rate per length and exiting fluid temperature.

$$q_l[°C] = \left(0.8150 \ln\left(\frac{Sh\,[h]}{24}\right) + 0.2713\right) \cdot \ln\left(\frac{Wh\,[h] - 3672}{24}\right) - 13.3214 \ln\left(\frac{Sh\,[h]}{24}\right) - 4.7938 \quad (46)$$

$$T_{exit}[W/m] = \left(-0.0393 \ln\left(\frac{Sh\,[h]}{24}\right) - 4.7938\right) \cdot \ln\left(\frac{Wh\,[h] - 3672}{24}\right) + 0.6382 \ln\left(\frac{Sh\,[h]}{24}\right) + 2.2746 \quad (47)$$

Table 34. Cooling rate per length as a function of summer and winter time (SD stands for Summer Day and WD stands for Winter Day)

	SD1	SD10	SD20	SD30	SD40	SD50	SD60	SD70	SD80	SD90
WD 1	-15	-34	-44	-50	-54	-57	-60	-62	-64	-66
WD 2	-14	-32	-42	-48	-51	-55	-57	-59	-61	-63
WD 3	-14	-31	-41	-46	-50	-53	-56	-58	-60	-61
WD 4	-14	-31	-40	-46	-49	-52	-55	-57	-58	-60

Cichong Liu
400079
cichong@aalto.fi

W D 5	-13	-30	-39	-45	-49	-52	-54	-56	-58	-59
W D 6	-13	-30	-39	-44	-48	-51	-53	-55	-57	-58
W D 7	-13	-30	-38	-44	-47	-50	-53	-55	-56	-58
W D 8	-13	-29	-38	-43	-47	-50	-52	-54	-56	-57
W D 9	-13	-29	-38	-43	-47	-50	-52	-54	-55	-57
W D 10	-13	-29	-37	-43	-46	-49	-51	-53	-55	-56
W D 15	-12	-28	-36	-42	-45	-48	-50	-52	-53	-55
W D 20	-12	-28	-36	-41	-44	-47	-49	-51	-52	-54
W D 25	-12	-27	-35	-40	-43	-46	-48	-50	-51	-53
W D 30	-12	-27	-35	-39	-43	-45	-47	-49	-51	-52
W D 40	-12	-26	-34	-39	-42	-44	-46	-48	-49	-51
W D 50	-11	-26	-33	-38	-41	-44	-45	-47	-49	-50
W D 60	-11	-25	-33	-37	-40	-43	-45	-47	-48	-49
W D 80	-11	-25	-32	-36	-39	-42	-44	-45	-47	-48
WD100	-11	-24	-31	-36	-39	-41	-43	-45	-46	-47
WD120	-11	-24	-31	-35	-38	-40	-42	-44	-45	-46
WD150	-10	-23	-30	-34	-37	-40	-41	-43	-44	-46
WD180	-10	-23	-30	-34	-37	-39	-41	-42	-44	-45
WD210	-10	-23	-29	-33	-36	-39	-40	-42	-43	-44
WD240	-10	-23	-29	-33	-36	-38	-40	-41	-43	-44
WD270	-10	-22	-29	-33	-35	-38	-39	-41	-42	-43

Table 35. Mean exiting fluid temperature as a function of summer and winter time (SD stands for Summer Day and WD stands for Winter Day)

	SD1	SD10	SD20	SD30	SD40	SD50	SD60	SD70	SD80	SD90
W D 1	2.74	3.64	4.11	4.40	4.61	4.78	4.88	5.00	5.08	5.16
W D 2	2.73	3.61	4.05	4.32	4.51	4.68	4.82	4.88	5.00	5.08
W D 3	2.70	3.53	4.00	4.25	4.48	4.59	4.72	4.83	4.90	4.97
W D 4	2.67	3.52	3.97	4.21	4.43	4.53	4.66	4.77	4.83	4.95
W D 5	2.70	3.52	3.96	4.18	4.35	4.50	4.63	4.73	4.79	4.90
W D 6	2.68	3.48	3.90	4.18	4.34	4.48	4.61	4.70	4.76	4.82
W D 7	2.67	3.44	3.91	4.12	4.34	4.48	4.54	4.63	4.75	4.80
W D 8	2.65	3.47	3.87	4.13	4.28	4.42	4.54	4.63	4.69	4.80
W D 9	2.64	3.44	3.83	4.09	4.24	4.43	4.49	4.58	4.69	4.74
W D 10	2.63	3.41	3.86	4.05	4.26	4.39	4.50	4.59	4.64	4.75
W D 15	2.62	3.39	3.81	4.02	4.18	4.31	4.45	4.52	4.57	4.66
W D 20	2.61	3.37	3.76	3.98	4.10	4.28	4.39	4.46	4.50	4.60
W D 25	2.59	3.36	3.73	3.94	4.09	4.23	4.32	4.42	4.48	4.53
W D 30	2.57	3.34	3.70	3.90	4.08	4.18	4.27	4.34	4.44	4.47
W D 40	2.61	3.26	3.60	3.87	4.04	4.13	4.22	4.28	4.38	4.48
W D 50	2.58	3.28	3.61	3.86	3.95	4.11	4.19	4.25	4.35	4.37

Cichong Liu
400079
cichong@aalto.fi

WD60	2.56	3.24	3.55	3.80	3.95	4.03	4.19	4.25	4.34	4.35
WD80	2.53	3.17	3.53	3.77	3.92	3.99	4.15	4.20	4.29	4.30
WD100	2.51	3.19	3.55	3.69	3.83	3.98	4.05	4.18	4.18	4.27
WD120	2.49	3.15	3.49	3.71	3.84	3.99	4.06	4.10	4.18	4.27
WD150	2.55	3.18	3.51	3.72	3.85	3.90	4.05	4.09	4.17	4.17
WD180	2.53	3.14	3.45	3.65	3.78	3.91	3.97	4.10	4.09	4.17
WD210	2.52	3.10	3.40	3.60	3.81	3.85	4.00	4.03	4.11	4.19
WD240	2.50	3.07	3.46	3.65	3.76	3.89	3.95	3.97	4.05	4.13
WD270	2.49	3.14	3.42	3.61	3.72	3.85	3.90	4.02	4.09	4.08

10.2.3 Scenario 3 (mass flow rate in summer = 0.5 kg/s, winter mass flow rate in winter = 0.1 kg/s)

In Scenario 3, case for mass flow rate in winter = 0.1 kg/s while mass flow rate in summer remaining 0.5 kg/s is analyzed.

Since the conditions are exactly same as the baseline scenario in summer, the heating rate per length and the exiting fluid temperature equations are the same as equations (14) and (15). And the ground temperature distribution after summer also remains the same as figure 16.

However, in winter, the change in mass flow rate results in a change in the exiting fluid temperature of cooling rate in winter. Table 36 and Table 37 show the cooling rate per length and the mean exiting temperature of the circulating fluid from the U-tube respectively and equation (48) and (49) present the predicting function for cooling rate per length and exiting fluid temperature.

$$q_l\,[\mathrm{W/m}] = \left(0.3537 \ln\left(\frac{\mathrm{Sh\,[h]}}{24}\right) + 0.0892\right) \cdot \ln\left(\frac{\mathrm{Wh\,[h]} - 3672}{24}\right) - 7.9872 \ln\left(\frac{\mathrm{Sh\,[h]}}{24}\right) - 2.56 \quad (48)$$

$$T_{exit}\,[°\mathrm{C}] = \left(-0.0842 \ln\left(\frac{\mathrm{Sh\,[h]}}{24}\right) - 0.0325\right) \cdot \ln\left(\frac{\mathrm{Wh\,[h]} - 3672}{24}\right) + 1.9070 \ln\left(\frac{\mathrm{Sh\,[h]}}{24}\right) + 2.9290 \quad (49)$$

Table 36. Cooling rate per length as a function of summer and winter time (SD stands for Summer Day and WD stands for Winter Day)

	SD1	SD10	SD20	SD30	SD40	SD50	SD60	SD70	SD80	SD90
WD1	-8	-20	-26	-30	-32	-34	-35	-37	-38	-39
WD2	-8	-19	-25	-29	-31	-33	-34	-36	-37	-38
WD3	-8	-19	-25	-28	-31	-32	-34	-35	-36	-37
WD4	-8	-19	-24	-28	-30	-32	-33	-34	-36	-37
WD5	-8	-18	-24	-27	-30	-32	-33	-34	-35	-36
WD6	-8	-18	-24	-27	-30	-31	-33	-34	-35	-36
WD7	-8	-18	-24	-27	-29	-31	-32	-34	-35	-36

Cichong Liu
400079
cichong@aalto.fi

W D 8	-8	-18	-24	-27	-29	-31	-32	-33	-35	-35
W D 9	-8	-18	-23	-27	-29	-31	-32	-33	-34	-35
W D 10	-8	-18	-23	-27	-29	-31	-32	-33	-34	-35
W D 15	-8	-17	-23	-26	-28	-30	-31	-32	-33	-34
W D 20	-7	-17	-22	-26	-28	-30	-31	-32	-33	-34
W D 25	-7	-17	-22	-25	-28	-29	-30	-32	-33	-33
W D 30	-7	-17	-22	-25	-27	-29	-30	-31	-32	-33
W D 40	-7	-17	-22	-25	-27	-29	-30	-31	-32	-33
W D 50	-7	-16	-21	-25	-27	-28	-29	-30	-31	-32
W D 60	-7	-16	-21	-24	-26	-28	-29	-30	-31	-32
W D 80	-7	-16	-21	-24	-26	-27	-29	-30	-31	-31
WD100	-7	-16	-21	-24	-26	-27	-28	-29	-30	-31
WD120	-7	-16	-21	-23	-25	-27	-28	-29	-30	-31
WD150	-7	-15	-20	-23	-25	-27	-28	-29	-30	-30
WD180	-7	-15	-20	-23	-25	-26	-27	-28	-29	-30
WD210	-7	-15	-20	-23	-25	-26	-27	-28	-29	-30
WD240	-7	-15	-20	-22	-25	-26	-27	-28	-29	-30
WD270	-7	-15	-20	-22	-24	-26	-27	-28	-29	-29

Table 37. Mean exiting fluid temperature as a function of summer and winter time (SD stands for Summer Day and WD stands for Winter Day)

	SD1	SD10	SD20	SD30	SD40	SD50	SD60	SD70	SD80	SD90
W D 1	4.38	6.95	8.40	9.34	9.92	10.35	10.70	11.05	11.27	11.47
W D 2	4.31	6.91	8.30	9.11	9.78	10.18	10.53	10.76	11.08	11.27
W D 3	4.27	6.79	8.16	9.06	9.59	10.11	10.33	10.66	10.98	11.17
W D 4	4.23	6.71	8.16	8.93	9.57	9.96	10.30	10.50	10.81	10.99
W D 5	4.20	6.76	8.07	8.82	9.46	9.84	10.17	10.50	10.80	10.98
W D 6	4.17	6.70	7.99	8.86	9.36	9.86	10.06	10.39	10.69	10.86
W D 7	4.15	6.65	7.93	8.78	9.28	9.78	10.10	10.29	10.59	10.76
W D 8	4.13	6.60	7.87	8.71	9.34	9.70	10.02	10.34	10.50	10.80
W D 9	4.11	6.56	7.95	8.65	9.27	9.63	9.95	10.26	10.56	10.72
W D 10	4.09	6.53	7.90	8.60	9.21	9.56	9.88	10.20	10.49	10.65
W D 15	4.03	6.53	7.71	8.52	9.12	9.46	9.77	10.07	10.36	10.51
W D 20	4.13	6.42	7.73	8.37	8.95	9.28	9.58	9.88	10.16	10.31
W D 25	4.10	6.34	7.62	8.40	8.82	9.29	9.59	9.73	10.00	10.31
W D 30	4.07	6.28	7.54	8.30	8.87	9.18	9.47	9.76	10.03	10.17
W D 40	4.03	6.17	7.40	8.14	8.70	9.16	9.28	9.57	9.83	9.97
W D 50	3.99	6.26	7.46	8.19	8.56	9.02	9.31	9.59	9.85	9.98
W D 60	3.97	6.19	7.38	8.10	8.63	8.91	9.19	9.46	9.72	9.84
W D 80	3.92	6.09	7.24	7.94	8.46	8.91	9.00	9.27	9.52	9.82
WD100	3.88	6.01	7.13	7.82	8.33	8.77	9.04	9.31	9.55	9.66

Cichong Liu
400079
cichong@aalto.fi

WD120	3.86	5.94	7.24	7.91	8.42	8.66	8.93	9.19	9.42	9.53
WD150	3.82	6.06	7.14	7.79	8.29	8.52	8.78	9.04	9.27	9.57
WD180	3.79	5.99	7.05	7.70	8.18	8.61	8.87	9.12	9.35	9.45
WD210	3.76	5.94	6.98	7.61	8.09	8.52	8.77	9.02	9.24	9.34
WD240	3.74	5.89	6.92	7.54	8.02	8.44	8.69	8.93	9.15	9.25
WD270	3.72	5.85	6.86	7.69	8.16	8.37	8.61	8.85	9.07	9.38

10.2.4 Scenario 4 (mass flow rate in summer = 0.5 kg/s, mass flow rate in winter =1 kg/s)

In Scenario 4, case for mass flow rate in winter = 1 kg/s while mass flow rate in summer remaining 0.5 kg/s is analyzed.

Same as Scenario 3, the summer conditions remain the same while the winter results change with the change in mass flow rate in winter.

Table 38 and Table 39 show the cooling rate per length and the mean exiting temperature of the circulating fluid from the U-tube respectively and equation (50) and (51) present the predicting function for cooling rate per length and exiting fluid temperature.

$$q_l[\mathrm{W/m}] = \left(0.8639 \ln\left(\frac{\mathrm{Sh\ [h]}}{24}\right) + 0.3198\right) \cdot \ln\left(\frac{\mathrm{Wh\ [h]} - 3672}{24}\right) - 13.5712 \ln\left(\frac{\mathrm{Sh\ [h]}}{24}\right) - 5.4638 \quad (50)$$

$$T_{exit}[°\mathrm{C}] = \left(-0.0208 \ln\left(\frac{\mathrm{Sh\ [h]}}{24}\right) - 0.0099\right) \cdot \ln\left(\frac{\mathrm{Wh\ [h]} - 3672}{24}\right) + 0.3246 \ln\left(\frac{\mathrm{Sh\ [h]}}{24}\right) + 2.1541 \quad (51)$$

Table 38. Cooling rate per length as a function of summer and winter time (SD stands for Summer Day and WD stands for Winter Day)

	SD1	SD10	SD20	SD30	SD40	SD50	SD60	SD70	SD80	SD90
WD1	-16	-35	-45	-51	-56	-59	-61	-63	-65	-67
WD2	-15	-33	-43	-49	-53	-56	-58	-61	-63	-64
WD3	-15	-32	-42	-48	-52	-55	-57	-59	-61	-63
WD4	-14	-32	-41	-47	-51	-54	-56	-58	-60	-61
WD5	-14	-31	-40	-46	-50	-53	-55	-57	-59	-60
WD6	-14	-31	-40	-45	-49	-52	-54	-56	-58	-60
WD7	-14	-30	-39	-45	-49	-52	-54	-56	-57	-59
WD8	-14	-30	-39	-44	-48	-51	-53	-55	-57	-58
WD9	-14	-30	-39	-44	-48	-51	-53	-55	-56	-58
WD10	-13	-30	-38	-44	-48	-50	-52	-54	-56	-57
WD15	-13	-29	-37	-42	-46	-49	-51	-53	-54	-56
WD20	-13	-28	-37	-42	-45	-48	-50	-51	-53	-54
WD25	-13	-28	-36	-41	-44	-47	-49	-51	-52	-53

Cichong Liu
400079
cichong@aalto.fi

WD30	-12	-27	-35	-40	-44	-46	-48	-50	-51	-53
WD40	-12	-27	-35	-39	-43	-45	-47	-49	-50	-51
WD50	-12	-26	-34	-39	-42	-44	-46	-48	-49	-51
WD60	-12	-26	-33	-38	-41	-44	-45	-47	-49	-50
WD80	-11	-25	-33	-37	-40	-43	-44	-46	-47	-49
WD100	-11	-25	-32	-36	-40	-42	-43	-45	-47	-48
WD120	-11	-24	-31	-36	-39	-41	-43	-44	-46	-47
WD150	-11	-24	-31	-35	-38	-40	-42	-43	-45	-46
WD180	-11	-23	-30	-35	-37	-40	-41	-43	-44	-45
WD210	-10	-23	-30	-34	-37	-39	-41	-42	-43	-44
WD240	-10	-23	-30	-34	-36	-39	-40	-41	-43	-44
WD270	-10	-23	-29	-33	-36	-38	-40	-41	-42	-43

Table 39. Mean exiting fluid temperature as a function of summer and winter time (SD stands for Summer Day and WD stands for Winter Day)

	SD1	SD10	SD20	SD30	SD40	SD50	SD60	SD70	SD80	SD90
WD1	2.39	2.85	3.10	3.26	3.35	3.43	3.50	3.53	3.59	3.64
WD2	2.38	2.83	3.07	3.21	3.30	3.37	3.43	3.49	3.54	3.56
WD3	2.36	2.78	3.04	3.17	3.28	3.35	3.40	3.46	3.51	3.52
WD4	2.37	2.78	3.02	3.15	3.25	3.31	3.37	3.42	3.47	3.48
WD5	2.36	2.78	2.98	3.13	3.23	3.29	3.35	3.40	3.44	3.45
WD6	2.35	2.75	2.98	3.10	3.19	3.28	3.33	3.38	3.42	3.44
WD7	2.34	2.76	2.95	3.10	3.19	3.25	3.29	3.34	3.38	3.43
WD8	2.33	2.75	2.96	3.07	3.19	3.25	3.29	3.34	3.38	3.42
WD9	2.36	2.73	2.94	3.08	3.16	3.22	3.26	3.31	3.38	3.39
WD10	2.35	2.71	2.95	3.06	3.14	3.23	3.27	3.32	3.35	3.39
WD15	2.32	2.69	2.91	3.04	3.11	3.16	3.24	3.28	3.31	3.35
WD20	2.30	2.68	2.89	3.01	3.08	3.16	3.20	3.24	3.27	3.31
WD25	2.33	2.69	2.85	2.97	3.07	3.11	3.18	3.22	3.25	3.28
WD30	2.31	2.66	2.86	2.97	3.07	3.10	3.14	3.21	3.24	3.27
WD40	2.30	2.66	2.84	2.94	3.04	3.07	3.14	3.17	3.20	3.23
WD50	2.28	2.63	2.80	2.94	2.99	3.06	3.09	3.16	3.18	3.21
WD60	2.27	2.60	2.81	2.90	2.99	3.06	3.09	3.11	3.17	3.20
WD80	2.30	2.61	2.80	2.88	2.97	3.04	3.06	3.08	3.14	3.17
WD100	2.28	2.57	2.76	2.89	2.97	2.98	3.05	3.07	3.13	3.16
WD120	2.27	2.60	2.78	2.85	2.93	2.99	3.00	3.07	3.08	3.11
WD150	2.26	2.57	2.74	2.85	2.93	2.98	3.00	3.06	3.07	3.10
WD180	2.24	2.59	2.75	2.81	2.89	2.94	3.01	3.02	3.07	3.10
WD210	2.29	2.57	2.73	2.84	2.90	2.96	2.97	3.03	3.04	3.06
WD240	2.28	2.55	2.70	2.81	2.87	2.93	2.99	3.00	3.05	3.08
WD270	2.27	2.54	2.74	2.79	2.90	2.95	2.96	3.02	3.02	3.05

Cichong Liu
400079
cichong@aalto.fi